UNIVERSITY OF OKLAHOMA

GRADUATE COLLEGE

# THE ANAEROBIC MICROBIAL METABOLISM OF ENERGY SUBSTRATES: AN EXPLORATION INTO COALBED METHANOGENESIS, THE BIODETERIORATION OF DIESEL FUEL, AND BIOCORROSION

A DISSERTATION

SUBMITTED TO THE GRADUATE FACULTY

in partial fulfillment of the requirements for the

Degree of

DOCTOR OF PHILOSOPHY

By

CHRISTOPHER NEIL LYLES
Norman, Oklahoma
2013

THE ANAEROBIC MICROBIAL METABOLISM OF ENERGY SUBSTRATES: AN EXPLORATION INTO COALBED METHANOGENESIS, THE BIODETERIORATION OF DIESEL FUEL, AND BIOCORROSION

A DISSERTATION APPROVED FOR
THE DEPARTMENT OF MICROBIOLOGY AND PLANT BIOLOGY

BY

_____
Dr. Joseph M. Suflita, Chair

_____
Dr. Michael J. McInerney

_____
Dr. Bradley S. Stevenson

_____
Dr. Paul A. Lawson

_____
Dr. Mark A. Nanny

## Dedication

I dedicate this work to my wife Laura, son Carson, and parents Linda and John Lyles.

## Acknowledgements

I would first like to thank Dr. Joseph M. Suflita. I am grateful for the research opportunities I was given in your laboratory and you have been very instrumental in my development as a researcher. I also want to thank you for the fishing trips, volleyball games, food, and advice. You and Taylor provided a home away from home and it was much appreciated. I would also like to thank my committee members Michael J. McInerney, Bradley S. Stevenson, Paul A. Lawson, and Mark A. Nanny for all of your insights into my various research projects.

I would like to send a special thank you to Drs. Irene Davidova and Kathleen Duncan. You two taught me how to work at the bench and I will forever be grateful for that experience. Dr. Victoria Parisi, Dr. Cody Sheik, Dr. Jessica Seiber, Neil Wofford, Robert Grizzle, Huynh Le, Bryan Crable, Chris Marks, Dr. Cat Isom, Dr. Will Beasley, and Dr. Mathew Caldwell, we had a lot of fun over the last six years and somewhere along the way we also did some research together (or at least tried). Truly everyone elevated me as a scientist and for that I am extremely grateful to have such great friends. Additional thanks goes to Drs. Michael A. Land and Ramaraj Boopathy. You encouraged me to pursue a career in microbiology and helped me realize my dream of doing research at the highest level.

Finally, to my family there are no words to express what your love and support has meant to me through this process. Laura you are wonderful, you have been there with me since the beginning, I would have never made it through this degree without you. To my parents Linda and John Lyles thank you for supporting me during my time at the University of Oklahoma.

# Table of Contents

# List of Tables

# List of Figures

Chapter 3

# Preface

As the world energy consumption rises and more stringent regulations on chemical emissions become implemented, there is increasing interest to understand the metabolic consequences of energy substrates under anaerobic conditions such as: the modern bioconversion of coal to methane, the biodeterioration of diesel fuel, or the deleterious process of biocorrosion. The anaerobic biotransformations of hydrocarbons, coal, or organic acid intermediates typically follow an overarching metabolic pathway, which requires nutritionally diverse microorganisms including fermenters, syntrophs, and methanogens. The parent substrate is activated by fermentative microorganisms and oxidized to intermediate compounds (i.e. fatty acids). These fatty acids are then syntrophically degraded to acetate, carbon dioxide, and hydrogen for use by methanogens in electron-acceptor limited environments or by other bacteria associated with the predominate terminal electron accepting process. Under anaerobic conditions, the complete mineralization of these compounds requires a thermodynamically based microbial syntrophism, that is, degradation of the parent substrate does not occur unless the resulting end products (i.e. hydrogen, formate) are maintained at low concentrations by a microbial partner. This generalized anaerobic metabolic pathway is a common theme throughout this dissertation whether discussing the production of coal bed methane, the degradation of diesel fuels, or the impact of syntrophic hydrocarbon and fatty acid metabolism on biocorrosion.

Arguably, biocorrosion is the most important ecological consequences associated with anaerobic metabolism. In a general sense, the corrosion of a metal sample is defined by the movement of electrons from an anode to cathode. Under

anaerobic conditions the accumulation of electrons on the cathode leads to the evolution of molecular hydrogen and subsequent liberation of Iron (II) from the anode. Microorganisms can substantially influence this process by directly utilizing the evolved hydrogen or electrons associated with the metal surface, through the production of biological components such as extracellular polymeric substance, creating microenvironments by forming biofilms on the metal surface, and through heterotrophic or autotrophic metabolism that leads to the production of corrosive end products (i.e. carbon dioxide, acetate, and hydrogen sulfide). Thus, biocorrosion is a complex process that requires understanding the relationships between microorganisms and carbon sources, the prevailing environmental conditions, and the elemental composition of the metal sample in question.

This dissertation is comprised of three chapters; each describes the anaerobic biotransformation of energy substrates and the latter two describe the potential impact these biodegradation processes can have on the biocorrosion of carbon steel. Chapter one discusses the ecological factors governing the bioconversion of coal to methane across the Illinois and Powder River Basins, as well as the Cook Inlet gas field. Chapter two examines the biological stability of ultra low sulfur diesel (ULSD), specifically the relationship between the concentration of organosulfur compounds and rates of sulfate reduction. Finally, Chapter three describes how the syntrophic degradation of both *n*-alkanes and fatty acids impacts both instantaneous corrosion rates ($1/R_p$) and pitting under methanogenic and sulfate reducing conditions.

Chapter one was written and formatted for the journal *FEMS Microbiology Ecology*. For this study 17 water samples were obtained spanning three coalfields

across the United States. We used three different methods to investigate the ecological factors influencing the bioconversion of coal to methane. These methods included anaerobic incubations inoculated with water from the 17 sample sites amended with various $C_1$-$C_5$ fatty acids, the extraction of polar organic compounds from acidified production water, and the use of a functional gene microarray to investigate the genetic potential at each sample site. The results suggested that the degradation of softer lignite coal leads to the production of more fatty acid intermediates, and thus the bioconversion of these fatty acids by syntrophic bacteria is ultimately the rate-limiting step for biological coalbed methanogenesis. Thus, we propose the major ecological factor influencing the modern production of coalbed methane is the recalcitrant nature of coal itself. My major contribution to this work was setting up the anaerobic incubations and monitoring methane production from the oxidation of the various fatty acid amendments.

Chapter two was written and formatted for the journal *Environmental Science and Technology*. This work was part of a larger project looking at the biological stability of fuel for the United States Navy. Previous work had already shown that fuel additives such as soy-based biodiesel substantially increased biofouling of ULSD fuel as well as increased corrosion of carbon steel by sulfidogenic bacteria. I was a contributing author on this work entitled "Anaerobic metabolism of biodiesel and its impact on metal corrosion" which was published in the journal *Energy & Fuels* (Appendix A). However, anecdotal evidence still suggested that ULSD that did not contain biodiesel was still predisposed to biodeterioration compared to traditional diesel fuel formulations. We hypothesized that the intense process of desulfurization

produced lower molecular weight hydrocarbons that would be more amenable to decay than non-desulfurized diesel fuels. Additionally, we hypothesized that the removal of anti-microbial organosulfur compounds would allow for the improved proliferation of hydrocarbon-carbon degrading sulfate reducing bacteria (SRB) in ULSD. In contrast to our hypotheses we found that microbial communities and rates of sulfate reduction were not significantly different between ULSD and other traditional diesel fuel formulations. Thus, reasons for the predisposition of ULSD to microbial attack must be sought elsewhere. My major contribution to this work was monitoring sulfate depletion in the diesel fuel amended incubations inoculated with water from a seawater compensated fuel ballast tank from a US Navy ship as well as the molecular analysis for the various incubations.

Throughout the previous study it was clear that hydrocarbon-degrading SRB, such as *Desulfatibacillum alkenivorans* strain AK-01, were present within seawater compensated fuel ballast tanks. However, the mere presence of these bacteria does not elucidate their impact on biocorrosion. Therefore, we used a model hydrocarbon-degrading SRB, *Desulfoglaeba alkanexedens* strain ALDC to investigate the corrosion of carbon steel coupons. A concentrated cell suspension of this bacterium was incubated with *n*-decane in an electrochemical cell and the instantaneous corrosion rate ($1/R_p$) was monitored periodically for 10 days compared to an abiotic control. Sulfide was added to the control at a concentration that was the theoretically expected amount based on the complete conversion of the available sulfate in the medium. The *D. alkanexedens* strain ALDC cell suspension produced a higher instantaneous corrosion rate compared to the abiotic control, even though only about 25% of the available

sulfate was consumed during the incubation. This was also confirmed by scanning electron microscopy which revealed a much more profound pitting attack on the metal sample exposed to *D. alkanexedens* strain ALDC. The results suggested that hydrocarbon-degrading SRB can catalyze biocorrosion and propagate localized pitting. This study was published as part of a book chapter entitled "Biocorrosion issues associated with ultra low sulfur diesel and biofuel blends" in *Understanding Biocorrosion: Fundamentals & Applications* (Appendix B).

Presumably the production of sulfide by *D. alkanexedens* strain ALDC was responsible for the increase in corrosivity above the abiotic control. In chapter three we explore this prospect by culturing *D. alkanexedens* strain ALDC with both sulfate and *Methanospirillum hungatei* strain JF-1 as electron acceptors. *D. alkanexedens* strain ALDC can syntrophically degrade *n*-alkanes in co-culture with a methanogen, that is, hydrocarbon degradation can still occur without the production of corrosive sulfide. Considering that anaerobic hydrocarbon degradation is also achieved through syntrophic partnerships in microbial consortia, we investigated the corrosive ability of the fatty acid-oxidizing bacterium *Syntrophus aciditrophicus* strain SB in axenic culture, as well as in co-culture with both *Desulfovibrio sp.* strain G11 and *M. hungatei* strain JF-1. The genus *Syntrophus* has been identified as numerically important in methanogenic hydrocarbon-degrading consortia. The results suggested that the corrosion of carbon steel decreased when *D. alkanexedens* strain ALDC was in co-culture with the methanogen *M. hungatei* strain JF-1 and increased when *S. aciditrophicus* strain SB was co-cultured with the SRB *Desulfovibrio sp.* strain G11. Thus, sulfide production was seemingly an important variable in determining the

corrosion of carbon steel. However, the standard deviations observed for instantaneous corrosion rates and pitting throughout biological replicates were high for both *D. alkanexedens* strain ALDC and *S. aciditrophicus* strain SB experiments and could not be explained by differences in the amount of biomass, initial substrate concentrations, metabolic activity, end product formation, or other experimental conditions within the incubations. Therefore, we were forced to attribute this variability to compositional differences associated with individual metal samples. Chapter three is written and formatted for the journal *Frontiers of Microbiology*, and my major contributions to this work include monitoring crotonate and sulfate depletion and measuring corrosion using both electrochemical and profilometry techniques. Part of this work was also published in the *Proceedings of the VI International Scientific Conference: Microbial Biodegradation and Biodeterioration of Technical Materials* (Appendix C).

## Abstract

Under anaerobic conditions the complete mineralization of energy substrate can be achieved by specialized individual microorganisms or through syntrophic partnerships involving bacteria and archaea that ultimately convert parent compounds to methane and carbon dioxide. Such biotransformations generally result in the production of several fatty acids (i.e. acetate, propionate, butyrate, benzoate) that are particularly diagnostic for *in situ* microbial activity as well as postulated intermediates for anaerobic hydrocarbon degradation. The metabolic fate of these organic acid intermediates has been the subject of multiple investigations. However, what seems clear is that fatty acid-oxidizing bacteria generally catalyze the subsequent conversion of these intermediate compounds under a thermodynamically-based microbial syntrophism in co-culture with hydrogen/formate-utilizing microorganisms. Thus, $C_1$-$C_5$ volatile fatty acid (VFA) compounds are used throughout these chapters to represent metabolic intermediates of coal or hydrocarbon degradation. The ecological consequences of these anaerobic bioconversions are highly dependent on the prevailing geochemical conditions as well as the interrelationships between microorganisms and carbon sources. This dissertation focuses on the degradation of hydrocarbons or proposed fatty acid intermediates either relating to the production of coal bed methane (CBM) or the biodeterioration of fuels and how the latter subsequently impacts the biocorrosion of carbon steel.

Coal is extremely difficult to chemically characterize; the organic fraction varies based on the starting plant material, the conditions of decomposition, and the physical and chemical changes that occur during the process of coalification. Thus, coal does

not make for amenable methanogenic substrate, and requires a diverse microbial assemblage along with a thermodynamically based microbial syntrophism for the bioconversion of coal to methane. Considering the vast worldwide reserves of coal, the ever-expanding need for energy across the globe, and the environmental benefits of methane utilization as an energy source, there is considerable interest in stimulating the modern bioconversion of coal to methane. It has been previously proposed that ecological factors such as substrate bioavailability, coal recalcitrance, the absence of the requisite microorganisms, and chemical/nutrient limitations might contribute to the inhibition of biogenic CBM production. To assess coalfield methanogenesis, formation water from 17 sites collected from the Illinois and Powder River Basins as well as the Cook Inlet gas field was used as inocula for nutrient-replete incubations amended with $C_1$-$C_5$ fatty acids. Methanogenic rates for these incubations were extremely slow with long lag times and expected stoichiometric values of methane were typically not produced. Additionally, a functional gene microarray indicated that the genetic potential associated with a variety of microbial functions was present in all samples. Out of the three coalfields, the Cook Inlet incubations produced the most methane, particularly when amended with butyrate or valerate, a result that correlated with the number of unique *mcr* gene sequences and is consistent with the *in situ* detection of $C_4$-$C_5$ alkanoic acids. Collectively, these results suggested that the soft lignite coal in the Cook Inlet is easier to degrade than the sub-bituminous and bituminous coals of the Illinois and Powder River Basins. The degradation of the lignite coal in turn leads to the production of intermediate polar organic compounds (i.e. butanoic, pentanoic acids) within production waters that are then syntrophically converted to methane. These

findings highlight the role of syntrophy in CBM production, and we concluded that coal methanogenesis is probably not limited by the inherent lack of metabolic potential, the presence of alternate electron acceptors, or the lack of available nutrients, but more likely restricted by the recalcitrant nature of the coal itself.

Stringent regulations have been imposed worldwide mandating that diesel fuels contain ≤15 ppm sulfur; as a consequence ultra-low sulfur diesel (ULSD) has been fully integrated into the worldwide infrastructure to reduce chemical and particulate emissions. The process of desulfurization results in several changes to the physical properties of diesel fuel, which might differentially impact the biodeterioration of ULSD, compared to traditional diesel fuel formulations. We hypothesized that the removal of potentially inhibitory organosulfur compounds could alleviate the negative impact of these substances on the microbes responsible for diesel fuel biodegradation and that the intense process of desulfurization leads to the production of residual lower-molecular weight by products, which might increase the proliferation of problematic microbes relative to the fuel hydrocarbons. To test these hypotheses, an inoculum from a seawater-compensated ballast tank, along with two other known hydrocarbon-degrading inocula, were amended with fuel from the same ship or with refinery fractions of ULSD, low- (LSD), and high sulfur diesel (HSD) and monitored for sulfate depletion. The rates of sulfate removal in incubations amended with the refinery fuels were elevated relative to the fuel-unamended controls, but indistinguishable from one another. Thus, anaerobic hydrocarbon metabolism likely occurred in these incubations regardless of fuel sulfur content. The microbial community structure from each incubation was also largely independent of the fuel amendment type, based on

molecular analysis of 16S rRNA gene sequences. Our results suggest that removal of organosulfur compounds and the production of easily amenable low molecular weight hydrocarbons via desulfurization do not significantly influence sulfate reduction rates or the structure of microbial communities. Thus, the process of desulfurization cannot explain the propensity of ULSD to decay faster than traditional diesel fuel formulations. The major implications of this work are that the biodegradation of diesel hydrocarbons or, by inference, the degree of biocorrosion is not influenced by the concentration of organosulfur species in the fuel.

There is no doubt that the anaerobic degradation of hydrocarbons can be accomplished axenically by microbial pure cultures under a variety of electron accepting conditions as well as syntrophically by nutritionally diverse microbial consortia. However, the environmental consequences of anaerobic hydrocarbon transformation depend on the geochemical setting. Under sulfate-reducing conditions the production of sulfide can lead to health and safety concerns, reservoir souring, and metal biocorrosion; whereas the consequences under methanogenic conditions include the overall diminishment of petroleum quality and the production of methane, a greenhouse gas. Given that syntrophic bacteria are common in oil production facilities, we focused our efforts to understanding the impact of syntrophic hydrocarbon and fatty acid intermediates on the deleterious process of biocorrosion under both methanogenic and sulfate reducing conditions. Thus, defined microbial incubations using the hydrocarbon-degrading, sulfate-reducing bacterium *Desulfoglaeba alkanexedens* strain ALDC, was cultured with either sulfate or *Methanospirillum hungatei* strain JF-1 as electron acceptors and tested for the ability to corrode carbon steel coupons. The

anaerobic biodegradation of hydrocarbons can also lead to the formation of a suite of fatty acid intermediates that can then be syntrophically metabolized, thus the corrosive potential of a model fatty acid-oxidizing bacteria *S. aciditrophicus* strain SB was assessed both in axenic culture, as well as syntrophically in co-culture with both *Desulfovibrio sp.* strain G11 and *M. hungatei* strain JF-1. Corrosion was measured using both electrochemical and profilometry techniques. Our results suggested that the corrosion of carbon steel decreased when *D. alkanexedens* strain ALDC was in co-culture with *M. hungatei* strain JF-1 and increased when *S. aciditrophicus* strain SB was co-cultured with *Desulfovibrio sp.* strain G11. The results highlight the role of acetate and sulfide production on the corrosion of carbon steel, and suggest that the metabolic interactions between syntrophs and hydrogen/formate utilizing microorganisms can substantially influence both instantaneous corrosion rates ($1/R_p$) and localized corrosion of the metal coupon. Despite these trends, corrosion was highly variable between replicate incubations. Differences in the amount of biomass, initial substrate concentrations, metabolic activity, end product production, and experimental conditions within the defined incubations did not account for this variation. Thus, the variability was ascribed to differences in the elemental composition of the metal coupons.

# Chapter 1: Ecological factors influencing the bioconversion of coal to methane


## Abstract

The potential for modern coalfield methanogenesis was assessed using formation water from the Illinois Basin, Powder River Basin, and Cook Inlet gas field as inocula for nutrient-replete incubations amended with $C_1$-$C_5$ fatty acids as presumed intermediates formed during anaerobic coal biodegradation. Instead of the expected rapid mineralization of these substrates, methanogenesis was inordinately slow (~1 $\mu mol \bullet d^{-1}$), following long lag periods (>100d), and methane yields typically did not reach stoichiometrically expected levels. However, a gene microarray confirmed the potential for a wide variety of microbiological functions, including methanogenesis, at all sites. The Cook Inlet incubations produced methane at a relatively rapid rate when amended with butyrate ($r$=0.98; $p$=0.001) or valerate ($r$=0.84; $p$=0.04), a result that correlated with the number of unique *mcr* gene sequences and was consistent with the *in situ* detection of $C_4$-$C_5$ alkanoic acids. This finding highlighted the role of syntrophy for the biodegradation of the soft lignitic coal in this formation, but methanogenesis from the harder sub-bituminous to bituminous coals in the other fields was less apparent. We conclude that coal methanogenesis is probably not limited by the inherent lack of metabolic potential, the presence of alternate electron acceptors, or the lack of available nutrients, but more likely restricted by the inherent recalcitrance of the coal itself.

## Introduction

Coal has been considered an unconventional natural gas reservoir where thermogenic or biogenic methane is stored predominantly in an adsorbed state (Suárez-Ruiz, 2012). There are consistent reports in the literature that suggest a small fraction of methane from coal beds is of modern origin (Thielemann et al., 2004; Klein et al., 2008; Jones et al., 2008; Jones et al., 2010). Biogenic coal bed methane (CBM), formed eons ago or relatively recently is believed to contribute about 3-4% of the total natural gas production in the United States (Strąpoć et al. 2011). Considering the vast worldwide reserves of coal (Strąpoć et al. 2011; Moore, 2012), the ever-expanding need for energy across the globe, and the environmental benefits that attend methane utilization as an energy source, there is considerable interest in stimulating the modern bioconversion of coal to methane (Ünal et al., 2012, Ulrich and Bower, 2008; Green et al, 2008; Harris et al., 2008; Penner et al., 2010; Wawrik et al., 2011).

However, coal is an extremely heterogeneous organic material that is challenging to fully chemically characterize (Strąpoć et al. 2011; Moore, 2012). Given its inherent chemical complexity, coal is far from an ideal substrate for methanogenic fermentation processes. However, it can reasonably be assumed that, like other forms of organic matter, the anaerobic mineralization of coal will require a nutritionally diverse assemblage of anaerobic bacteria that attack large molecular weight labile components and convert them to simpler chemical residues. The latter components ultimately get converted to a suite of volatile fatty acid (VFA) and alcohol intermediates (Beckmann et al., 2011; Faiz and Hendry, 2006; Fry et al., 2009; Green et al., 2008; Leschine, 1995; Strąpoć et al., 2008; Wawrik et al., 2011). The anaerobic

bioconversion of these critical intermediates has been the subject of many investigations. What seems clear is that the ultimate conversion of the small molecular weight intermediates to methane is often a rate-limiting process that requires a thermodynamically-based microbial syntrophism. That is, substrate bioconversion by one microorganism occurs only when the resulting products, typically hydrogen, formate, or acetate, are maintained at very low concentrations by a cooperating microbial partner. In electron-acceptor limited environments, these simple electron donors are maintained at the requisite low levels by acetoclastic, methylotrophic, and hydrogenotrophic methanogens (McInerney et al., 2008; Thauer et al., 1977; Berry et al., 1987; Widdel and Rabus, 2001).

Of course, in addition to the presence of the requisite microorganisms, there should also be an environment that is suitable for microbial activity and growth. For efficient methanogenesis, this implies the lack of alternate electron acceptors, an appropriate and available supply of nutrients (C, N, P, S, and trace elements), as well as pH and temperature conditions that are nominally compatible with the requirements of the indigenous microflora. Similarly, we presume that the major microbial activities in coalfields would be co-associated with the ready availability of moisture.

A considerable amount of research has been dedicated to identifying the requisite microorganisms associated with the bioconversion of coal to methane, and convincingly a large body of work has been assembled identifying the presence of known fermenting and syntrophic bacteria as well as methanogenic archaea in coalfields worldwide (Fry et al., 2009; Harris et al., 2008; Kimura et al., 2010; Midgley et al., 2010; Papendick et al., 2011; Thielemann, 2004; Strąpoć et al., 2008; Strąpoć et

al., 2011; Wawrik et al., 2011; Green et al., 2008). Based on these studies it would seem that biogenic CBM production is not likely to be hindered by a fundamental lack of metabolic potential (Wawrik et al., 2011).

While coalfield waters harbor a diverse indigenous microflora, the major ecological factors that influence the bioconversion of coal to methane remain unresolved. Jones et al. (2008, 2010) identified several possible limitations to biogenic CBM, mainly *in situ* nutrient limitations and the bioavailability of the carbon within coal. Bates et al. (2011) suggests that carbon, nitrogen, and phosphorous species are relatively low throughout groundwater in the Powder River Basin. Conceivably the depletion of these nutrients could alone or in combination limit *in situ* methanogenesis. Nevertheless, multiple enrichment studies from this basin have reported the bioconversion of coal to methane *in vitro* when incubated with coal or potential intermediate compounds (i.e. acetate). The same studies have also shown dramatic increases in methane production when incubations were amended with trace elements, acetate, yeast extract, or slight changes in temperature or pH (Ünal et al., 2012, Ulrich and Bower, 2008; Green et al, 2008; Harris et al., 2008). Similar results have been reported from enrichment studies in other coalfields such as the San Juan Basin (Wawrik et al., 2011) and coal beds in Alberta, Canada (Penner, et al., 2010). Taken collectively these studies suggest that indigineous microbial communities within coalfield waters could produce modern methane from coal-related organic matter. However, under laboratory conditions lag times for methane production from coal or coal-related intermediates can ranged from ~120-450 days (Harris et al., 2008; Ulrich and Bower, 2008; Krüger et al., 2008; Wawrik et al., 2011), suggesting that even with

adequate nutrient supply, methanogenesis from these substrates was still a relatively slow process.

The maturity of coal can also substantially impact the production of methane. Previous studies have reported that lower rank coal typically produced more biogenic methane than mature coals (Kotarba, 2001; Harris et al., 2008; Formolo et al., 2008; Strąpoć et al., 2011). Glombitza et al. (2008) and Vieth et al. (2008) reported that the concentrations of formate and acetate extracted from coals appeared to depend on coal rank, thus potentially providing a carbon source for deep subsurface microbial communities. In contrast, other studies have indicated that coal maturity and methanogenesis are not highly correlated (Wawrik et al., 2011; Jones et al., 2008; Faiz and Hendry, 2006; Formolo et al. 2008); suggesting that rank alone is not a reliable indicator of the susceptibility of coal to methanogenesis.

To investigate the ability of coalfield microbial communities to generate methane we obtained formation water samples from multiple locations in the Illinois and Powder River coal basins as well as the Cook Inlet Alaska gas field. The formation water samples were used as inocula for nutrient-sufficient anaerobic incubations that were amended with formate or acetate to assay for the methanogenic archaea. Similarly, methanogenesis was assessed in other incubations that were amended with the individual VFAs, propionate, butyrate, or valerate to assay for the requisite syntrophic bacteria. We reasoned that if *in situ* CBM was an active and ongoing process, the indigenous microflora should be able to readily utilize these simple electron donors given their presumed importance in anaerobic coal biodegradation. The genetic potential for organic matter utilization was also assessed at each site using a functional

gene microarray (GeoChip 3.2 or 4.0). Lastly, the low molecular weight polar organic compounds in the formation waters, presumed metabolites associated with coal biodegradation processes, were also analyzed by mass spectrometry. Our findings suggest that the bioconversion of coal is not limited by the inherent lack of metabolic potential but more likely restricted by the recalcitrant nature of the coal itself.

## Materials and Methods

**Sample Collection and Site Description.** Water samples were obtained from multiple sites within three coalfields in the United States: the Illinois Basin, Cook Inlet gas field, and Powder River Basin. A total of 17 samples were collected throughout the three coalfields. Formation water (~160 mls) was collected in serum bottles that were then sealed with butyl-rubber stoppers and aluminum crimps and shipped to the University of Oklahoma. Coal maturity in the three coalfields differ markedly (AOGCC, 2011; Calderwood and Fackler, 1972; Hartz et al., 2009; Pratt et al., 1999; Strąpoć et al., 2007; Walters, 2002; Strąpoć et al., 2011). The Illinois Basin encompasses the state of Illinois and parts of Indiana and Kentucky. The basin consists of high volatile bituminous coals (Strąpoć et al., 2007). Five samples were collected and designated 1-5. The Cook Inlet gas field is located along the western shoreline of Alaska (AOGCC, 2011) and contains thin intercalated beds of claystone, sandstone, siltstone, and lignitic to subbituminous coal (Calderwood and Fackler, 1972). Six water samples were collected and designated 6-11. The Powder River Basin is located in Montana and northeast Wyoming and consists of subbituminous coals (Walters, 2002). Six water samples were collected and designated 12-17.

**Anaerobic Incubations**. A basal medium was prepared as previously described in McInerney et al. (1979), except rumen fluid and sulfate were omitted. Final concentrations of mineral components were as follows: 0.87 mM $K_2HPO_4$, 1.54 mM $MgCl_2 \bullet 6H_2O$, 0.365 mM NaCl, 0.345 mM $NH_4Cl$, and 0.005 mM $CaCl_2 \bullet 2H_2O$. The medium was also amended with a trace metal and vitamin solution described in Tanner (2002), a 0.001% solution of resazurin used as a redox indicator, and 24 mM sodium bicarbonate ($NaHCO_3$). The medium was reduced using a 2.5% solution of cysteine sulfide. Strict anaerobic conditions were maintained as described by Widdel and Bak (1992). Nine ml aliquots of the basal medium were dispensed into sterile 25 ml serum tubes in an anaerobic chamber (5% $H_2$ in $N_2$ gas phase). The serum tubes were closed with butyl rubber stoppers, crimped with aluminum seals, and the headspace was exchanged to a $N_2$:$CO_2$ (80:20) atmosphere.

The basal medium was inoculated with one ml of a water sample from each of the 17 coalfield locations. Incubations were then amended with five mM of a specific low molecular weight volatile fatty acid (VFA) that included either: formate, acetate, butyrate, propionate, or valerate. Using the empirical equation derived by Buswell and Mueller (1952) theoretical yields of methane were predicted based on the initial concentration of VFA. The theoretical yields for formate, acetate, propionate, butyrate, and valerate were 25, 50, 87.5, 125, and 162.5 μmol methane, respectively. Negative controls included sterile, VFA-unamended, and uninoculated incubations. Incubations were monitored for methane production with time and values are corrected for the background level in the VFA-unamended controls.

**Analytical Techniques.** Methane production was measured using a gas chromatograph (Packard model 427, Downers Grove, Ill.), equipped with a flame ionization detector and a Porapack Q column (Supleco, Inc., Bellefonte, Penn). The oven, detector, and injector temperatures were set to 100, 100, and 125°C, respectively. The concentration of chloride, nitrate, and sulfate were measured using ion chromatography (Dionex model DX500, Sunnyvale, CA) equipped with an IonPac™ AS4A column, ASRS 300 4mm self-regenerating suppressor, and a conductivity detector. The eluent consisted of 1.7 mM sodium bicarbonate and 1.8 mM sodium carbonate and was diluted 1:100 from a ready to use concentrate. The flow rate was 2.0 ml/min and the suppressor was set to 54 mA.

**GeoChip Functional Gene Array Hybridization.** The DNA extraction protocols were previously described by He et al. (2010) and Lu et al. (2011). Approximately 100 ng of DNA was amplified using a Templiphi kit (GE Healthcare, Piscataway, NJ), and labeled with Cy3 fluorescent dye (GE Healthcare) by random priming (Wu et al., 2006). The DNA was then purified with a QIAquick purification column (Qiagen, Valencia, CA) and dried in a SpeedVac (ThermoSavant, Milford, MA) at 45°C for 45 min before hybridization. GeoChip analysis was performed using either version 3.2 or 4.0. The Cook Inlet gas field samples (6, 8-11) were analyzed using GeoChip 3.2. This version of the microarray contained 28,000 gene probes for more than 56,500 gene targets in 292 functional gene categories (He et al., 2010). The Illinois Basin and Powder River samples (1-5 and 12-15, respectively) were analyzed using GeoChip 4.0. This updated version of the microarray contains 83,992 gene probes and targets 152,414 genes in 410 functional gene categories (Lu et al., 2011).

**GeoChip Statistical Analysis.** Approximately 800 unique functional genes were measured within each sample from the three coalfield basins. These genes were placed into "gene categories" covering several fundamental microbial processes (He et al., 2010). Three changes were made to the organizational structure described in He et al. (2010), the methyl coenzyme M reductase (*mcr*AB) genes, the dissimilatory sulfite reductase (*dsr*AB) genes, and the adenosine-5'-phosphosulfate (*aps*AB) genes were recategorized as methane production and (the latter two) as sulfate reduction genes, respectively. In order to reduce the complexity of the functional gene analysis, the nine most relevant categories are discussed within this paper. The relative abundance of a gene category for each sample is equal to the sum of the detected genes in the category, divided by the sum of detected genes in the basin. To compare if the nine categories were significantly different from one another, a mean percentage ($\overline{X}$) was calculated for the nine functional gene categories. The standard error ($n$=14) represents the samples assayed using the functional gene array. Correlation coefficients ($r$) were used to indicate the strength and direction of the linear relationship between rates of methanogenesis from the various anaerobic incubations and the diversity and quantity of *mcr* genes detected by the GeoChip.

**Metabolite Profiling**. Water samples from each of the coalfield sites were acidified with 50% HCl to a pH <2 and kept at 4°C until analyzed. One liter of acidified sample was extracted with ethyl acetate (10% vol/vol, 4 times) and dried over anhydrous $Na_2SO_4$. Extracted samples were concentrated by rotary evaporation and reduced further to approximately 100 µl under a flow of nitrogen gas (Duncan et al., 2009). The extract was derivatized using *N,O*-bis(trimethylsilyl)trifluoroacetamide (BSTFA)

(Pierce Chemical Co., Rockford, IL). Putative metabolites were identified using gas chromatography (Agilent model 6890, Santa Clara, California) coupled with a mass spectrometer (Agilent model 5973, Santa Clara, California). Separations were performed using a HP-5 ms capillary column (30m X 0.25 mm inner diameter X 0.25 μm film, J&W Scientific, Folsom, CA) with an initial oven temperature of 45 °C for 5 mins that was increased at 4°C/min to 270 °C and held for 10 min (Aktas et al. 2010). All metabolite identifications were made by comparison with features of authentic standards.

## Results

### Water Chemistry and Metabolite Analysis

Seventeen samples from the Illinois Basin, Cook Inlet gas field, and Powder River Basin were analyzed for chloride, sulfate, and nitrate anions (Table 1). The waters from the three coalfields were found to contain <0.5 mM of sulfate and nitrate, suggesting that alternate electron acceptors were unlikely to impact the endogenous rates of methanogenesis within the coalfields. The mean chloride concentrations for the Illinois Basin, Cook Inlet gas field, and the Powder River Basin were 41.0 ± 39.2, 8.90 ± 13.4, and 0.843 ± 0.293 mM respectively. Thus, the low chloride levels are also unlikely to be a substantive detriment to coalfield methanogenesis (Waldron et al., 2007).

Mass spectral analysis of water samples from the three coalfields was used to detect the presence of 71 polar organic compounds that could be putative intermediates associated coal biotransformation (Figure 1). The anaerobic metabolites for alkylbenzene degradation (benzylsuccinic acid through propylbenzylsuccinic acid) and

polycyclic aromatic compounds (naphthylsuccinic through phenanthrene carboxylic acid) were only identified in a few samples throughout the Cook Inlet gas field. However, monoaromatic compounds (benzoate through 3-propyl phenol) were intermittently identified throughout the samples in the three coalfields. Additionally, alkylsuccinic acids ($C_1$ through $C_{16}$) were only identified in the Cook Inlet gas field samples. Nineteen alkanoic acids were detected throughout the 17 sample sites (Figure 2). The detection of $C_1$-$C_5$ alkanoic acids was particularly notable since we used the same compounds as substrates in the anaerobic biodegradation assays (below). Only one sample out of five in the Illinois Basin contained acetic, propionic, and butanoic acids. Five out of six sites in the Cook Inlet gas field were positive for butanoic and pentanoic acids. Additionally, two sites contained acetic and propionic acid. Only one site within the Powder River Basin was positive for pentanoic acid. Longer chain fatty acids (octanoic through octadencanoic acids) were identified throughout the samples from the three coalfields, though to a lesser extent within the Cook Inlet gas field. Overall, The Cook Inlet gas field had about twice the number of polar organic compounds than either the Illinois or Powder River Basins.

**Anaerobic Biodegradation Assays**

When laboratory incubations of coalfield water samples were amended with $C_1$-$C_5$ VFA compounds, inordinately slow rates of methanogenesis and long lag times were detected, and the stoichiometric expected amount of methane was not typically produced (Figure 3). Prokaryotic biomass levels were estimated for each of the 17 samples (Table 2). Cell numbers estimated based on the amount of DNA recovery ranged from ~$10^5$ to $10^7$ cells•$ml^{-1}$ (Kubitschek and Freedman, 1971; Button and

Robertson, 2001). There was no correlation between the estimated cell biomass levels and metabolic activity (Figure 3; Table 2). The Illinois Basin (Figure 3A) had two samples (1 and 2) out of five, where the inocula metabolized at least one of the $C_1$-$C_5$ VFAs to the theoretically expected amount of methane. Organisms within sample 1 incubations metabolized formate, acetate, butyrate, and valerate to methane at a rate of 0.42 ± 0.10, 1.2 ± 0.8, 2.3 ± 0.88, and 0.48 ± 0.08 μmol $CH_4 \bullet d^{-1}$, respectively, following a 54-200 day lag period depending on the particular substrate. The microflora in sample 2 incubations amended with formate and acetate, produced methane at a rate of 0.36 ± 0.04 and 0.52 ± 0.11 μmol $CH_4 \bullet d^{-1}$ after a 50 and 25 day lag, respectively. Samples 3,4, and 5 had negligible methanogenesis activity, with some lag times well in excess of one year. The Cook Inlet gas field (Figure 3B) contained three samples (6,7, and 8) out of six where the inoculum produced the theoretically expected amount of methane from the VFAs amendments. The microbes in sample 6 incubations metabolized formate, acetate, propionate, butyrate, and valerate to methane at a rate of 0.37 ± 0.08, 0.67 ± 0.06, 0.60 ± 0.003, 0.80 ± 0.10, 1.1 ± 0.14 μmol $CH_4 \bullet d^{-1}$ respectively. The lag time for these VFAs ranged from 35-150 days depending on the substrate. Sample 7 incubations metabolized formate, acetate, and butyrate to methane at a rate of 0.03 ± 0.2, 0.34 ± 0.27, and 0.69 ± 0.02 μmol $CH_4 \bullet d^{-1}$, respectively after a 36-152 day lag period. Sample 8 incubations metabolized acetate and butyrate at a rate of 0.23 ± 0.3 and 0.98 ± 0.06 μmol $CH_4 \bullet d^{-1}$, respectively. The microflora in samples 9-11 did produce some methane from various VFA substrates, but none reached the theoretically expected amount after ~400 day incubation period. The Powder River Basin (Figure 3C) had only one sample (13) out of six where the inoculum produced the

theoretically expected amount of methane from the VFAs amendments. These incubations metabolized propionate at a rate of 0.73 ± 0.2 μmol $CH_4 \bullet d^{-1}$ with a lag time of 149 days. Samples 12, 14-17 produced negligible methane after 450 days.

**Functional Gene Analysis**

A functional gene microarray (GeoChip 3.2 or 4.0) was used to assess the genetic potential in 14 of the 17 samples from the three coalfields. Samples 7, 16, and 17 were not included in this assay because the amount of DNA extracted was too low to amplify. We presume there was an inhibitor present that interfered with either the extraction or amplification procedures. The two versions of GeoChip used in this study differ in the number of functional gene probes. In order to compare the microarray data between the three coalfields, the data sets were normalized to relative abundance by dividing the sum of detected genes in a particular category for each sample by the total number of detected genes in each basin. The microarray analysis revealed that genes encoding for the same or similar microbial activities were ubiquitous throughout the three coalfields (Figure 4). In order to see if any gene category was relatively more variable than the others, the mean percentage ($n$=14 samples) for each gene category was calculated and the standard error was determined. The variability of the nine gene categories across the 14 samples was not significantly different (Bartlett test of homogeneity of variances: $K^2$=4.2, $p$=0.83). Additionally, no significant difference was observed between the mean percentages for each of the nine gene categories ($F$(8, 117)=0.4, $p$=0.9). The results suggest that the variability and mean percentage of the functional gene categories are relatively the same throughout the three coalfields (Figure 4).

**Relationships between putative metabolites, rates of methanogenesis, and functional genes**.

Generally, the *in situ* presence of $C_1$-$C_5$ alkanoic acids (Figure 2) in the coalfield samples was not associated with the ability of a particular inoculum to metabolize the same compounds *in vitro* (Figure 3). However, exceptions were noted at the Cook Inlet site, in which butanoic and pentanoic acids were identified in the production waters from samples 6 and 8-10. Correlations between the diversity or quantity of *mcr* genes and rates of methanogensis from anaerobic incubations amended with the methanogenic substrates (i.e. formate, acetate) or the syntrophic substrate (i.e. propionate, butyrate, valerate) were generally quite low in most coalfield samples ($r \leq 0.60$; Table 3). To investigate how the diversity of *mcr* genes impacts methanogenesis within the coalfields, the number of unique gene sequences were totaled and compared to methanogenic rates measured with the various VFA amendments. The strongest correlation was noted between the number of unique *mcr* genes detected via the GeoChip assay and rates of methanogenesis observed for Cook Inlet gas field samples when amended with butyrate ($r$=0.98, $p$=0.001) and valerate ($r$=0.84, $p$=0.04) (Table 3). Additionally, in the Powder River Basin a correlation was observed between the rates of methanogenesis in samples amended with acetate ($r$=0.76, $p$=0.065) and the number of unique *mcr* genes detected *in situ* (Table 3).

However, it is not obvious why gene diversity *per se* would correlate with microbial activity. That point notwithstanding, we also investigated if the quantity of *mcr* genes, measured as signal intensity during the GeoChip analysis, correlated with the rates of methanogenesis. Previous work demonstrated a quantitative relationship

between signal intensity and the concentration of DNA on the functional gene microarray (Wu et al. 2006). Thus, *mcr* gene signal intensities were totaled as a crude measure of methanogen biomass and compared to the rates of methanogenesis calculated from VFA-amended incubations. However, these relationships were generally not strong ($r \leq 0.33$; Table 3) with the highest r-value observed between the quantity of *mcr* genes and rate of methanogenesis in the Powder River Basin incubations amended with acetate ($r$=0.78, $p$=0.11; Table 3).

## Discussion

Biogenic CBM is estimated to contribute ~3-4% of the total natural gas production in the United States (Strąpoć et al., 2011). Jones et al. (2008, 2010) proposed that substrate bioavailability, coal recalcitrance, the absence of the requisite microorganisms, and chemical/nutrient limitations are potential ecological factors that inhibit the bioconversion of coal to methane. To assess these factors, production water samples were collected from three different coalfields and used as inocula for anaerobic incubations consisting of a basal medium and $C_1$-$C_5$ VFA substrates. The medium contained nitrogen and phosphorous sources as well as trace metals and vitamins in an attempt to overcome potential nutrient limitations that might restrict methanogenesis *in vitro*. The concentration of electron acceptors (Table 1; nitrate and sulfate) was low enough that methanogenesis would likely not be substantively inhibited in the 17 coalfield samples. Additionally, the chloride levels (Table 1) fall within the range that is compatible with methanogenesis (Waldron et al., 2007). The fact that methane was produced from various $C_1$-$C_5$ VFA amendments in several incubations across the three

coalfields suggests that the medium itself was sufficient and was therefore unlikely to restrict methanogenesis.

Low molecular weight VFAs were chosen as assay substrates because they have previously been identified as potential intermediates formed during the anaerobic bioconversion of coal to methane (Ulrich and Bower, 2008; Vieth et al., 2008; Glombitza et al., 2009; Wawrik et al., 2011). We added formate and acetate as methanogenesis precursors and other VFAs as substrates requiring syntrophic interactions for ultimate mineralization. The $C_1$-$C_5$ VFAs are water-soluble and coal was specifically not added in the incubations to eliminate complications associated with substrate adsorption limiting bioavailability and concomitant methanogenesis. We expected the coalfield inocula to easily biodegrade these low molecular weight VFAs and produce the stoichiometrically expected amount of methane. However, this was rarely the case. Anaerobic incubations using coalfield production waters as inocula exhibited long lag periods (~100 days) and methanogenesis rates that were rather slow (~1 μmol $CH_4 \bullet d^{-1}$). Moreover, these incubations typically did not reach the stoichiometrically expected amounts of methane, even after ~400 days of incubation (Figure 3). Additionally, the slow rates of methanogenesis measured in the VFA-amended incubations (Figure 3) could not be explained by differences in total or methanogen biomass levels (Table 2). Of the three coalfield basins, several samples from the Cook Inlet gas field were the only ones that harbored the inherent microbial community that completely mineralized the VFA amendments. The negative values of methane production in Figure 3 indicate that several VFA amendments had a slight inhibitory impact on methanogenesis relative to substrate-unamended controls. In the

few cases where it was observed, we presume it was most likely due to the relatively high concentration of VFAs employed. Methane production exceeding 100% of the theoretical value was undoubtedly due to endogenous electron donors already in the coalfield production waters as detected in the metabolite profiling assay (Figures 1 and 2).

The metabolic results from the anaerobic incubations were surprising, considering that the microbial communities from some of these coalfields, specifically the Powder River Basin, have been shown to oxidize coal in the laboratory (Green et al., 2008; Harris et al., 2008; Ulrich and Bower, 2008). However, there is much debate whether or not planktonic communities in production water reflect the sessile communities associated with coal. In most CBM studies production water is used as inocula due to the difficulty of obtaining actual coal samples from investigation sites (Strąpoć et al. 2011). Klein et al. (2008) suggests that methanogens associated with coal *per se* are both phylogenetically and functionally different than those identified in coal production waters of the Powder River Basin. Thus, despite the potential differences in planktonic and sessile microbial communities throughout the three coalfields, the GeoChip analyses indicates that the genetic potential for complex carbon biodegradation and methanogenesis is present in all samples (Figure 4), and that the mean relative abundance and variability between gene categories across the three coalfields was not significantly different. Thus, methane production was not likely inhibited due to a lack of functional genes, and by extension, the absence of requisite microorganisms.

If the genetic potential is present, but no methane is being produced from the $C_1$-$C_5$ VFA amendments this might imply that the microbial communities within the coalfields are not frequently exposed to these low molecular weight substrates. Within the Illinois and Powder River Basins, the *in situ* presence of $C_1$-$C_5$ alkanoic acids in the coalfield samples was generally not associated with the ability of a particular inoculum to metabolize the same compounds. Previous research from the Illinois Basin suggests that methanogenesis is primarily hydrogenotrophic (Strąpoć et al., 2007), and that the dominant Archaea is *Methanocorpusculum* (Strąpoć et al., 2008) a methanogen capable of producing methane from $H_2/CO_2$, formate, 2-propanol/$CO_2$ and 2-butanol/$CO_2$ (Zellner et al., 1989). Thus, if formate is a common intermediate for methanogenesis within the Illinois Basin, then it should be rapidly utilized within the laboratory incubations. Only two samples (1 and 2) metabolized formate to the theoretically expected extent (Figure 3A). No correlation was observed between rates of methanogenesis when the samples were amended with formate and the either diversity or quantity of *mcr* genes (Table 3). Perhaps formate and other VFAs may not be particularly common coal biodegradation intermediates in the Illinois Basin samples. Previous research has shown a gradient in coal maturity across the Illinois Basin. Biogenic methane from $CO_2$-reduction is common in areas with less mature coal (Indiana portion) while the methane from areas containing harder and more mature coal (western Kentucky portion) is derived principally of thermogenic origin (Strąpoć et al. 2007). It is unknown if such gradients exist in the areas where the samples were obtained.

The Powder River Basin samples had a slightly different result when compared to the Illinois Basin. Stable isotope probing suggests that biogenic methane production within the Powder River Basin is derived from acetoclastic reactions (Faiz and Hendry, 2006), and the dominant Archaea was identified as *Methanosarcina*, a methanogen capable of acetate, $CO_2/H_2$, and methyl/methanol utilization (Green et al., 2008). Therefore, it is reasonable to predict that methane production should occur within anaerobic incubations of Powder River Basin samples amended with acetate. Some samples (12, 14, 16, and 17) produced methane from acetate amendments, though these did not reach the predicted value of methane. Despite the lack of methane production, a correlation was observed between the rates of methanogenesis from acetate-amended incubations and the diversity and quantity of *mcr* genes observed in the four samples (Table 3). Presumably acetate is a relatively common methanogenic intermediate in the Powder River Basin even though methane production was minimal and lag times were in excess of a year.

Compared to the methane production using the Illinois and Powder River Basin inocula, methanogenesis from $C_1$-$C_5$ VFA metabolism was substantially higher in comparable Cook Inlet incubations. That is, methane was produced when formate, acetate, butyrate, or valerate were used as an amendment, though sometimes the mineralization of these substrates was incomplete (Figure 3B). The differences between the Cook Inlet gas field and the Illinois or Powder River coalfield is particularly apparent when assessing the polar organic compound profiles. The abundance of putative metabolites in production waters from the Cook Inlet (Figure 1) suggests that the metabolic fate of the softer lignitic coal within this formation was substantially

different than the subbituminous to high volatile bituminous coals found within the Powder River or Illinois Basins. Harris et al. (2008) previously reported that coals collected from Fort Yukon, Alaska contained higher concentrations of organic-extractable carbon (maltene fraction) than the coals from the Powder River Basin. Therefore, it is likely that the lignite coal from the Cook Inlet provides a higher concentration of labile carbon for bacteria to metabolize, thus producing more total polar organic molecules within production waters. The presence of butanoic and pentanoic acids (Figure 2; samples 6, 8-10) in the Cook Inlet gas field corresponded with the ability of the inocula to metabolize butyrate and valerate amendments (Figure 3B). A strong correlation was also observed between the number of unique *mcr* genes *in situ* and rates of methanogensis when amended with butyrate and valerate *in vitro* (Table 3). The Cook Inlet gas field has previously been reported to have a high diversity of universal and obligate acetoclastic, methylotrophic, and hydrogenotrophic methanogens (Strąpoć et al. 2011). Thus, the strong correlations between rates of methanogenesis in butyrate- and valerate- amended incubations and the diversity of *mcr* genes suggests that the metabolic coupling between the syntrophic bacteria and methanogens is an important process potentially limiting anaerobic bioconversions in coal seams. However, the GeoChip assay does not contain functional genes that differentially target syntrophic bacteria, and we were unable to correlate the relationship between the quantity of syntrophs and rates of methanogenesis. Regardless, the only possible fate for butyrate and valerate was the syntrophic bioconversion of these VFAs to the stoichiometrically predicted values of methane.

Collectively, these results suggest that the soft lignite coal in the Cook Inlet is easier to degrade than the sub-bituminous and bituminous coals of the Illinois and Powder River Basins. The degradation of the lignite coal in turn leads to the formation of more polar organic compounds (i.e. butanoic, pentanoic acids) within production waters that are then syntrophically converted to methane. Thus, the major ecological difference between the Cook Inlet and the Illinois and Powder River Basins is the recalicitrant nature of the coal itself. Therefore, we propose that the inherent biodegradability of coal and the subsequent production of polar organic substrates that require syntrophic microbial metabolism is ultimately what governs the bioconversion of coal to methane. Of course, we do acknowledge that our analysis of a limited number of samples may not reflect the ecological conditions inherent throughout the entirety of the coalfields. Such coalfields are major deposits of organic carbon and it is certainly conceivable that other ecological factors could positively or negatively impact the ultimate bioconversion of coal to methane at individual locations. Nevertheless, the general trends that we observe would indicate that modern CBM production is slow at best and primarily limited by the chemistry of the coal itself.

**Acknowledgements**

This work was funded by ConocoPhillips Corporation, Houston TX. We would like to thank Darius Strąpoć and Courtney Turich for collecting the water samples used in this study.

## References


Aktas DF, Lee JS, Little BJ, Ray RI, Davidova IA, Lyles CN, & Suflita JM (2010) Anaerobic metabolism of biodiesel and its impact on metal corrosion. *Energ Fuel* **24** (12): 2924–2928.

Alaska Oil and Gas Conservation Commission (AOGCC) (2011) Beluga River unit, Beluga River undefined gas pool. http://doa.alaska.gov/ogc/annual/current/17_Gas_Pools/Beluga%20River%20-%20Gas/1_Gas_1.htm. Accessed: April 22, 2013.

Bates BL, McIntosh JC, Lohse KA, & Brooks PD (2011) Influence of groundwater flowpaths, residence times, and nutrients on the extent of microbial methanogenesis in coal beds: Powder River Basin, USA. *Chem Geol* **284** (1-2): 45–61.

Beckmann S, Krüger M, Engelen B, Gorbushina AA, & Cypionka AA (2011) Role of bacteria , archaea and fungi involved in methane release in abandoned coal mines. *Geomicrobiol J* **28** (4): 347–358.

Berry DF, Francis AJ, & Bollag J-M (1987) Microbial metabolism of homocyclic and heterocyclic aromatic compounds under anaerobic conditions. *Microbiol Rev* **51** (1): 43–59.

Buswell AM & Mueller HF (1952) Mechanism of methane fermentation. *J Ind Eng Chem* **44** (3): 550–552.

Button DK & Robertson BR (2001) Determination of DNA content of aquatic bacteria by flow cytometry. *Appl Environ Microbiol* **67** (4): 1636–1645.

Calderwood KW & Fackler WC (1972) Proposed stratigraphic nomenclature for Kenai Group, Cook Inlet Basin, Alaska. *AAPG Bull* **56** (4): 730–754.

Duncan KE, Gieg LM, Parisi VA, Tanner RS, Tringe SG, Bristow J, & Suflita JM (2009) Biocorrosive thermophilic microbial communities in Alaskan North Slope oil facilities. *Environ Sci Technol* **43** (20): 7977-7984.

Faiz M & Hendry P (2006) Significance of microbial activity in Australian coal bed methane reservoirs -- a review. *B Can Petrol Geol* **54** (3): 261–272.

Formolo MJ, Martini AM, & Petsch, ST (2008) Biodegration of sedimentary organic matter associated with coalbed methane in the Powder River and San Juan Basins, U.S.A. *Int J Coal Geol* **76** (1-2): 86–97.

Fry JC, Horsfield B, Sykes R, Cragg BA, Heywood C, et al. (2009) Prokaryotic populations and activities in an interbedded coal deposit, including a previously

deeply buried section (1.6–2.3 Km) above ~ 150 Ma basement rock. *Geomicrobiol J* **26** (3): 163–178.

Glombitza C, Mangelsdorf K, & Horsfield B (2009) A novel procedure to detect low molecular weight compounds released by alkaline ester cleavage from low maturity coals to assess its feedstock potential for deep microbial life. *Org Geochem* **40** (2): 175–183.

Green MS, Flanegan KC, & Gilcrease PC (2008) Characterization of a methanogenic consortium enriched from a coalbed methane well in the Powder River Basin, U.S.A. *Int J Coal Geol* **76** (1-2): 34–45.

Harris SH, Smith RL, & Barker CE (2008) Microbial and chemical factors influencing methane production in laboratory incubations of low-rank subsurface coals. *Int J Coal Geol* **76** (1-2): 46–51.

Hartz JD, Kremer MC, Krouskop DL, Silliphant LJ, Houle JA, Anderson PC, & LePain DL (2009) Preliminary engineering and geological evaluation of remaining Cook Inlet gas reserves (Decker PL, ed) pp 1-37. *Alaska Division of Oil and Gas Report* http://dog.dnr.alaska.gov/ResourceEvaluation/Documents/Preliminary_Engineering_and_Geological_Evaluation_of_Remaining_Cook_Inlet_Gas_Reserves.pdf. Accessed: April 22, 2013.

He Z, Deng Y, Van Nostrand JD, et al. (2010) GeoChip 3.0 as a high-throughput tool for analyzing microbial community composition, structure and functional activity. *ISME J* **4** (9): 1167–1179.

Jones EJP, Voytek MA, & Warwick PD (2008) Bioassay for estimating the biogenic methane-generating potential of coal samples. *Int J Coal Geol* **76** (1-2): 138–150.

Jones EJP, Voytek MA, Corum MD, & Orem WH (2010) Stimulation of methane generation from nonproductive coal by addition of nutrients or a microbial consortium. *Appl Environ Microb* **76** (21): 7013–7022.

Kimura H, Nashimoto H, Shimizu M, Hattori S, Yamada K, Koba K, Yoshida N, & Kato K (2010) Microbial methane production in deep aquifer associated with the accretionary prism in Japan. *ISME J* **4** (4): 531–541.

Klein DA, Flores RM, Venot C, Gabbert D, Schmidt R, Stricker GD, Pruden A, & Mandernack K. (2008) Molecular sequences derived from Paleocene Fort Union Formation coals vs. associated produced waters: Implications for CBM regeneration. *Int J Coal Geol* **76** (1): 3-13.

Kotarba MJ (2001) Composition and origin of coalbed gases in the upper Silesian and Lublin Basins, Poland. *Org Geochem* **32** (1): 163–180.

Krüger M, Beckmann S, Engelen B, et al. (2008) Microbial methane formation from hard coal and timber in an abandoned coal mine. *Geomicrobiol J*, **25** (6), pp.315–321.

Kubitschek HE & Freedman ML (1971) Chromosome replication and the division cycle of Escherichia coli B/r. *J bacteriol* **107** (1): 95–99.

Leschine SB (1995) Cellulose degradation in anaerobic environments. *Annu Rev Microbiol* **49**: 399–426.

Lu Z, Deng Y, Van Nostrand JD, et al. (2011) Microbial gene functions enriched in the Deepwater Horizon deep-sea oil plume. *ISME J* **6** (2): 451-460.

McInerney M, Bryant M, & Pfennig N (1979) Anaerobic bacterium that degrades fatty acids in syntrophic association with methanogens. *Arch Microbiol* **122** (2): 129–135.

McInerney MJ, Struchtemeyer CG, Sieber J, Mouttaki H, Stams AJM, Schink B, Rohlin L, & Gunsalus RP (2008) Physiology, ecology, phylogney, and genomics of microorganisms capable of syntrophic metabolism. *Ann NY Acad Sci* **1125**: 58–72.

Midgley DJ, Hendry P, Pinetown KL, Fuentes D, Gong S, Mitchell DL, & Faiz M (2010) Characterisation of a microbial community associated with a deep, coal seam methane reservoir in the Gippsland Basin, Australia. *Int J Coal Geol* **82** (3-4): 232–239.

Moore TA (2012) Coalbed methane: a review. *Int J Coal Geol* **101:** 36-81.

Penner TJ, Foght JM, & Budwill K (2010) Microbial diversity of western Canadian subsurface coal beds and methanogenic coal enrichment cultures. *Int J Coal Geol* **82** (1-2): 81–93.

Papendick SL, Downs KR, & Vo KD (2011) Biogenic methane potential for Surat Basin, Queensland coal seams. *Int J Coal Geol* **88** (2): 123-134.

Pratt T, Mavor M, & DeBruyn R (1999) Coal gas resource and production potential of subbituminous coal in the Powder River Basin. In *SPE Rocky Mountain Regional Meeting* Gillette, Wyoming.

Strąpoć D, Ashby M, Wood L, Levinson R, & Huizinga B (2011) Significant contribution of methyl/methanol-utilising methanogenic pathway in a subsurface biogas environment. *Applied Microbiology and Molecular Biology in Oilfield Systems* (Whitby C & Skovhus TL, eds), pp. 211–216. Dordrecht: Springer Netherlands.

Strąpoć D, Mastalerz M, Dawson K, Macalady J, Callaghan AV, Wawrik B, Turich C, & Ashby M (2011) Biogeochemistry of microbial coal-bed methane. *Annu Rev Earth Pl Sc* **39** (1): 617–656.

Strąpoć D, Mastalerz M, Eble C, & Schimmelmann A (2007) Characterization of the origin of coalbed gases in southeastern Illinois Basin by compound-specific carbon and hydrogen stable isotope ratios. *Org Geochem* **38** (2): 267–287.

Strąpoć D, Picardal FW, Turich C, et al. (2008) Methane-producing microbial community in a coal bed of the Illinois Basin. *Appl Microbiol* **74** (8): 2424–2432.

Suárez-ruiz (2012) Organic petrology: an overview. *Petrology - New Perspectives and Applications* (Ismail Al-Juboury A, ed). Intech. Available from: http://www.intechopen.com/books/petrology-new-perspectives-and-applications/organic-petrology-an-overview.

Tanner RS (2002) Cultivation of bacteria and fungi. *Manual of Environmental Microbiology*, 2nd ed (Crawford RL, Knudsen GR, McInerney MJ, and & Stetzenback LD, eds), pp 62–70. ASM Press, Washington, DC.

Thauer RK, Jungermann K, & Decker K (1977) Energy conservation in chemotrophic anaerobic bacteria. *Microbiol Mol Biol R* **41** (1): 100-180.

Thielemann T (2004) Coalbed methane in the Ruhr Basin, Germany: a renewable energy resource? *Org Geochem* **35** (11-12): 1537–1549.

Ulrich G & Bower S (2008) Active methanogenesis and acetate utilization in Powder River Basin coals, United States. *Int J Coal Geol* **76** (1-2): 25–33.

Ünal B, et al. (2012) Trace elements affect methanogenic activity and diversity in enrichments from subsurface coal bed produced water. *Front Microbiol* doi: 10.3389/fmicb.2012.00175

Vieth A, Mangelsdorf K, Sykes R, and Horsfield B (2008) Water extraction of coals – potential for estimating low molecular weight organic acids as carbon feedstock for the deep terrestrial biosphere. *Org Geochem* **39** (8): 985–991.

Waldron PJ, Petsch ST, Martini AM, & Klaus N (2007) Salinity constraints on subsurface archaeal diversity and methanogenesis in sedimentary rock rich in organic matter. *Appl Environ Microbiol* **73** (13): 4171–4179.

Walters BA (2002) Coalbed gas systems, resources, and production and a review of contrasting cases from the San Juan and Powder River Basin." *AAPG Bull* **86** (11): 1853–1890.

Wawrik B, Mendivelso M, Parisi VA, et al. (2011) Field and laboratory studies on the bioconversion of coal to methane in the San Juan Basin. *FEMS Microbiol Ecol* **81** (1): 26–42.

Widdel F & Rabus R (2001) Anaerobic biodegradation of saturated and aromatic hydrocarbons. *Curr Opin Biotech* **12** (3): 259–76.

Widdel F & Bak F (1992) Gram-negative mesophilic sulfate-reducing bacteria. *The Prokaryotes,* 2nd ed (Balows A, Truper HG, Dworkin M, Harder W, & Schleifer KH, eds) pp 3352–3378. Springer-Verlag, New York, NY.

Wu L, Liu X, Schadt CW, & Zhou J (2006) Microarray-based analysis of subnanogram quantities of microbial community DNAs by using whole-community genome amplification. *Appl Environ Microb* **72** (7): 4931–4941.

Zellner G, Stackebrandt E, Messner P, Tindall BJ, Conway De Maeario E, Kneifel H, Sleytr UB, & Winter J (1989) Methanocorpusculaceae Fam. Nov., represented by Methanocorpusculum Parvum, Methanocorpusculum Sinense Spec. Nov. and Methanocorpusculum Bavaricum Spec. Nov. *Arch Microbiol* **151**: 381–390.

**Table 1:** Chloride, nitrate, and sulfate concentrations from 17 sample sites throughout three coalfield basins. BDL= below detectable limit

| Sample Sites | Chloride (mM) | Nitrate (mM) | Sulfate (mM) |
|---|---|---|---|
| **Illinois Basin** | | | |
| 1 | 93.3 | BDL | 0.038 |
| 2 | 58.7 | 0.058 | 0.075 |
| 3 | 48.7 | 0.050 | 0.143 |
| 4 | 2.92 | BDL | 0.090 |
| 5 | 1.20 | BDL | 0.625 |
| **Cook Inlet gas field** | | | |
| 6 | 3.23 | BDL | 0.066 |
| 7 | 4.23 | 0.018 | 0.072 |
| 8 | 9.42 | BDL | 0.037 |
| 9 | 35.4 | BDL | 0.063 |
| 10 | 0.58 | BDL | 0.035 |
| 11 | 0.59 | BDL | 0.034 |
| **Powder River Basin** | | | |
| 12 | 0.56 | 0.141 | 0.111 |
| 14 | 0.80 | BDL | 0.167 |
| 13 | 1.10 | BDL | 0.062 |
| 15 | 1.21 | BDL | 0.059 |
| 16 | 0.93 | 0.196 | 0.088 |
| 17 | 0.47 | 0.152 | 0.061 |

**Table 2:** Biomass estimates calculated from DNA stock solutions for sample sites in the Illinois and Powder River Basins as well as the Cook Inlet gas field.

| Sample Sites | Kubitschek and Freedman* (Cells/ml) | Button and Robertson+ (Cells/ml) |
|---|---|---|
| | **Illinois Basin** | |
| **1** | 5.51E+06 | 9.26E+06 |
| **2** | 6.72E+05 | 1.13E+06 |
| **3** | 7.24E+05 | 1.22E+06 |
| **4** | 1.49E+05 | 2.50E+05 |
| **5** | 4.47E+05 | 7.50E+05 |
| | **Cook Inlet gas field** | |
| **6** | 6.98E+05 | 1.17E+06 |
| **8** | 7.67E+05 | 1.29E+06 |
| **9** | 1.71E+06 | 2.87E+06 |
| **10** | 9.29E+05 | 1.56E+06 |
| **11** | 8.66E+05 | 1.46E+06 |
| | **Powder River Basin** | |
| **12** | 5.11E+05 | 8.59E+05 |
| **13** | 8.38E+06 | 1.41E+07 |
| **14** | 1.40E+06 | 2.36E+06 |
| **15** | 3.22E+06 | 5.41E+06 |
| **16** | 2.41E+05 | 4.04E+05 |
| **17** | 3.94E+05 | 6.62E+05 |

* 4.2 fg DNA/genome, we assumed 1 genome per cell
+ 2.5 fg DNA/cell

**Table 3:** Correlation coefficients (*r*) between rates of methanogenesis from $C_1$-$C_5$ amended incubations and the diversity and quantity of *mcr* genes observed within the Illinois Basin, Cook Inlet gas field, and Powder River Basin samples. Values indicated by bold type suggest strong correlations.

| Correlation Coefficient (*r*) Values | | | |
|---|---|---|---|
| **Fatty Acid Substrate** | **Illinois Basin** | **Cook Inlet gas field** | **Powder River Basin** |
| **Number of unique *mcr* genes** | | | |
| **Formate** | -0.21 | 0.35 | 0.09 |
| **Acetate** | -0.43 | 0.57 | **0.87** |
| **Propionate** | -0.56 | 0.25 | 0.23 |
| **Butyrate** | -0.57 | **0.98** | -0.29 |
| **Valerate** | -0.60 | **0.84** | 0.32 |
| **Quantity of *mcr* genes** | | | |
| **Formate** | -0.59 | -0.05 | 0.12 |
| **Acetate** | -0.51 | -0.39 | **0.78** |
| **Propionate** | -0.59 | -0.17 | 0.27 |
| **Butyrate** | -0.56 | -0.43 | -0.18 |
| **Valerate** | -0.59 | -0.23 | 0.33 |

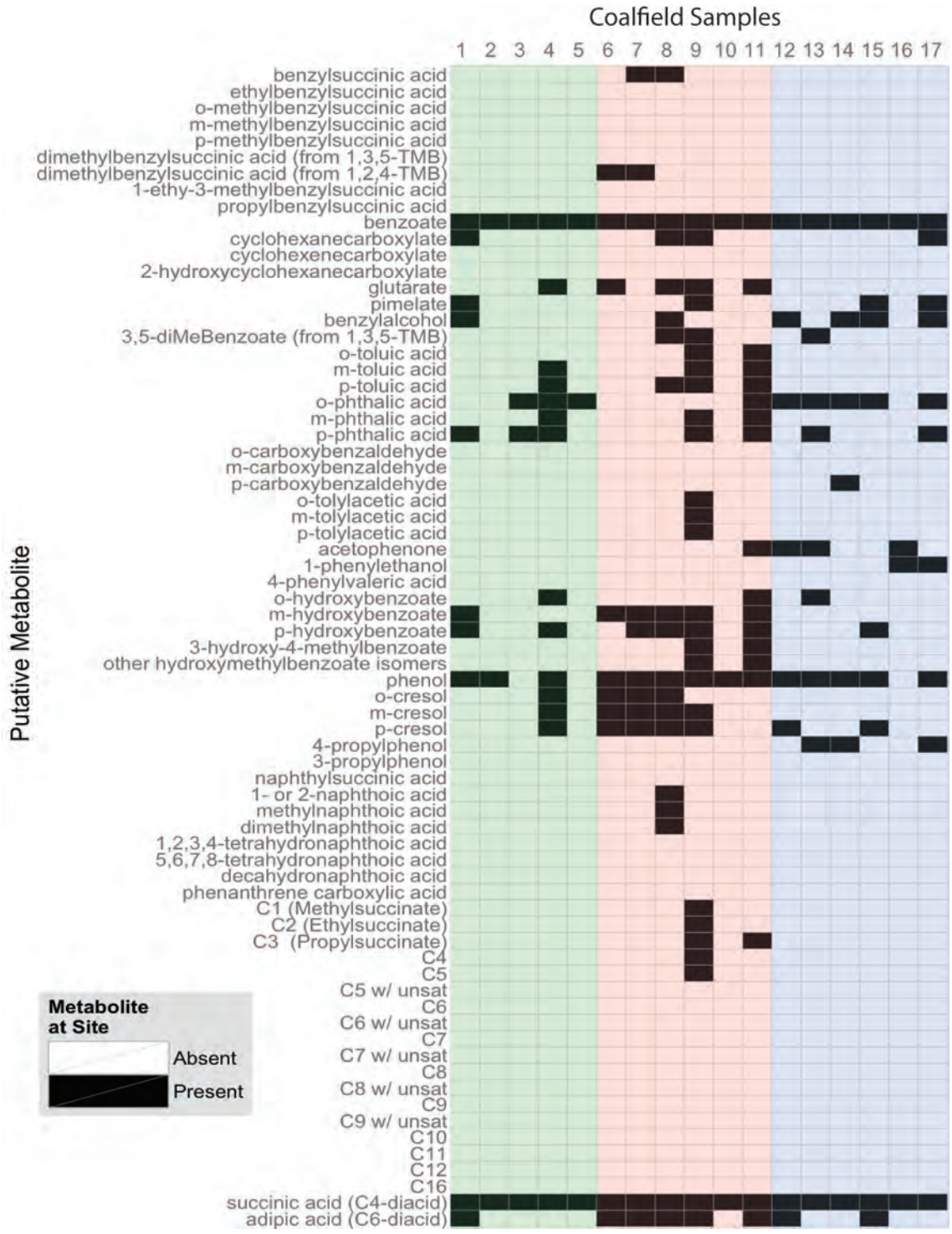


**Figure 1:** Analysis of 71 polar organic compounds from the 17 sample sites within the Illinois Basin (Green), Cook Inlet gas field (Red), and Powder River Basin (Blue).

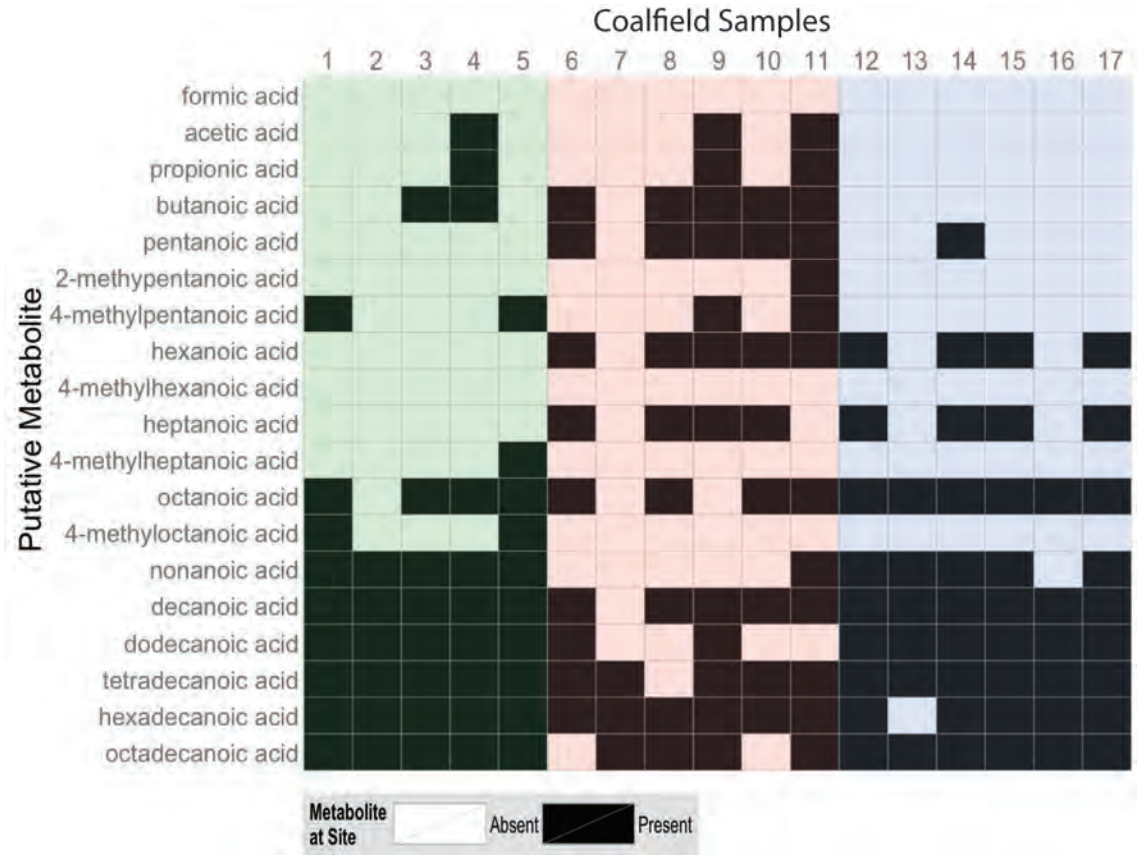


**Figure 2**: Alkanoic acids identified within the 17 sample sites from the Illinois Basin (Green), Cook Inlet gas field (Red), and Powder River Basin (Blue).

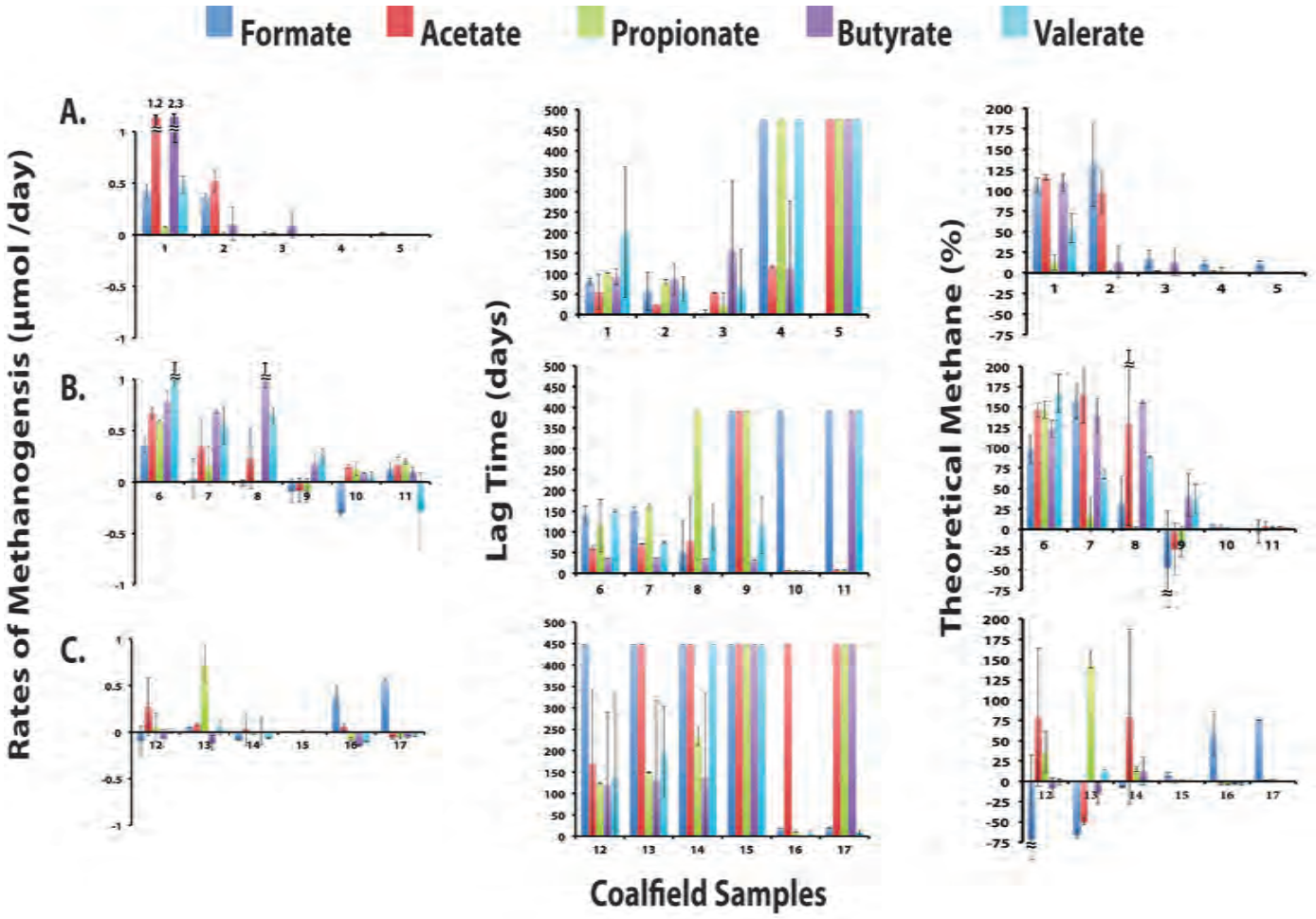


**Figure 3:** Rates of methanogenesis, lag time, and the percent of theoretical methane produced in incubations of the A) Illinois Basin, B) Cook Inlet gas field, and C) Powder River Basin.

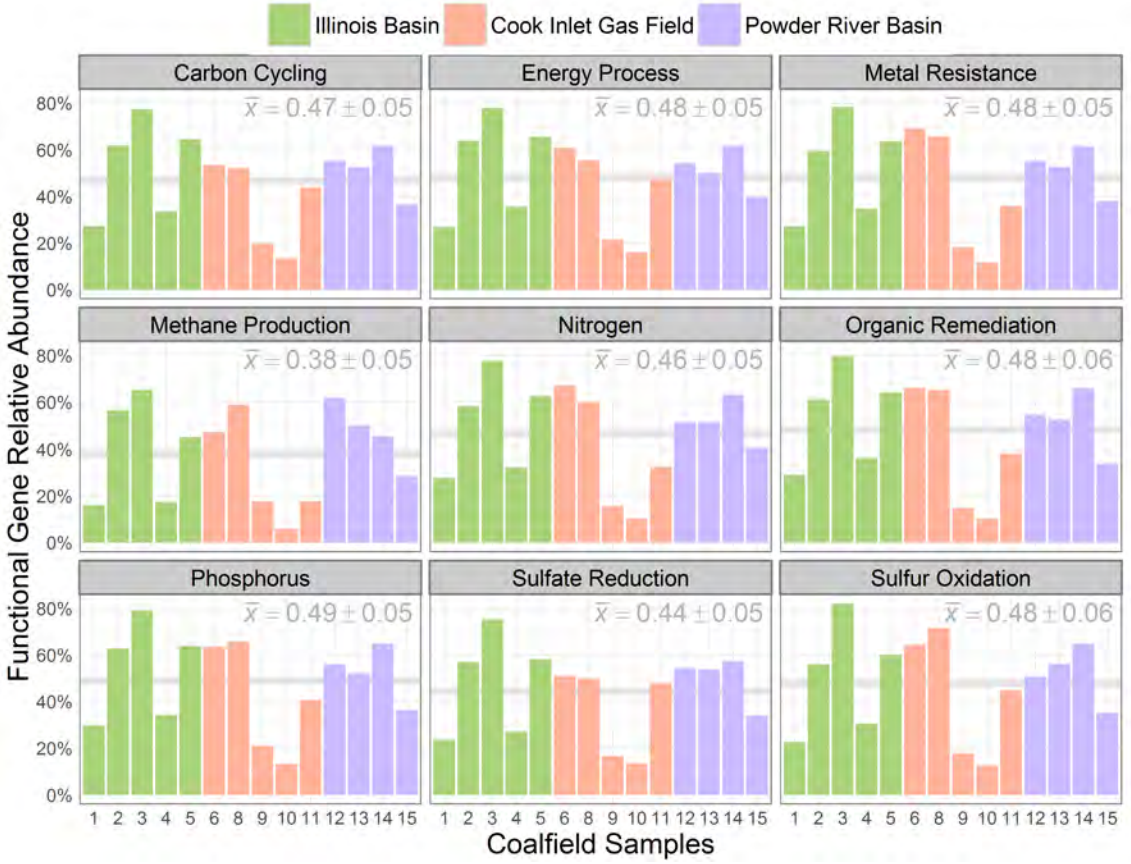


**Figure 4:** Relative abundance of functional genes associated with nine gene categories observed in coalfield production waters. The grey line represents the mean percentage ($\overline{X}$) of the relative abundance of each gene category (standard error *n*= 14 samples).

# Chapter 2: Impact of organosulfur content on diesel fuel stability and implications for carbon steel corrosion


## Abstract

Ultra-low sulfur diesel (ULSD) fuel has been integrated into the worldwide fuel infrastructure to help meet a variety of environmental regulations. However, desulfurization alters the properties of diesel fuel in ways that could potentially impact its biological stability. Fuel desulfurization might predispose ULSD to biodeterioration relative to sulfur-rich fuels, and in marine systems accelerate rates of sulfate reduction, sulfide production, and carbon steel biocorrosion. To test such prospects, an inoculum from a seawater-compensated ballast tank was amended with fuel from the same ship or with refinery fractions of ULSD, low- (LSD), and high sulfur diesel (HSD) and monitored for sulfate depletion. The rates of sulfate removal in incubations amended with the refinery fuels were elevated relative to the fuel-unamended controls, but statistically indistinguishable (~50 μM $SO_4$/day), but was found to be roughly twice as fast (~100 μM $SO_4$/day) when the ship's own diesel was used as a source of carbon and energy. Thus, anaerobic hydrocarbon metabolism likely occurred in these incubations regardless of fuel sulfur content. Microbial community structure from each incubation was also largely independent of the fuel amendment type, based on molecular analysis of 16S rRNA gene sequences. Two other inocula known to catalyze anaerobic hydrocarbon metabolism showed no differences in fuel-associated sulfate reduction or methanogenesis rates between ULSD, LSD, and HSD. These findings suggest that the stability of diesel is independent of the fuel organosulfur compound status and reasons

for the accelerated biocorrosion associated with the use of ULSD should be sought elsewhere.

## Introduction

The United States, European Union, and Japan have imposed regulations mandating that diesel fuels must contain ≤15 ppm sulfur.[1–8] Advances in desulfurization procedures and catalyst technology have allowed refineries to essentially achieve sulfur-free diesel fuel,[9–14] resulting in the decline of both particulate and chemical emissions to the atmosphere. Lim et al.[15] tested tailpipe exhaust from 12 diesel engines operated at various conditions using either ultra-low sulfur diesel (ULSD) or low-sulfur diesel (LSD). The results indicated that ULSD combustion produced lower levels of carbon dioxide, sulfur and nitrogen oxides, polycyclic aromatic hydrocarbons, and other emissions. Additionally, sulfur-rich diesel fuels are known to have a direct impact on engine wear due to the production of sulfuric acid from fuel and exhaust gas condensate.[16] Thus, the removal of sulfur compounds from diesel fuel may also decrease corrosive wear on engine parts.

The process of desulfurization results in several changes to the physical properties of diesel fuel,[17] most notably a reduction in fuel lubricity. Additives are regularly used to improve fuel performance characteristics. The blending of ULSD with biodiesel to improve lubricity is common.[18,19] However, biodiesel can be readily metabolized by sulfidogenic anaerobic microorganisms resulting in increased corrosion of low-alloy steel.[20] In a study by Lee et al.[21] incubations containing ULSD, distilled water, and carbon steel coupons had higher electrochemical corrosion rates than biodiesel or ULSD-biodiesel blended fuels, but biodiesel had the highest propensity for

biofouling. The full impact of fuel desulfurization and the prospective use of additives on the microbial metabolism of ULSD are not fully understood.

The removal of organosulfur compounds might differentially impact the biodeterioration of diesel fuel through multiple mechanisms. Organosulfur compounds are known anti-microbial agents[22] and have been detected in over 200 structurally diverse forms in diesel fuels and other petroleum products including thiols, thiophenes, and sulfide derivatives.[23] Their concentration can range from 0.05% to 14% by weight in crude oils and natural bitumens.[24] Thus, the removal of potentially inhibitory organosulfur compounds could alleviate the negative impact of these substances on the microbes responsible for diesel fuel biodegradation. Further, to achieve ≤15 ppm/w sulfur, diesel fuel is reacted with hydrogen under elevated temperature and pressure conditions in the presence of a catalyst.[14] The intense nature of this process leads to the destruction of some hydrocarbon components and the production of residual lower-molecular weight byproducts.[25] Such byproducts might represent preferred substrates that allow for the proliferation of problematic microbes relative to the fuel hydrocarbons.

Fuels were taken from a refinery at various stages in the desulfurization process to explore the connection between organosulfur content and the susceptibility of fuels to anaerobic biodegradation, and by inference, their propensity to exacerbate biocorrosion in marine systems. We focused our efforts on a seawater-compensated ballast tank inoculum from a United States naval vessel. We then compared the findings with the same fuels incubated in sediments from a gas condensate-contaminated aquifer known

to harbor anaerobes capable of hydrocarbon metabolism[26] and an oil-degrading methanogenic consortium capable of metabolizing a broad range of hydrocarbons.[27]

Our findings suggest that the organosulfur status of diesel fuels does not significantly influence anaerobic hydrocarbon biodegradation with any of the tested inocula. Moreover, the enrichment of microbial communities, while different for various inocula, was independent of the fuel type used in the incubations.

## Experimental Section

**Ballast Tank Sampling.** Military ships often use seawater-compensated fuel ballast tanks. As the ship engines use fuel, seawater is pumped aboard to compensate for weight and volume losses. In this system, there is direct contact between seawater and fuel, increasing the opportunity for developing anaerobic conditions and biocorrosion. A seawater-diesel fuel sample was collected from a ballast tank aboard a US Navy ship and used for experimental purposes. Seawater was jettisoned out of a port on the side of the ship and collected in a clean container. The water sample was then transferred into multiple 1L Schott bottles, reduced with 10 ml of a 2.5% $Na_2S$ as a reductant, and sealed to provide anaerobic conditions. The samples were packed with ice and shipped overnight to the laboratory. Once received, the bottles were placed in an anaerobic chamber for 24 hrs before use. Prior to the initiation of experiments, biomass from 1 L of the ballast tank water was filtered through a cellulose nitrate membrane filter (0.2 μm, 47mm; Whatman, Piscataway, NJ) and stored at -80°C for later DNA extraction.

**Fuel Characterization and Metabolite Analysis.** Since diesel fuels are often amended with a variety of additives that can complicate experimental interpretations, ULSD, LSD, and HSD were obtained directly from a cooperating refinery. The ballast tank

inoculum was used to compare the anaerobic biodegradation of the additive-free refinery fuel fractions. The same assessment was also used to compare the shipboard diesel fuel and a soy-based biodiesel obtained from a different refinery.

Fuels were diluted (10:1) in ethyl acetate for gas chromatographic analyses and injected (50:1 split) into an Agilent 6890 instrument equipped with an Agilent 5973 mass spectrometer. Components were separated using a HP-5 ms capillary column (30m X 0.25 mm inner diameter X 0.25 μm film, J&W Scientific, Folsom, CA). The initial oven temperature was 45°C, held for 5 min, followed by a linear increase at 4°C/min to 270 °C and held again for 10 min. The carrier gas was helium and flowed at a rate of 1 ml/min. The sulfur content of each fuel type (except biodiesel) was determined by an external laboratory (Phillips 66 Bartlesville, OK, USA), using the standard test method ASTM D2622.[28] The production of putative microbial metabolites in the incubations was also assayed as described in Aktas et al.[20]

**Ballast Water-Diesel Fuel Incubations.** A mineral medium[29] (40 ml) amended with 20 mM of $Na_2SO_4$ was added to sterile serum bottles, inoculated with 10 ml of ballast tank water, and crimp sealed with butyl rubber septa. The headspace was adjusted to $N_2$:$CO_2$ (80%: 20%) and triplicate incubations were amended aseptically with 1g of a particular diesel fuel by sterile syringe. All serum bottles were incubated in the dark at room temperature (21 ± 2°C). Diesel fuel biodegradation was evidenced by the loss of sulfate relative to the fuel-unamended controls.

Sulfate depletion was analyzed by ion chromatography (Dionex model IC-3000, Sunnyvale, CA) using an IonPac™ AS4A column, ASRS 300 4mm self-regenerating suppressor, and a conductivity detector. The eluent was a sodium carbonate/sodium

bicarbonate buffer diluted 1:100 from an AS4A ready-to-dilute concentrate (Dionex, Sunnyvale, CA). The system was operated isocratically at 2.0 ml/min and the electrochemical suppressor was set at 54 mA.

**Diesel Fuel Incubations with Other Anaerobic Inocula.** To further examine the stability of the diesels to anaerobic biodegradation, the same fuels were tested with other inocula known to catalyze hydrocarbons. We used sediments from a gas-condensate contaminated aquifer (Ft. Lupton, Colorado) previously documented to harbor anaerobes capable of hydrocarbon metabolism under both sulfate-reducing and methanogenic conditions.[26] We also used a methanogenic oil-degrading enrichment that was capable of metabolizing a broad range of hydrocarbons.[27] Incubations were identical to the ballast water incubations except these inocula required a freshwater medium.[27] The aquifer sediment incubations were amended with 10 mM $Na_2SO_4$, and sulfate depletion was monitored using the previously described ion chromatography system. The methanogenic oil-degrading enrichment was grown in the same freshwater media[27] as the aquifer sediment, but contained no sulfate. Methane production was monitored by gas chromatography previously described in Gieg et al.[27]

**Molecular Analysis of the Ballast Tank Inoculum**

**Alkylsuccinate Synthase Gene Survey.** Seawater was collected from the ballast tanks as described above and assayed for the presence of *ass*A, which encodes the catalytic subunit of the glycyl radical enzyme alkylsuccinate synthase (ASS; also known as MAS). ASS/MAS has been implicated in the anaerobic activation of n-alkanes via addition to fumarate.[30,31] For this analysis, DNA was extracted using a method adapted from Rainey et al.[32] Fifty μL PCR reactions contained PCR SuperMix (Invitrogen,

Carlsbad, CA), 5 to 50 ng of DNA template, 1 μM of 1432F and *ass*/*bss* R primers (Table S1),[33] and 5 units of GoTaq (Promega, Madison, WI). Thermal cycling conditions were as follows: 95°C for 3 minutes followed by 40 cycles of 95°C for 45 seconds, 55°C for one minute, 72°C for two minutes, and a final extension step at 72°C for 10 minutes. PCR products were gel-purified (Qiagen, Valencia, CA) and cloned into *E.coli* using either the pCRII or pCR4-TOPO vectors (Invitrogen, Carlsbad, CA). Colonies were picked into individual wells of a 96-well microtiter plate containing tryptone-yeast extract broth with ampicillin and kanamycin and grown overnight. Inserts of the correct size were sequenced using either M13 primers or the 1432F primer. Sequences were assembled into operational taxonomic units (OTUs) of ≥97% sequence identity using Lasergene 8.0 (DNASTAR Inc., Madison, WI), and aligned using the ClustalW algorithm within Megalign (DNASTAR Inc., Madison, WI). A phylogenetic tree was constructed in MEGA4 using the Tajima-Nei distance method[34] with pairwise deletion and performing 5,000 bootstrap replicates. Representative sequences for each OTU was deposited into the NCBI GenBank archive with following accession numbers: KC503834-KC503837

**Characterization of Microbial Communities.** Triplicate water samples from the various diesel fuel incubations were stored in 1.5 μl tubes. The tubes were centrifuged at 14,000g for 15 mins. The supernatants were discarded and the pellets resuspended in 1 X phosphate buffered saline (Ambion® 10x concentrate) The pellets were then concentrated into 1 tube and washed 3 times with 500 μl of the phosphate buffered saline. DNA was extracted using a PowerSoil® Kit (MO BIO Laboratories, Inc, Carlsbad, CA) and a mini-beading instrument (Biospec product, Bartlesville, OK)

operated at 25 rpm for one minute. High quality DNA bands were observed by agarose gel electrophoresis.

Amplification of the 16S rRNA gene was achieved by using eubacterial primers M13F-27F and M13R-338R (Table S1). Reactions contained ~ 10-50 ng of DNA, 20 μM of each primer, and PCR SuperMix (Invitrogen, Carlsbad, CA). Thermal cycling conditions were as follows: 95°C for 3 minutes, followed by 35 cycles of 95°C for 30 seconds, 53°C for 45 seconds, and 72°C for 1 minute. Successful amplification was confirmed by agarose gel electrophoresis and amplified products were purified using a QIAquick PCR purification column (Qiagen, Valencia, CA) to remove primer dimer and unused nucleotide. Five microliters of purified PCR product were then 'tagged' by re-amplification, using PCR primers for multiplex pyrosequencing (Table S1) as described by Hamady et al.[35] The thermal cycling conditions were as follows: 95°C for 2 minutes followed by 6 cycles of 95°C for 30 seconds, 52°C for 30 seconds, and 72°C for 40 seconds. Each diesel fuel treatment received a different tagged forward primer (Table S2) containing a specific 'barcode' sequence. Tagging was confirmed by comparing the sizes of tagged and un-tagged PCR products by agarose gel electrophoresis. PCR products were mixed and sequenced via parallel 454-sequencing at the Advanced Center for Genome Technology at the University of Oklahoma.[36] Diesel fuel treatments were sorted according to their tags using computational analysis. Bacterial 16S rRNA gene library sequences were analyzed using QIIME, an open-source bioinformatics software package for comparison and analysis of microbial communities.[37] The multiplexed reads were assigned to samples based on their nucleotide barcode, trimmed to remove those that contain any errors in the forward

primer or barcode regions, ambiguities, or an average quality score <25. Sequences were denoised,[38] assigned to operational taxonomic units (OTUs), and chimeras were identified and removed.[39] Sequences were aligned using the PyNAST alignment program.[40] Each OTU was assigned a phylogenetically consistent taxonomy based on a naïve Bayesian rRNA classifier available through the Ribosomal Database Project II.[41] Closest relatives of unclassified OTUs were identified with ARB[42] using the Greengenes 16S rRNA database.[43] Additionally, QIIME was used to compare the libraries using analysis of similarity (ANOSIM). Raw sequences were deposited into the NCBI sequence read archive (SRA) accession number: SRX264455

**DGGE Analysis.** Amplification of the 16S rRNA gene used a previously described touchdown PCR protocol[44] and eubacterial primers GM5F and 907R (Table S1).[45] The PCR reaction contained ~10-50 ng DNA, 2.5 pmol of each primer, 10X platinum buffer diluted to 1X concentration, 500 mM Betaine, 2.5mM $MgCl_2$, 0.2 mM deoxyribonucleotide, and 0.04 U of Platinum® Taq DNA polymerase (Invitrogen, Carlsbad, CA), and PCR grade $H_2O$. Gel electrophoresis was used to confirm PCR amplification. The DGGE analysis was done using a D-Code 16/16-cm gel apparatus (Bio-Rad, Hercules, CA) with a 6% (wt/vol) polyacrylamide gel. The gradient was formed of 7% polyacrylamide in 1 X TAE (Tris base, acetic acid, and EDTA, Sigma-Aldrich) buffer between 20 and 80% denaturant (7M urea and 40% formamide defined as 100% denaturant). Electrophoresis was run at 65V for 16 hours at 60°C.

## Results

### Fuel Characterization

The gas chromatographic profile associated with ULSD, LSD, and HSD, as well as the shipboard diesel confirm that these fuels were chemically similar (Figure 1). That is, each of the fuels had a similar range of resolvable hydrocarbons in this analysis. The linear alkanes ranged from $C_9$ –$C_{20}$ in all of the fuels tested, which is typical for many diesels. Diesel fuels also contained branched alkanes ranging from $C_7$-$C_{12}$, and alkylated benzene and naphthalene compounds. The only major difference observed in this analysis was that ULSD had a greater ratio of high molecular ($C_{16}$-$C_{22}$) to low molecular ($C_{10}$-$C_{14}$) alkanes compared to the other fuels. In contrast, the organosulfur analysis revealed that the sulfur content for ULSD, LSD, and HSD varied from 4 to 441 ppm, while the shipboard fuel was in excess of 1,528 ppm (Figure 1).

**Characterization of Initial Ballast Tank Seawater**

Water samples from a seawater compensated ballast tank were investigated for the presence of the *assA* gene as a biomarker for the genetic potential for anaerobic alkane degradation. Four *assA* genotypes were detected (Figure 2). Based on BlastX and BlastN the ballast water *assA* clone sequences are similar to *assA2* in *Desulfatibacillum alkenivorans* AK-01[30] and *assA* clone sequences from the Arthur Kill Waterway[33] and a methanogenic enrichment[46] (Figure 2). The presence of *ass*A in the initial ballast tank seawater is indicative of anaerobic microorganisms capable of anaerobic alkane degradation via the "fumarate addition" pathway.

The microbial community in the ballast tank waters was further investigated by high-throughput pyrosequencing (Figure 3). Replicate microbial assemblages collected when ballast tank water was filtered (Figure 3 lanes 1-3) prior to the incubation revealed a total of 16,097 sequences that were binned into 244 OTUs at a 97% similarity. The

alphaproteobacteria were the dominant bacterial taxa (>60% relative abundance), and were classified as the genera *Pelagibacter* or *Dinoroseobacter*. The epsilonproteobacteria represented ~5-7% of the ballast tank water microbial community, and sequences were classified as the genera *Arcobacter* and *Sulfurimonas*. The deltaproteobacteria contributed <5% of the initial ballast tank water microbial community and were primarily associated with the family *Desulfobacteraceae*. The major deltaproteobacterial genera identified were *Desulfatibacillum*, *Desulfuromusa, Desulfotignum, Desulfobacterium, Pelobacter, Desulfosalina, Desulfobacter*, and *Desulfovibrio* (Figure 4). The unclassified taxa represented in Figure 4 were similar to uncultured bacterial clones associated with marine sediments (unpublished study: Genbank ID FJ716967.1). The gamma-proteobacteria contributed <5% of the initial ballast tank water bacterial community, but harbored sequences representative of the genera *Alteromonas, Haliea, Marinobacter, Colwellia, Pseudoalteromonas, Alcanivorax, Halomonas, Thiomicrospira*, and *Vibrio*. The ballast tank microbial community also contained members of the classes *Clostridia* (<1%)*, Mollicutes* (~5-7%)*, Deferribacteres* (~3%)*, Thermotogae* (<1%)*, and Flavobacteria* (~3%). The unclassified taxa represented in Figure 3 consisted primarily of OTUs similar to the major candidate division FW128[47] and an undefined species similar to *Acholeplasma parvum* str. H23M (AY538170.1).

**Ballast Tank Incubations**

Ballast tank water was incubated under strict anaerobic conditions and either amended with a diesel fuel or biodiesel. After incubation for 310 days, dramatic shifts in the microbial community profile were evident compared to the initial bacterial

community observed in the fuel ballast tank. An analysis of similarity (ANOSIM) indicated that the microbial communities associated with the initial ballast tank water community (Figure 3 lanes 1-3), diesel fuel-amended incubations (ULSD, LSD, HSD, and US Navy fuel; Figure 3 lanes 4-7), the diesel-unamended control (Figure 3 lane 8), and the biodiesel-amended incubations (Figure 3 lane 9) were all significantly different from one another (R=0.94).

The microbial community structures in the diesel fuel incubations were compared by DGGE analysis (Figure 5). The microbial communities enriched by the diesel-fuel amendments were not inherently different from each other as evidenced by the respective DNA banding patterns, but were substantially different from the biodiesel-amended incubation. High throughput sequencing provided higher resolution of the microbial community, and yielded a total of 16,773 16S rRNA gene sequences, which were binned into 111 OTUs at 97% sequence identity. After anaerobic incubation, the alpha- epsilon-, and gammaproteobacterial populations were negligible (<1%), whereas the deltaproteobacteria, unclassified Bacteroidetes, and the unclassified group were enriched and became the dominant bacterial taxa (Figure 3).

The deltaproteobacteria comprised ~20% of the total bacterial community in the diesel fuel-amended incubations (Figure 3). A majority (>70%) of OTUs were related to the family *Desulfobacteraceae*. The relative abundance of the genera within this family changed compared to the start of the incubation (Figure 4). Most notable was the loss of the genus *Desulfatibacillum* within the diesel fuel-amended incubations, although it was at low relative abundance (≤ 1%) within the ULSD enrichments (Figure 4). The primary genera identified from the ULSD, LSD, and HSD incubations were

*Desulfotignum, Desulfobacterium, Pelobacter*, and *Desulfosalina* (Figure 4). The shipboard fuel incubations had a similar population of deltaproteobacteria, except they were enriched (~44%) with the genus *Desulfobacter* (Figure 4 lane 7). The unclassified Bacteroidetes constituted between 16-30% of the microbial community post-incubation (Figure 3) and primarily consisted of OTUs related to uncultured Bacteroidales clones associated with a hydrocarbon-degrading methanogenic culture found in Canadian oil sands (unpublished study: Genbank ID EU522665.1). Additionally, the unclassified taxa consisted almost entirely of OTUs phylogenetically associated with *Thermotogales* str. BHI80-139 (unpublished study: Genbank ID AJ431248.1).

The diesel-unamended control contained a different microbial community from the diesel-amended incubations, but the dominant taxa were still deltaproteobacteria and the unclassified group, consisting of approximately 50% and 30% of the microbial community, respectively (Figure 3). In contrast to the diesel-amended incubations, the deltaproteobacteria in the fuel-free incubations consisted of sequences similar to the family *Desulfovibrionaceae*, primarily the genus *Desulfovibrio* (Figure 4). The unclassified group was phylogenetically similar to *Thermotogales* str. BHI80-139 (unpublished study: Genebank ID AJ431248.1) and an unclassified order (PBS-18) in the phylum Spirochaetes (Figure 3).

When the ballast tank inoculum was amended with a soy-based biodiesel a completely different microbial community was enriched compared to the diesel-amended or diesel-unamended incubations. This assemblage consisted primarily of the taxonomic classes *Clostridia*, unclassified Bacteroidetes, and the unclassified group (Figure 3). The *Clostridia* accounted for ~15% of the microbial community, and

consisted of an unclassified genus within the family XI of the *Clostridiales*. The unclassified Bacteroidetes represented ~30% of the microbial community and were phylogenetically similar to uncultured bacteria clones associated with coastal sediments.[48] The unclassified group mainly consisted of undescribed genera in the family *Dethiosulfovibrionaceae*, however, some OTUs were classified as *Thermotogales* str. BHI80-139 (unpublished study: AJ431248.1). Note that in these biodiesel incubations the deltaproteobacteria made up <2% of the microbial community and were almost completely associated with the genus *Desulfovibrio* (Figure 4).

Anaerobic incubations containing the ballast tank inoculum and amended with ULSD, LSD, and HSD fuel, reduced sulfate at rates of 65 ± 18, 47 ± 8, and 48 ± 10 μM $SO_4$/day, respectively (Figure 6). Additionally, this inoculum reduced sulfate at a rate of 102 ± 10 μM $SO_4$/day when amended with shipboard fuel (Figure 6). No significant sulfate depletion was noted in the diesel-unamended controls. For comparison when the ballast tank inoculum was incubated in the presence of biodiesel, the rate of sulfate reduction was far greater (827 ± 224 μM/day) attesting to the greater lability of biodiesel as a carbon source for the resident microflora.[20]

**Other Anaerobic Inocula**

The reduction of sulfate in the presence of fuel, regardless of its organosulfur status, is consistent with the anaerobic biodegradation of these carbon sources. However, major compositional differences in the fuel hydrocarbon profile were not evident when the hydrocarbon layers were analyzed (not shown). In addition, diagnostic anaerobic metabolites were not detected. Therefore, the relative biodegradability of the same fuels was tested using inocula previously shown to

catalyze anaerobic hydrocarbon decay: An inoculum from a gas-condensate contaminated aquifer[26] and an oil-degrading methanogenic consortium.[27] Sulfate was replete in the aquifer incubations and net (corrected for diesel-unamended controls) sulfate reduction rates of 42 ± 9, 37 ± 11, and 35 ± 9 μM $SO_4$/day were measured when amended with ULSD, LSD, and HSD, respectively. The oil-degrading methanogenic consortium metabolized ULSD, LSD, and HSD and produced methane at rates of 105 ± 37, 84 ± 2, 85 ± 37 μmol $CH_4$/day, respectively. Thus, no significant difference in the rate of biodegradation was observed as a function of organosulfur composition when two other inocula, known to catalyze anaerobic hydrocarbon metabolism, were incubated with the same fuels (Figures S1 and S2).

## Discussion

The global shift toward reducing atmospheric particulate emissions led many governments to reduce the sulfur content of transportation fuels (e.g. see http://www.epa.gov/otaq/fuels/dieselfuels/index.htm). The production of ULSD requires extensive processing of crude oil to reduce the amount of sulfur to a maximum of 15 ppmS. This refining tends to alter the properties of ULSD[17] such that additives are typically required to improve lubricity and corrosion resistance characteristics. Nevertheless, there are many reports of increased corrosion in the fuel infrastructure[49] associated with the introduction and use of ULSD. We hypothesized that these reports might be due to either the removal of organosulfur compounds that would normally inhibit biodegradation and biocorrosion activities or to the acceleration of these activities through the differential microbial metabolism of fuel components formed or added during oil refining. One report suggests that small molecular weight components

can be formed as a consequence of the refining process used to produce ULSD.[21] To address these hypotheses, we compared the susceptibility of additive-free ULSD, LSD, and HSD to anaerobic biodegradation by microorganisms from a seawater-compensated ballast tank. We also tested the influence of a soy-based biodiesel as this is regularly blended with ULSD to improve its lubricity characteristics.[20]

A comparison of the gas chromatographic profiles of ULSD, LSD, HSD, and the US Navy shipboard diesel revealed that the fuels were qualitatively similar in terms of their range and nature of the component hydrocarbons (Figure 1). However, a separate analysis of the organosulfur content of the fuels revealed that they varied widely (4 - >1500 ppmS). Therefore, if the organosulfur content of fuels was a major factor influencing their susceptibility to biodegradation and biocorrosion, it should have been evident in our experiments.

An initial screen of the ballast tank water for the presence of organisms harboring the alkylsuccinate synthase gene (*ass*A) was positive (Figure 2). Thus, the prospect for the anaerobic metabolism of the fuel hydrocarbons was inherent in ballast tanks at the start of the incubation. The endogenous bacterial community of the ballast tank of a U.S. Naval vessel was characterized using high throughput sequencing of 16S rRNA genes. The bacterial community profile at the start of the experiment was determined from the initial filtered ballast tank water samples (Figure 3 Lanes 1-3). The bacterial community profiles among triplicate filters were indistinguishable (ANOSIM $P<0.001$) and primarily consisted of alphaproteobacteria (Figure 3). The genera *Pelagibacter* and *Dinoroseobacter* constituted the majority of the alphaprotoeobacteria. The genus *Pelagibacter* is part of the SAR11 clade, which is

ubiquitous in seawater. This group accounts for approximately 26% of all rRNA genes found within pelagic marine bacterioplankton communities.[50] The genus *Dinoroseobacter* is a group of aerobic anoxygenic phototrophic bacteria isolated from marine dinoflagellates.[51] Sequences related to the epsilon-proteobacteria were found to be similar to the genera *Arcobacter* and *Sulfuricurvales,* both of which are known sulfide-oxidizing bacterial groups.[52,53] Conceivably, these organisms might be involved in the oxidation of sulfide formed during biodegradation and biocorrosion processes. The gammaproteobacteria sequences noted in the ballast tank community were closely associated with known hydrocarbon-degrading genera *Marinobacter*, *Alcanivorax,* and *Vibrio*.[54–56] These organisms could be responsible for the initial attack on the fuel hydrocarbon substrates, which would result in oxygen consumption and the development of anaerobic conditions. Such a scenario has been previously suggested for fuel decay linked to metal biocorrosion in seawater microbial communities.[57] Other genera including, *Alteromonas, Pseudoalteromonas, Haliea, Colwellia, Halomonas,* and *Thiomicrospira* found in the ballast tank communities are common in marine environments.[58–62] The deltaproteobacteria were initially in low relative abundance (~5%). The identification of the genus *Desulfatibacillum* and the detection of *assA* (Figure 2) suggest the *in situ* presence of hydrocarbon-degrading sulfate-reducing bacteria. For example *Desulfatibacillum alkenivorans* strain AK-01 and *Desulfatibacillum aliphaticivorans* strain CV2803$^{T}$ are well characterized sulfate-reducing bacteria that activate alkanes via addition to fumarate.[63,64] Additionally, the sulfate-reducing bacterial genera *Desulfotignum*, *Desulfocella, Desulfocarcina, Desulfobacterium,* and *Desulfobacter* were present within the ballast tank water prior to

incubation. These are members of the deltaproteobacteria family *Desulfobacteraceae* are capable of using long-chain fatty acids, alcohols, polar aromatic compounds, as well as aliphatic or aromatic hydrocarbons as electron donors to support their respiratory metabolism.[65]

The initial microbial community profile from the ballast tank water can be compared to coastal seawater analyzed in a similar manner.[57,66] In both samples, there is a relatively high abundance of alpha- and gammaproteobacteria. However, deltaproteobacteria were well below the relative detection limits in pristine seawater and thus quite different from the ballast tank waters. In fact, the presence of anaerobic organisms in general were also relatively unimportant.[57,66] Thus, seawater compensated fuel ballast tanks on board at least one marine vessel clearly represents a different microbial community profile than pristine seawater.

The microbial community profile changed substantially upon the imposition of anaerobic conditions with or without an amendment of different fuels (Figure 3). If the organosulfur content of the fuels influenced microbial succession patterns or if the fuels differed markedly in the susceptibility to anaerobic biodegradation, clear changes in both the bacterial composition patterns and sulfate reduction rates would be expected. However, when the ballast tank inoculum was anaerobically incubated, amended with various fuels, and analyzed with high throughput sequencing, deltaproteobacteria, unclassified Bacteroidetes, and an unclassified group of organisms became the relatively dominant bacterial taxa. The family *Desulfobacteraceae* comprised ≥70% of the deltaproteobacteria identified in the ULSD, LSD, HSD, and shipboard fuel incubations. In addition, the sulfate-reducing bacterial genera associated with the

ULSD, LSD, and HSD incubations were very similar (Figure 4). When the ballast tank inoculum was incubated with the diesel fuel taken from the same ship, *Desulfobacter* (Figure 4) was a relatively more imporant proportion of the deltaproteobacterial community. *Desulfobacter* is an acetate-utilizing sulfate-reducing bacterium common in marine environments and, has been previously associated with biocorrosion.[67] In contrast to the diesel-amended incubations, the composition of deltaproteobacteria within the diesel-unamended control consisted mostly of *Desulfovibrio*. Clearly, the deltaproteobacteria were enriched under anaerobic conditions, but the fuel amendments resulted in the differential selection of sulfate-reducing bacterial communities. The results suggest, that while there is some variation in the composition of microbial communities among ULSD, LSD, HSD, and shipboard fuel incubations, the overall bacterial community profiles were not significantly different (ANOSIM $P<0.001$). Similarly, the community profiles among the diesel fuel treatments were indistinguishable via DGGE analyses (Figure 5). Therefore, our results suggest that small molecular weight biodegradable components formed during fuel desulfurization are unlikely to substantively influence the composition of the resident microflora.

The rates of sulfate reduction measured within the ballast tank incubations were not inherently different among ULSD, LSD, and HSD diesel incubations (Figure 6). Thus, the different concentrations of sulfur associated with each diesel fuel did not inhibit biodegradation processes. Gas chromatographic evidence of pre- and post-incubation diesel layers was not significantly different, undoubtedly due to the inability to detect small compositional changes relative to the large background amount of parent fuel. In fact, we estimate that far more sulfate (>150 mM) than that depleted in our

experiments would be required to completely metabolize only the $C_{12}$, $C_{15}$, and $C_{18}$ n-alkanes in the diesel incubations (calculations not shown). To test whether hydrocarbon metabolism was a reasonable interpretation for the sulfate consumption evidence, we looked for the presence of diagnostic metabolites,[68] but these intermediates were not detected. This suggests that either the characteristic metabolite was at a concentration below our analytical limit or that hydrocarbon-degradation was occurring by a physiological mechanism other than fumarate addition.

We therefore incubated the same fuels with inocula known to catalyze anaerobic hydrocarbon biodegradation and hypothesized that if the amount of organosulfur compounds in the fuels did not influence anaerobic hydrocarbon decay, the same rates of either sulfate reduction or methanogenesis should be detected with the known hydrocarbonoclastic inocula. This was indeed the observation as no difference was measured between the sulfate reduction or methanogenic rates in the HSD, LSD, or ULSD amended incubations, but the rates were well above the diesel-unamended control (Figures S1 & S2). Thus, it is clear that the mere removal of sulfur from the diesel had no substantive influence on the susceptibility of the resulting fuel to anaerobic biodegradation.

Despite the superficial similarity among the fuels (Figure 1), the ballast tank inoculum, amended with the shipboard diesel, reduced sulfate at a rate that was approximately twice that of the refinery fuels (Figure 5). The shipboard diesel contained the highest concentration of sulfur (1,528 ppm), again suggesting that the organosulfur content played little if any role in inhibiting anaerobic metabolic processes. The increase in sulfate reduction rate observed with the shipboard diesel

may, therefore be a function of the acclimation of the resident microflora to the metabolism of the fuel components to which they are chronically exposed. Alternatively, the shipboard fuel may have included additives that were not present in the refinery fuels. This suggestion is supported by the differential and strong enrichment of *Desulfobacter* in these incubations relative to the other fuel incubations. Presumably the shipboard fuel contained some additive that was being metabolized to acetate and subsequently oxidized by the *Desulfobacter*. Fuel additives such as methyesters associated with biodiesel have been previously reported to increase biofouling and biocorrosion.[20] Thus, it is clear that fuel additives can have a profound impact on the composition of the microbial community, as well as the rates of sulfate depletion and, by extension, biocorrosion.

The major implication of this work is that ULSD, LSD, HSD and even a traditional diesel fuel formulation can undergo biodegradation to a similar extent and stimulate sulfate reduction when oxygen becomes limiting in seawater compensated ballast tanks. This process would produce higher levels of hydrogen sulfide ($H_2S$) and thus an elevated biocorrosion rate. However, it is unlikely that either the biodegradation of diesel hydrocarbons or, by inference, the degree of biocorrosion is likely to be influenced by the concentration of organosulfur species in the fuel.

**Acknowledgement**

This work was supported by a grant (Award N0001408WX20857) from the Office of Naval Research and in part by a National Science Foundation grant (MCB-0921265). We thank Dr. Paul M. Ryder of ConocoPhillips for obtaining the refinery diesel samples, the soy biodisel, and for the organosulfur quantification. Additionally, we are grateful to the Captain and crew of the *USS Gettysburg* for help obtaining ballast water and shipboard fuel samples.

## References


(1) Kilbane, J. J. Microbial biocatalyst developments to upgrade fossil fuels. *Curr. Opin. In Biotechnol.* **2006**, *17* (3), 305–14.

(2) Swaty, T. Global refining industry trends: the present and future. *Hydrocarb. Processing* **2005**, *84* (9), 35–46.

(3) Song, C and Ma, X. New design approaches to ultra-clean diesel fuels by deep desulfurization and deep dearomatization. *Appl. Catal. B: Environ.* **2003**, *41* (1), 207–238.

(4) Song, C. An overview of new approaches to deep desulfurization for ultra-clean gasoline, diesel fuel and jet fuel. *Catal. Today* **2003**, *86* (1), 211–263.

(5) Alsolami, B.; Carneiro, J. T.; Moulijn, J. a.; Makkee, M. On-site low-pressure diesel HDS for fuel cell applications: Deepening the sulfur content to ⩽1ppm. *Fuel* **2011**, *90* (10), 3021–3027.

(6) Ho, T. C. Deep HDS of diesel fuel: chemistry and catalysis. *Catal. Today* **2004**, *98* (1), 3–18.

(7) Ho, T. C.; Markley, G. Property–reactivity correlation for hydrodesulfurization of prehydrotreated distillates. *Appl. Catal. A: Gen.* **2004**, *267* (1), 245–250.

(8) Rheinberg, O. van; Lucka, K.; Kohne, H.; Schade, T.; Andersson, J. Selective removal of sulphur in liquid fuels for fuel cell applications. *Fuel* **2008**, *87* (13), 2988–2996.

(9) Mei, H.; Mei, B.; Yen, T.F. A new method for obtaining ultra-low sulfur diesel fuel via ultrasound assisted oxidative desulfurization. *Fuel* **2003**, *82* (4), 405–414.

(10) Guo, W.; Wang, C.; Lin, P.; Lu, X. Oxidative desulfurization of diesel with TBHP/isobutyl aldehyde/air oxidation system. *Appl. Energ.* **2011**, *88* (1), 175–179.

(11) García-Gutiérrez, J. L.; Fuentes, G. A.; Hernández-Terán, M. E.; Murrieta, F.; Navarrete, J.; Jiménez-Cruz, F. Ultra-deep oxidative desulfurization of diesel fuel with H2O2 catalyzed under mild conditions by polymolybdates supported on Al2O3. *Appl. Catal. A: Gen.* **2006**, *305* (1), 15–20.

(12) Dai, Y.; Qi, Y.; Zhao, D.; Zhang, H. An oxidative desulfurization method using ultrasound/Fenton's reagent for obtaining low and/or ultra-low sulfur diesel fuel. *Fuel Process. Technol.* **2008**, *89* (10), 927–932.

(13) Tailleur, R. G.; Ravigli, J.; Quenza, S.; Valencia, N. Catalyst for ultra-low sulfur and aromatic diesel. *Appl. Catal. A: Gen.* **2005**, *282* (1), 227–235.

(14) Knudsen, K. G.; Cooper, B. H.; Topsøe, H. Catalyst and process technologies for ultra low sulfur diesel. *Appl. Catal. A: Gen.* **1999**, *189* (1), 205–215.

(15) Lim, M. C. H.; Ayoko, G. A.; Morawska, L.; Ristovski, Z. D.; Jayaratne, E. R. The effects of fuel characteristics and engine operating conditions on the elemental composition of emissions from heavy duty diesel buses. *Fuel* **2007**, *86* (12), 1831–1839.

(16) Murakami, Y. Analysis of corrosive wear of diesel engines: relationship to sulfate ion concentrations in blowby and crankcase oil. *JSAE Rev.* **1995**, *16* (1), 43–48.

(17) Stanislaus, A.; Marafi, A.; Rana, M. S. Recent advances in the science and technology of ultra low sulfur diesel (ULSD) production. *Catal. Today* **2010**, *153* (1), 1–68.

(18) Abu-Jrai, A.; Rodríguez-Fernández, J.; Tsolakis, A.; Megaritis, A.; Theinnoi, K.; Cracknell, R. F.; Clark, R. H. Performance, combustion and emissions of a diesel engine operated with reformed EGR. Comparison of diesel and GTL fuelling. *Fuel* **2009**, *88* (6), 1031–1041.

(19) Di, Y.; Cheung, C. S.; Huang, Z. Experimental investigation on regulated and unregulated emissions of a diesel engine fueled with ultra-low sulfur diesel fuel blended with biodiesel from waste cooking oil. *Sci Total Environ.* **2009**, *407* (2), 835–46.

(20) Aktas, D. F.; Lee, J. S.; Little, B. J.; Ray, R. I.; Davidova, I. A.; Lyles, C. N.; Suflita, J. M. Anaerobic metabolism of biodiesel and its impact on metal corrosion. *Energ. Fuel.* **2010**, *24* (12), 2924–28.

(21) Lee, J. S.; Ray, R. I.; Little, B. J. Microbiological and corrosivity characterizations of biodiesels and advanced diesel fuels. *Nace Corrosion Conference & Expo* **2009**, 1–22.

(22) Heldreth, B.; Turos, E. Microbiological properties and modes of action of organosulfur-based anti-infectives. *Curr. Med. Chem.: Anti-Infect. Agents* **2005**, *4* (4), 295–315.

(23) Dean, R. A.; Whitehead, E. V. Status of work in separation and identification of sulphur compounds in petroleum and shale oil. In *7th World Petroleum Congress*; Mexico City, Mexico, 1967; p. 12.

(24) Orr, W. L.; Sinninghe Damste, J. S. Geochemistry of sulfur in petroleum systems. In *Geochemistry of Sulfur in Fossil Fuels*; Orr, W.; CM, W., Eds.; American Chemical Society: Washington, DC, 1990; pp. 2–29.

(25) Mochida, I.; Choi, K.-H. An overview of hydrodesulfurization and hydrodenitrogenation. *J. Jpn. Petrol. Inst.* **2004**, *47* (3), 145–163.

(26) Gieg, L. M.; Kolhatkar, R. V; Mcinerney, M. J.; Tanner, R. S.; Sublette, K. L.; Suflita, J. M. Intrinsic bioremediation of petroleum hydrocarbons in a gas condensate-contaminated aquifer. *Environ. Sci. & Technol.* **1999**, *33* (15), 2550–2560.

(27) Gieg, L. M.; Duncan, K. E.; Suflita, J. M. Bioenergy production via microbial conversion of residual oil to natural gas. *Appl. Environ. Microbiol.* **2008**, *74* (10), 3022–9.

(28) ASTM D2622 - 10 Standard test method for sulfur in petroleum products by wavelength dispersive x-ray fluorescence spectrometry.

(29) Widdel, F.; Bak, F. Gram-negative mesophilic sulfate-reducing bacteria. In *The Prokaryotes*; Balows, A.; Truper, H. G.; Dworkin, M.; Harder, W.; Schleifer, K. H., Eds.; Springer-Verlag: New York, NY, 1992; pp. 3352–3378.

(30) Callaghan, A. V; Wawrik, B.; Ní Chadhain, S. M.; Young, L. Y.; Zylstra, G. J. Anaerobic alkane-degrading strain AK-01 contains two alkylsuccinate synthase genes. *Biochem. Biophys. Res. Commun.* **2008**, *366* (1), 142–8.

(31) Grundmann, O.; Behrends, A.; Rabus, R.; Amann, J.; Halder, T.; Heider, J.; Widdel, F. Genes encoding the candidate enzyme for anaerobic activation of n-alkanes in the denitrifying bacterium, strain HxN1. *Environ. microbiol.* **2008**, *10* (2), 376–85.

(32) Rainey, F. A.; Ward-Rainey, N.; Kroppenstedt, R. M.; Stackebrandt, E. The genus Nocardiopsis represents a phylogenetically coherent taxon and a distinct actinomycete lineage: proposal of Nocardiopsaceae fam. nov. *Int. J. Syst. Bacteriol.* **1996**, *46* (4), 1088–92.

(33) Callaghan, A. V; Davidova, I. A.; Savage-Ashlock, K.; Parisi, V. A.; Gieg, L. M.; Suflita, J. M.; Kukor, J. J.; Wawrik, B. Diversity of benyzl- and alkylsuccinate synthase genes in hydrocarbon-impacted environments and enrichment cultures. *Environ. Sci. & Technol.* **2010**, *44* (19), 7287–94.

(34) Kumar, S.; Nei, M.; Dudley, J.; Tamura, K. MEGA: a biologist-centric software for evolutionary analysis of DNA and protein sequences. *Briefings Bioinf.* **2008**, *9* (4), 299–306.

(35) Hamady, M.; Walker, J. J.; Harris, J. K.; Gold, N. J.; Knight, R. Error-correcting barcoded primers for pyrosequencing hundreds of samples in multiplex. *Nat. Methods* **2008**, *5* (3), 235–237.

(36) Wawrik, B.; Mendivelso, M.; Parisi, V. A.; Suflita, J. M.; Davidova, I. A.; Marks, C. R.; Van Nostrand, J. D.; Liang, Y.; Zhou, J.; Huizinga, B. J.; Strąpoć, D.; Callaghan, A. V Field and laboratory studies on the bioconversion of coal to methane in the San Juan Basin. *FEMS microbiol. Ecol.* **2012**, *81* (1), 26–42.

(37) Caporaso, J.; Kuczynski, J.; Stombaugh, J.; Bittinger, K.; Bushman, F.; Cotello, E.; Fierer, N.; Gonzalez Pena, A.; Goodrich, J.; Gordon, J.; Huttley, G.; Kelley, S.; Knights, D.; Koening, J.; Ley, R.; Lozupone, C.; McDonald, D.; Muegge, B.; Pirrung, M.; Reeder, J.; Sevinsky, J.; Turnbaugh, P.; Walters, W.; Widmann, J.; Yatsunenko, T.; Zaneveld, J.; Knight, R. QIIME allows analysis of high-throughput community sequencing data. *Nat. Methods* **2010**, *7* (5), 335–36.

(38) Reeder, J.; Knight, R. Rapid denoising of pyrosequencing amplicon data: exploiting the rank-abundance distribution. *Nat. Methods* **2010**, *7*, 668–669.

(39) Edgar, R. C. Search and clustering orders of magnitude faster than BLAST. *Bioinformatics* **2010**, *26*, 2460–1.

(40) Caporaso, J. G.; Bittinger, K.; Bushman, F. D.; DeSantis, T. Z.; Andersen, G. L.; Knight, R. PyNAST: a flexible tool for aligning sequences to a template alignment. *Bioinformatics* **2010**, *26* (2), 266–7.

(41) Maidak, B. L.; Cole, J. R.; Lilburn, T. G.; Parker, C. T.; Saxman, P. R.; Farris, R. J.; Garrity, G. M.; Olsen, G. J.; Schmidt, T. M.; Tiedje, J. M. The RDP-II (Ribosomal Database Project). *Nucleic Acids Res.* **2001**, *29* (1), 173–4.

(42) Ludwig, W.; Strunk, O.; Westram, R.; Richter, L.; Meier, H.; Yadhukumar; Buchner, A.; Lai, T.; Steppi, S.; Jobb, G.; Förster, W.; Brettske, I.; Gerber, S.; Ginhart, A. W.; Gross, O.; Grumann, S.; Hermann, S.; Jost, R.; König, A.; Liss, T.; Lüssmann, R.; May, M.; Nonhoff, B.; Reichel, B.; Strehlow, R.; Stamatakis, A.; Stuckmann, N.; Vilbig, A.; Lenke, M.; Ludwig, T.; Bode, A.; Schleifer, K.-H. ARB: a software environment for sequence data. *Nucleic Acids Res.* **2004**, *32* (4), 1363–71.

(43) McDonald, D.; Price, M. N.; Goodrich, J.; Nawrocki, E. P.; DeSantis, T. Z.; Probst, A.; Andersen, G. L.; Knight, R.; Hugenholtz, P. An improved Greengenes taxonomy with explicit ranks for ecological and evolutionary analyses of bacteria and archaea. *ISME J.* **2012**, *6* (3), 610–8.

(44) Muyzer, G.; De Waal, E. C.; Uitterlinden, A. G. Profiling of complex microbial populations by denaturing gradient gel electrophoresis analysis of polymerase

chain reaction-amplified genes coding for 16S rRNA. *Appl. Environ. Microbiol.* **1993**, *59* (3), 695–700.

(45) Santegoeds, C.; Damgaard, L. R.; Hesselink, G.; Zopfi, J.; Lens, P.; Muyzer, G.; De Beer, D. Distribution of sulfate-reducing and methanogenic bacteria in anaerobic aggregates determined by microsensor and molecular analyses. *Appl. Environ. Microbiol.* **1999**, *65* (10), 4618–4629.

(46) Wang, L.; Wei, L.; Mbadinga, S.; Liu, J.; Gu, J.; Mu, B. Methanogenic Microbial Community Composition of Oily Sludge and Its Enrichment Amended with Alkanes Incubated for Over 500 Days. *Geomicrobiol. J.* **2012**, *29* (8), 716–726.

(47) Chouari, R.; Paslier, D. Le; Dauga, C.; Daegelen, J. W.; Sghir, A. Novel Major Bacterial Candidate Division within a Municipal Anaerobic Sludge Digester. *Appl. Environ. Microbiol.* **2005**, *71* (4), 2145–2153.

(48) Pavissich, J. P.; Silva, M.; González, B. Sulfate reduction, molecular diversity, and copper amendment effects in bacterial communities enriched from sediments exposed to copper mining residues. *Environ. Toxicol. Chem.* **2010**, *29* (2), 256–64.

(49) Battelle Memorial Institue *Corrosion in Systems Storing and Dispensing Ultra Low Sulfur Diesel ( ULSD ), Hypotheses Investigation*; Columbus, Ohio, 2012; p. 34.

(50) Rappé, M. S.; Connon, S. A.; Vergin, K. L.; Giovannoni, S. J. Cultivation of the ubiquitous SAR11 marine bacterioplankton clade. *Nature* **2002**, *418* (6898), 630–3.

(51) Biebl, H.; Allgaier, M.; Tindall, B. J.; Koblizek, M.; Lünsdorf, H.; Pukall, R.; Wagner-Döbler, I. Dinoroseobacter shibae gen. nov., sp. nov., a new aerobic phototrophic bacterium isolated from dinoflagellates. *Int. J. Syst. Evol. Microbiol.* **2005**, *55* (3), 1089–96.

(52) Fera, M.; Maugeri, T. Detection of Arcobacter spp. in the coastal environment of the Mediterranean Sea. *Appl. Environ. Microbiol.* **2004**, *70* (3), 1271–1276.

(53) Macalady, J. L.; Dattagupta, S.; Schaperdoth, I.; Jones, D. S.; Druschel, G. K.; Eastman, D. Niche differentiation among sulfur-oxidizing bacterial populations in cave waters. *ISME J.* **2008**, *2* (6), 590–601.

(54) Gauthier, M. J.; Lafay, B.; Christen, R.; Fernandez, L.; Acquaviva, M.; Bonin, P.; Bertrand, J.-C. Marinobacter hydrocarbonclasticus gen. nov., sp. nov., a new, extremely halotolerant, hydrocarbon-degrading marine bacterium. *Int. J. Syst. Evol. Microbiol.* **1992**, *42* (4), 568–576.

(55) Kasai, Y.; Kishira, H.; Sasaki, T.; Syutsubo, K.; Watanabe, K.; Harayama, S. Predominant growth of Alcanivorax strains in oil-contaminated and nutrient-supplemented sea water. *Environ. Microbiol.* **2002**, *4* (3), 141–7.

(56) Hedlund, B. P.; Staley, J. T. Vibrio cyclotrophicus sp. nov., a polycyclic aromatic hydrocarbon (PAH)-degrading marine bacterium. *Int. J. Syst. Evol. Microbiol.* **2001**, *51* (1), 61–6.

(57) Aktas, D. F.; Lee, J. S.; Little, B. J.; Duncan, K. E.; Perez-Ibarra, B. M.; Suflita, J. M. Effects of oxygen on biodegradation of fuels in a corroding environment. *Int. Biodeterior. Biodegrad.* **2012**. http://dx.doi.org/10.1016/j.ibiod.2012.05.006.

(58) Gauthier, G.; Gauthier, M.; Christen, R. Phylogenetic analysis of the genera Alteromonas, Shewanella, and Moritella using genes for small-subunit rRNA sequences and division of the genus Alteromonas into two genera, Alteromonas (emended) and Pseudoalteromonas gen. nov., and proposal of twelve new species combinations. *Int. J. Syst. Bacteriol.* **1995**, *45* (4), 755–761.

(59) Urios, L.; Intertaglia, L.; Lesongeur, F.; Lebaron, P. Haliea salexigens gen. nov., sp. nov., a member of the Gammaproteobacteria from the Mediterranean Sea. *Int. J. Syst. Evol. Microbiol.* **2008**, *58* (5), 1233–7.

(60) Ivanova, E. P.; Flavier, S.; Christen, R. Phylogenetic relationships among marine Alteromonas-like proteobacteria: emended description of the family Alteromonadaceae and proposal of Pseudoalteromonadaceae fam. nov., Colwelliaceae fam. nov., Shewanellaceae fam. nov., Moritellaceae fam. nov., Ferrimonadacea fam. nov. Idiomarinaceae fam. nov. and Psychromonadaceae fam. nov. *Int. J. Syst. Evol. Microbiol.* **2004**, *54* (5), 1773–88.

(61) Vreeland, R. H.; Litchfield, C. D.; Martin, E. L.; Elliot, E. Halomonas elongata, a new genus and species of extremely salt-tolerant bacteria. *Int. J. Syst. Bacteriol.* **1980**, *30* (2), 485–495.

(62) Kuenen, J.; Veldkamp, H. Thiomicrospira pelophila, gen. n., sp. n., a new obligately chemolithotrophic colourless sulfur bacterium. *Antonie van Leeuwenhoek* **1972**, *38* (1), 241–256.

(63) So, C.; Young, L. Isolation and Characterization of a Sulfate-Reducing Bacterium That Anaerobically Degrades Alkanes. *Appl. Environ. Microbiol.* **1999**, *65* (7), 2969–2976.

(64) Callaghan, A. V; Gieg, L. M.; Kropp, K. G.; Suflita, J. M.; Young, L. Y. Comparison of mechanisms of alkane metabolism under sulfate-reducing conditions among two bacterial isolates and a bacterial consortium. *Appl. Environ. Microbiol.* **2006**, *72* (6), 4274–82.

(65) Bergey, D. H.; Holt, J. G. Group 7: Dissimilatory sulfate- or sulfur reducing bacteria. In *Bergey's manual of Determinative Bacteriology 9th Ed.*; Henayl, W. R., Ed.; Williams and Wilkins, 1994; pp. 335–341.

(66) Lee, J.; Ray, R.; Little, B.; Duncan, K. Sulphide production and corrosion in seawaters during exposure to FAME diesel. *Biofouling* **2012**, *28* (5), 465–478.

(67) Brink, D. E.; Vance, I.; White, D. C. Detection of desulfobacter in oil field environments by non-radioactive DNA probes. *Appl. Microbiol. Biotechnol.* **1994**, *42* (2), 469–475.

(68) Kropp, K. G.; Davidova, I. A.; Suflita, J. M. Anaerobic oxidation of n-dodecane by an addition reaction in a sulfate-reducing bacterial enrichment culture. *Appl. Environ. microbiol.* **2000**, *66* (12), 5393–8.

**Table S1:** ASS, PCR, and DGGE primers used in this study

| Primer name | Position[a] | Sequence (5'-3') |
|---|---|---|
| 1432F | - | CCNACCACNAAGCAYGG |
| *ass*/*bss* R | - | TCGTCRTTGCCCCATTTIGGIGC |
| M13F-27F | 8-27 | **GTA AAA CGA CGG CCA G**AG AGT TTG ATC CTG GCT CAG |
| M13R-338R | 338-356 | **CAG GAA ACA GCT ATG AC**T GCT GCC TCC CGT AGG AGT |
| TiA-8nt-27F[b] | - | CCA TCT CAT CCC TGC GTG TCT CCG ACT CAG NNN NNN NN**C A**AG AGT TTG ATC CTG GCT CAG |
| TiB-338R[b] | - | CCT ATC CCC TGT GTG CCT TGG CAG TCT CAG **CA**T GCT GCC TCC CGT AGG AGT |
| GM5F[C] | 341-357 | CCT ACG GGA GGC AGC AG |
| 907R | 907-928 | CCG TCA ATT CCT TTG AGT TT |

[a]Position in the 16S rRNA of *E. coli*

[b] Life Sciences 454 Titanium "A" and "B" primers are underlined, N's designate location of unique barcode (see Table S2), and spacer nucleotides are in bold.

[c] a 40 base GC clamp was attached to primer (5'-CGC CCG CCG CGC CCC GCG CCC GTC CCG CCG CCC CCG CCC G-3')

**Table S2:** List of 8 nucleotide barcodes used for parallel pyrosequencing of multiple libraries

| Barcode (5'-3') | Library |
|---|---|
| CAAGCAAG | Ballast tank water filter 1 |
| CAAGCATC | Ballast tank water filter 2 |
| CAAGCTAC | Ballast tank water filter 3 |
| CAAGCTTG | US Navy ship diesel incubation |
| CAAGGAAC | Soy based biodiesel incubation |
| CAAGGATG | Ultra-low sulfur diesel incubation |
| CAAGGTAG | Low sulfur diesel incubation |
| CAAGGTTC | High sulfur diesel incubation |
| CAAGTCCA | Diesel-unamended control |

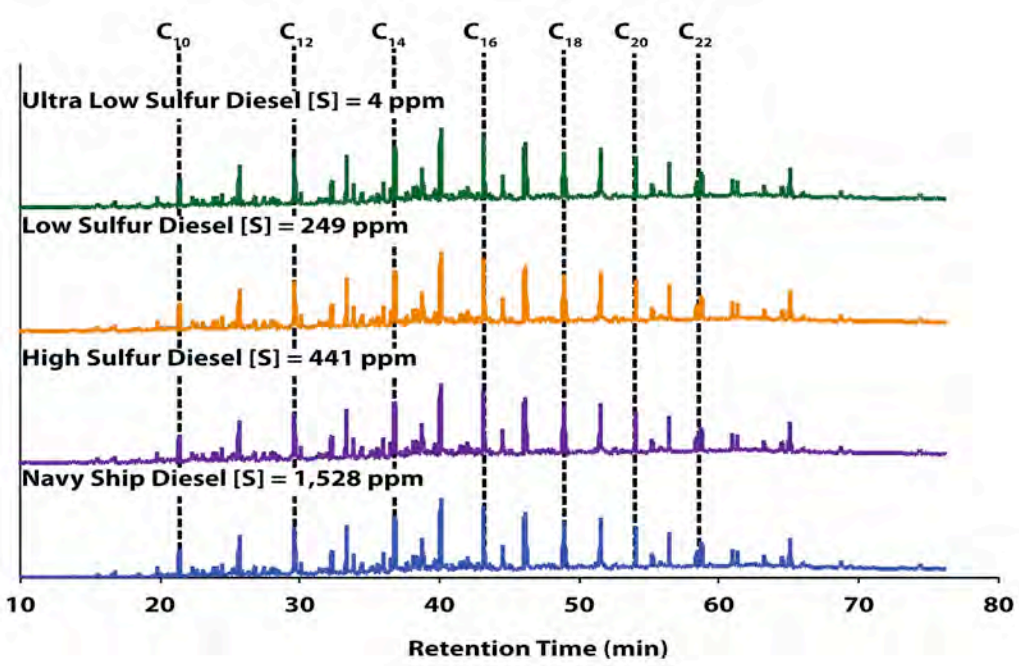


**Figure 1:** Gas chromotagraphic profiles of ultra low-, low-, and high- sulfur diesel refinery fuels as well as a shipboard fuel from a US Navy ship. The sulfur concentration [S] is indicated for each of the diesel fuels.

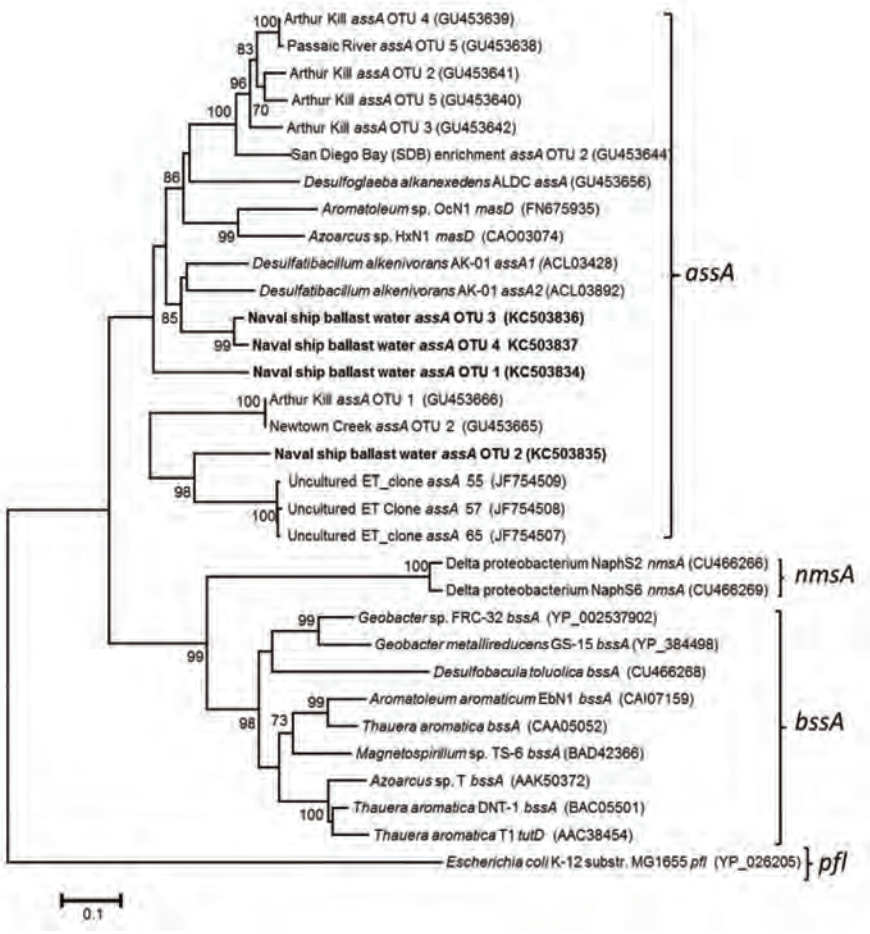


**Figure 2:** Neighbor-joining dendrogram of *assA* and *bssA* gene sequences from reference strains and the closest matches to each of the ballast water sequences. Naval ship ballast water *assA* sequences are in bold. Bootstrap values below 65% are not shown. Numbers in parentheses represent GenBank accession numbers. Abbreviations: *ass* (alkylsuccinate synthase), *mas* ((1-methylalkyl)succinate synthase)) *bss* (benzylsuccinate synthase), *tut* ("toluene-utilizing"; benzylsuccinate synthase), *nms* ((2-naphthylmethyl)succinate synthase)), and *pfl* (pyruvate formate lyase).

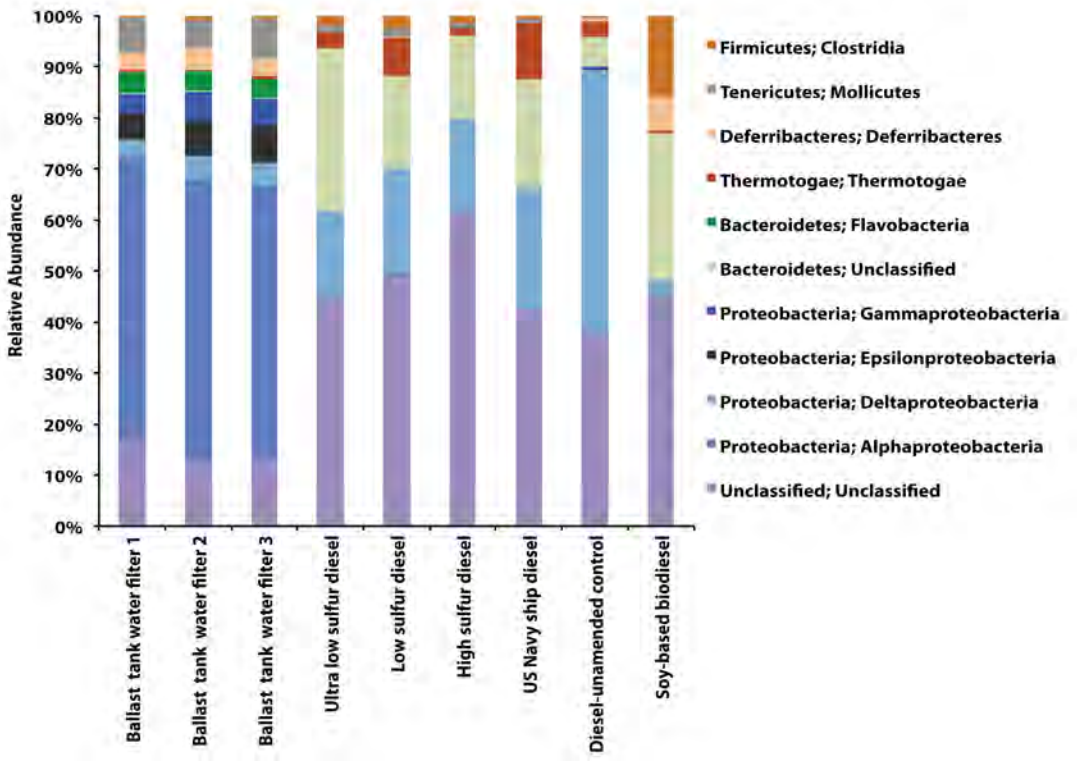


**Figure 3:** The relative abundances of different phyla and classes of bacteria based on 16S rRNA library analyses. Replicate filtered samples of ballast tank water (1-3) represent the microbial community structure at the start of the experiment. The other lanes reflect the changed bacterial community structure in ballast tank incubations exposed to various diesel fuels or to a diesel-unamended control.

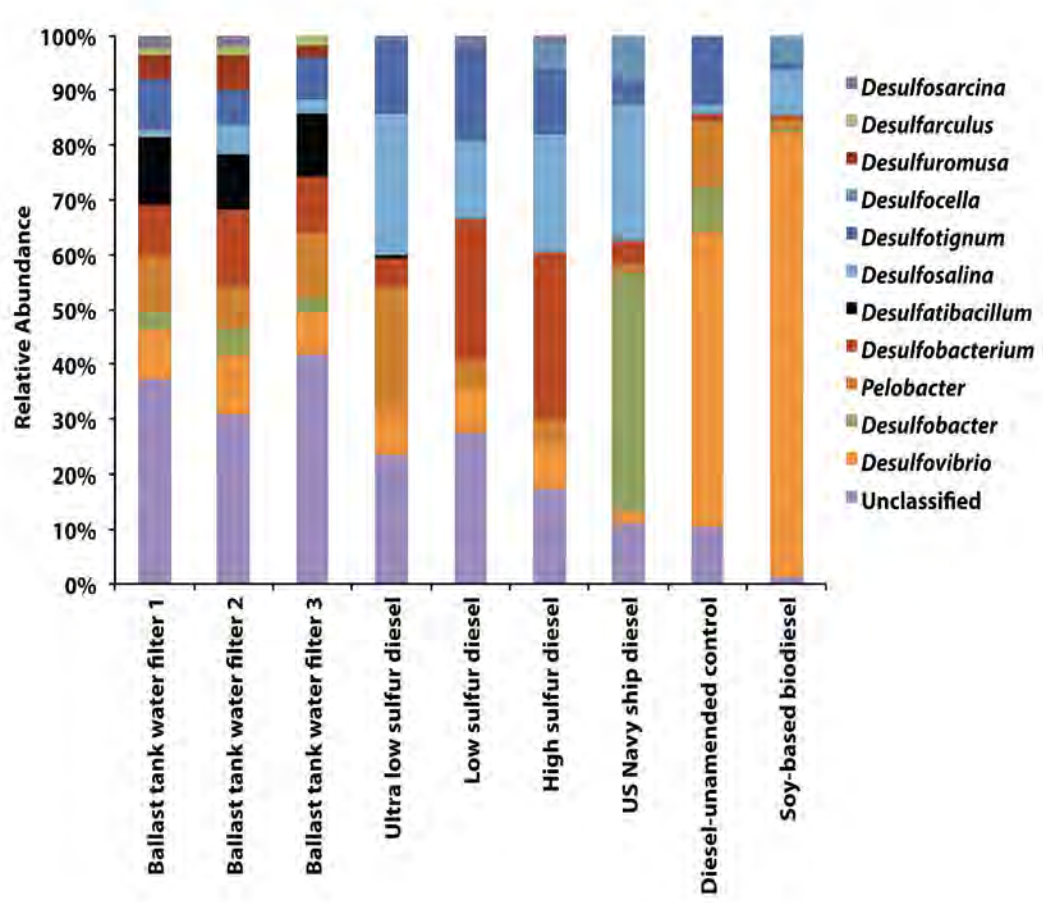


**Figure 4:** The relative abundances of genera within the deltaproteobacteria detected in various diesel fuel incubations (see Figure 3).

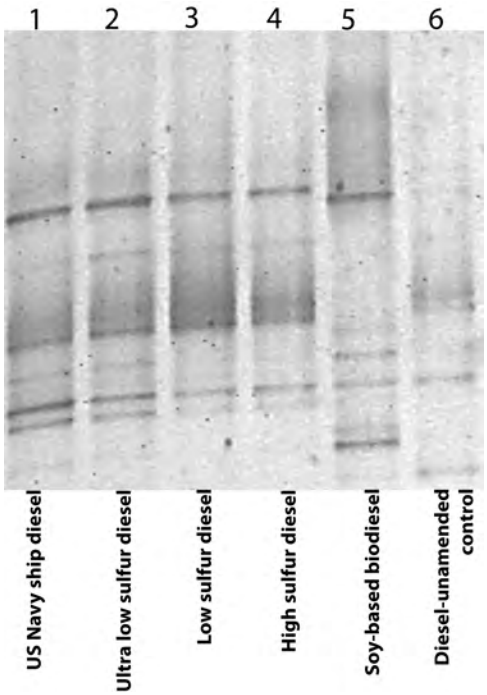


**Figure 5:** The DGGE profile of the bacterial communities in ballast tank incubations amended with shipboard diesel (Lane 1), ULSD (Lane 2), LSD (Lane 3), HSD (Lane 4), Soy-based biodiesel (Lane 5), and the diesel-unamended control (Lane 6)

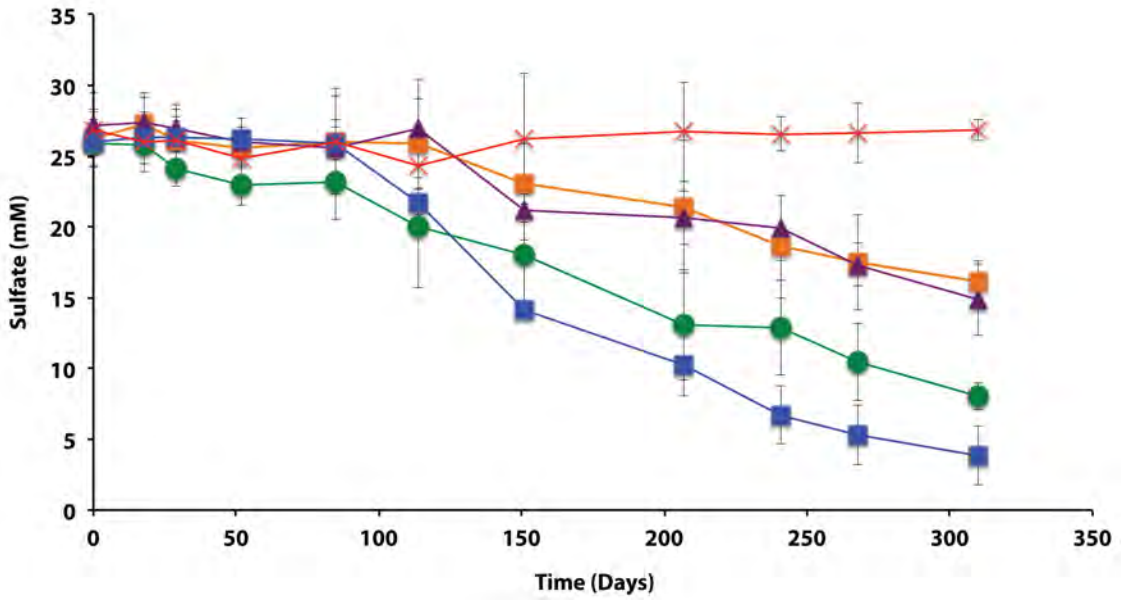


**Figure 6:** Sulfate depletion in ballast tank incubations containing various diesel fuels: ULSD (●), LSD (■), HSD (▲), and US Navy ship diesel (■). Rates of sulfate loss were determined after an 85 d lag period and were adjusted to background rates measured in the diesel-unamended control (✕).

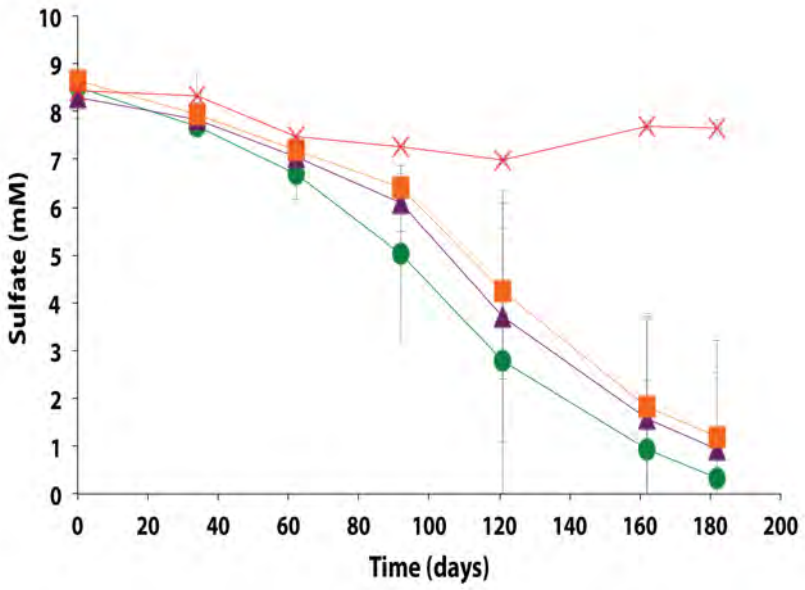


**Figure S1:** Sulfate depletion in gas-condensate contaminated aquifer incubations amended with various diesel fuels: ULSD (●), LSD (■), HSD (▲), and diesel-unamended control (✕).

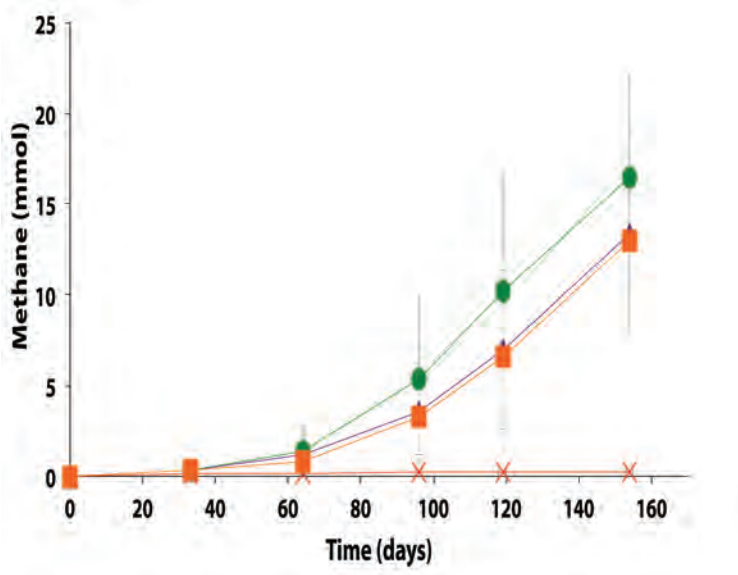


**Figure S2:** Methane production in oil-degrading methanogenic consortium incubations amended with various diesel fuels: ULSD (●), LSD (■), HSD (▲), and diesel-unamended control (×).

# Chapter 3: Anaerobic hydrocarbon and fatty acid metabolism by syntrophic bacteria and their impact on carbon steel corrosion


## Abstract

The microbial metabolism of hydrocarbons is increasingly associated with the corrosion of carbon steel in sulfate-rich marine waters. However, how such transformations influence metal biocorrosion in the absence of an electron acceptor is not fully recognized. We grew a marine alkane-utilizing, sulfate-reducing bacterium, *Desulfoglaeba alkanexedens* strain ALDC with either sulfate or *Methanospirillum hungatei* strain JF-1, as electron acceptors and tested the ability of the cultures to catalyze metal corrosion. Axenically, *D. alkanexedens* strain ALDC had a higher instantaneous corrosion rate and produced more pits in carbon steel coupons than when the same organism was grown in syntrophic co-culture with the methanogen. Since anaerobic hydrocarbon biodegradation pathways converge on fatty acid intermediates, the corrosive ability of a known fatty acid-oxidizing syntrophic bacterium, *Syntrophus aciditrophicus* strain SB was compared when grown in pure culture or in co-culture with a $H_2$-utilizing sulfate-reducing bacterium (*Desulfovibrio sp.,* strain G11) or a methanogen (*M. hungatei* strain JF-1). The instantaneous corrosion rates were not substantially different between the cultures, but the syntroph/sulfate-reducing co-culture produced more pits in coupons than other combinations of microorganisms. Lactate-grown cultures of strain G11 had higher instantaneous corrosion rates and coupon pitting compared to the same organism cultured with hydrogen as an electron donor. Thus, if sulfate is available as an electron acceptor, the same microbial assemblages produce sulfide and low molecular weight organic acids that generally exacerbate

biocorrosion. Despite these trends, a surprisingly high degree of variation was encountered with the corrosion assessments. Differences in biomass, initial substrate concentration, rates of microbial activity or the degree of end product formation did not account for the variations. We are forced to ascribe such differences to the metallurgical properties of the coupons.

## Introduction

Anaerobic hydrocarbon biodegradation is metabolically coupled with the consumption of a variety of terminal electron acceptors (for recent reviews see, Heider and Schühle, 2013; Callaghan, 2013). It is essential to understand the underlying geochemical settings for such bioconversions in order to reliably assess the attendant environmental consequences. Arguably, the greatest impact of this metabolism is manifest in sulfate-laden environments where petroleum metabolism may be coupled with sulfide production. Aside from the destruction of the hydrocarbons *per se*, the formation of sulfide has several important consequences including health and safety concerns (Reiffenstein et al., 1992), reservoir souring (Nemati et al., 2001; Hubert and Voordouw, 2007; Jenneman et al., 1986; McInerney et al., 1996) and metal biocorrosion (Hamilton, 1985). Not surprisingly, these problems are most acute in marine environments where sulfate-reducing bacterial communities thrive in petroleum deposits, hydrocarbon seeps, petroleum hydrothermal sediments, methane hydrates, oil field equipment, and in hydrocarbon-contaminated sediments (Teske, 2010). Moreover, in offshore and near coastal drilling operations where seawater is injected into petroleum reservoirs to maintain oil field formation pressures, efforts are regularly made to remove sulfate from seawater in order to control the deleterious consequences

of scale deposits as well as to minimize microbial sulfate reduction, reservoir souring, and sulfide-induced metal corrosion (Bader, 2007). When exogenous electron acceptors are limiting, anaerobic hydrocarbon mineralization can still proceed and result in the formation of methane (Heider and Schühle, 2013; Gieg et al., 2008; Jones et al., 2008; Dolfing et al., 2008). In fact, methanogenic enrichments and isolates are regularly obtained from hydrocarbon-rich marine ecosystems (Teske, 2010), even though these organisms are not known to directly utilize petroleum components. Rather, acetoclastic and hydrogenotrophic methanogens catalyze the terminal mineralization steps as members of thermodynamically-based hydrocarbonoclastic syntrophic microbial assemblages of varying complexity (Gieg et al., 2008; Jones et al., 2008; Dolfing et al., 2008). The consequences of methanogenic hydrocarbon metabolism minimally include the overall diminution in the quality of petroleum reserves (Head et al., 2010), and the formation of methane a powerful greenhouse gas (Blake and Rowland, 1988). The other end product of this bioconversion, carbon dioxide, can potentially alter the *in situ* mineralization pathways in petroliferous reservoirs. If carbon dioxide is in a high enough concentration, acetoclastic methanogenesis may become a dominant process and increase the rate of methane production and sequestration of carbon dioxide (Mayumi et al., 2013).

Thus, the complete mineralization of hydrocarbons under anaerobic conditions, like the biodegradation of other complex forms of organic matter, can be initiated or accomplished by specialized microbial isolates that can couple this metabolism to the consumption of exogenous electron acceptors or enter into complex syntrophic partnerships. Such bioconversions often result in the transient formation of fatty acid

metabolites (e.g. acetate, propionate, butyrate, and benzoate) that have been postulated as intermediates of anaerobic hydrocarbon metabolism under both methanogenic and sulfate-reducing conditions (Van Stempvoort et al., 2007; Van Stempvoort et al., 2009; Cozzarelli et al., 1994; Struchtemeyer et al., 2011). In syntrophic partnerships, it is well known that non-methanogens, such as hydrogen/formate-utilizing, sulfate-reducing bacteria (SRB), can fulfill the role of the terminal electron-accepting microorganisms (Jackson et al., 1999; Hopkins et al., 1995; Warikoo et al., 1996). Conversely, a syntrophic association with methanogens can also be realized even in environments with high sulfate concentrations (Struchtemeyer et al., 2011).

The role of SRB and methanogens as agents of metal corrosion, when grown as pure cultures or as members of syntrophic consortia, is not fully appreciated. These organisms have been implicated in the corrosion of metal via direct electron transfer from zero valent iron under electron donor-limited conditions (Dinh et al., 2004; Enning et al., 2012; Uchiyama et al., 2010). Additionally, when electron donors are sufficient, the inorganic and organic compounds produced during metabolism (e.g. hydrogen, fatty acids, carbon dioxide, and sulfides) have frequently been associated with metal biocorrosion (King et al., 1973a; King and Miller, 1971; King et al., 1973b; King and Wakerley, 1972; Kermani and Morshed, 2003; Hedges and Mcveigh, 1999; Garsany et al., 2003; Suflita et al., 2008; Crolet et al., 1999).

Given the diverse modes of existence for the requisite microorganisms, we used defined incubations of both pure and co-culture syntrophic bacteria to examine their impact on carbon steel biocorrosion. More specifically, we evaluated a known hydrocarbon-degrading bacterium grown with sulfate or syntrophically in co-culture

with a methanogen as the electron acceptor. We also evaluated biocorrosion with a known fatty acid-oxidizing syntrophic bacterium grown as a pure culture or with either a hydrogen/formate utilizing methanogen or SRB as the electron-accepting microorganism. Lastly, all pure cultures were individually evaluated for their ability to corrode metal coupons. Our results suggest that the corrosion of carbon steel was generally more evident when anaerobic microbial metabolism was linked to sulfate reduction rather than methanogenesis. However, a greater than expected standard deviation in corrosivity was measured in replicate incubations. After controlling and monitoring the biological and chemical characteristics of the incubations, we are forced to attribute the variability to presumed compositional differences in the metal used for the construction of the coupons.

## Materials and Methods

**Electrochemical cell construction.** Electrochemical cells were made from culture bottles (100 ml; Figure S1) fitted with rubber stoppers that were modified to hold a graphite counter electrode and a luggin probe filled with 1M potassium chloride (KCl) solution containing a saturated calomel reference electrode (Gamry Instruments, Warminster, PA; Figure S2). The working electrode was a 1020 carbon steel coupon (Alabama Specialty Products, Munford, AL) with dimensions of 0.95 cm diameter x 1.27 cm and a surface area of 4.5 $cm^2$. The metal was prepared using the specifications detailed in ASTM standard A576-90b (2006), and consisted of the elemental components listed in Table S1 according to the manusfacturer (above). A wire was attached to the coupon using rosin core soder and the entire assembly was sealed with epoxy resin (Figure S3). The working electrode assembly was then washed with

acetone and methanol, before being sterilized by immersion for 30 minutes in a 70% ethanol bath. The ethanol was evaporated with an open flame and the coupon was dried under nitrogen and handled aseptically. Sterile electrochemical probes (Figure S2) were placed in the incubations (Figure S4) while inside a well-working anaerobic chamber ($N_2$:$H_2$ 95:5%) and linear polarization resistance (LPR) curves were recorded every 5 minutes for a 30 minute period using computer controlled potentiostats (model 600, Gamry Instruments, Warminster, PA). The potential was swept ±10 mV above and below the corrosion potential ($E_{corr}$) at a rate of 0.125 mV/s. Tafel slope regions were used to extrapolate resistence polarization ($R_p$) values within ±5 mV of the $E_{corr}$. The instantaneous corrosion rate is derived by taking the inverse of the resistance polarization ($1/R_p$; $ohms^{-1}$ $cm^{-2}$). The LPR measurement was taken intermittently based on the metabolic activity measured within anaerobic incubations (below). Thus, the $1/R_p$ curves reflect various points along the curve shown in Figure 1. A $1/R_p$ value for each time point was selected based on the mean distribution of six LPR curves within the 30 minute measurement period. Finally, instantaneous corrosion rates were typically generalized as low <0.0254 millimeter per year (mmpy), moderate (0.0254-0.127 mmpy), or high (0.0254-0.508 mmpy) based on the $1/R_p$ logarithmic value (Figure 1).

**Cultivation of the hydrocarbon-degrading bacterium.** *Desulfoglaeba alkanexedens* strain ALDC (Davidova et al., 2006) is a marine alkane-degrading, sulfate-reducing bacterium, that can completely oxidize $C_6$-$C_{12}$ *n*-alkanes via the fumarate addition pathway. The bacterium can also syntrophically degrade the same suite of aliphatic hydrocarbons in a sulfate-free medium when co-cultured with the hydrogen/formate-

consuming methanogen, *Methanospirillum hungatei* strain JF-1 (Ferry et al., 1974). The mineral medium was prepared as previously described (McInerney et al., 1979), except rumen fluid and sulfate were omitted. The medium was amended with 10 ml/L of a trace metal and vitamin solution (Tanner, 2002), 0.0001% solution of resazurin as a redox indicator, sodium bicarbonate (24 mM), and 10 ml/L of a 2.5% solution of cysteine sulfide used as a reductant. The medium was dispensed into the electrochemical cells (50 ml) and inoculated with 20% transfers for the *D. alkanexedens* strain ALDC or *M. hungatei* strain JF-1 pure culture incubations or 10% transfers of each microorganism for the co-culture incubations. The mineral medium was the same for all axenic cultures or co-cultures, but the substrate, sulfate concentration, and headspace gas composition were adjusted for different incubation conditions (Table 1). The headspace for the axenic cultures of *M. hungatei* strain JF-1 was monitored and exchanged every 14 d to resupply $H_2/CO_2$ to support the hydrogenotrophic growth of the methanogen. Strict anaerobic conditions were maintained throughout the 44 d incubation period. Triplicate cultures were incubated at 32°C and monitored for corrosion with the potentiostats every 26 d after moving the cultures inside the anaerobic chamber. After each LPR measurement the culture bottles were resealed and the headspace exchanged to the appropriate atmosphere.

**Cultivation of the fatty acid-oxidizing syntroph.** *Syntrophus aciditrophicus* strain SB (Hopkins et al., 1995; Jackson et al., 1999) was used as a model culture to explore the corrosivity of fatty acid-oxidizing syntrophic bacteria. This bacterium metabolizes various saturated and unsaturated fatty acids, methyl esters of butyrate and hexanoate, benzoate, and alicyclic acids when in co-culture with a hydrogen/formate-consuming

microorganism (Mouttaki et al., 2007) including the methanogen *M. hungatei* strain JF-1 or the SRB, *Desulfovibrio sp*. strain G11 (McInerney et al., 1979). Its use of a primary sodium pump to create a chemostatic potential and to synthesize ATP using a sodium gradient mimics the bioenergetics scheme of many marine microorganisms (McInerney et al., 2007). Similarly, *M. hungatei* strain JF-1 also has the capacity to produce and use sodium gradients (Anderson et al., 2009). *S. aciditrophicus* strain SB can also be grown as a pure culture on crotonate whereupon it produces acetate, cyclohexane carboxylate, and benzoate as metabolic endproducts (Mouttaki et al., 2007). A basal medium was prepared as previously described (Tanner, 2002), and was amended with 10 ml/L trace metal and vitamin solution (Tanner, 2002), a 0.0001% solution of resazurin as a redox indicator, sodium bicarbonate (24 mM), and 20 ml/L of a 2.5% solution of cysteine sulfide used as a reductant. The medium was dispensed into the electrochemical cells (50 ml) and inoculuated with 20% transfers of *S. aciditrophicus* SB or *Desulfovibrio sp.* G11 pure cultures, or 10% transfers of each of the microorganisms for the syntrophic co-culture incubations. The basal medium was the same for all cultures and co-cultures, but the substrate, sulfate, and headspace atmosphere were adjusted depending on the desired incubation condition (Table 2). The headspace in autotrophically grown *Desulfovibrio sp.* strain G11 incubations was exchanged daily to resupply $H_2/CO_2$ to support the growth of this microorganism. Cultures were incubated in triplicate while medium controls were in duplicate. Incubations were held at 32°C and monitored electrochemically for the instantaneous corrosion rate as described above every 7 d (experiment 1) or 28 d (experiment 2) after

placing the cultures inside the anaerobic chamber. After each LPR measurement the culture bottles were resealed and the headspace exchanged to the original atmosphere.

**Spent medium experiments.** The corrositivity of the basal medium (Tanner, 2002) was assessed after amendment with various fatty acids with concentrations of crotonate and lactate ranging from 0 to 20 mM, as well as acetate ranging from 0 to 40 mM. These compounds were exogenously amended to mimic the concentration of substrates and endproducts produced by a crotonate grown co-culture of *S. aciditrophicus* strain SB and *Desulfovibrio sp.* strain G11 and lactate metabolism by a pure culture of *Desulfovibrio sp.* strain G11. Acetate was amended at a ratio of 2:1 for crotonate metabolism and 1:1 for lactate metabolism. To represent sulfide production within the uninocultated incubations sodium sulfide was amended at 10 mM and 20 mM concentrations. The pH for all incubations was ~7.0. The incubation conditions are described in Table 3. Duplicate uninoculated incubations were held at 32°C and monitored electrochemically every 17 d inside the anaerobic chamber as described above.

**Profilometry.** At the end of the incubation, the coupons were recovered and localized corrosion damage was assessed by counting pits using light profilometry (PS50 profilometer, Nanovea, Irvine, CA). The coupons were acid-cleaned to remove corrosion deposits according to ASTM standard method G1-03 (2003). The initial surface profiling of coupons was conducted by a cooperating external laboratory (Phillips 66, Bartlesville, OK, USA). However, a model PS50 profilometer (Nanovea, Irvine, CA) was eventually acquired for this purpose. Only the flat surface of the cylindrical coupons were analyzed for localized pitting evaluations. Line scans were

run at a data acquisition rate of 2000 Hz using a 300 μm optical pen at a 3.0 μm step size. All surface analysis was performed using 3D analysis software (Ultra v6.2 Nanovea, Irvine, CA). Pitting was defined as damage that was 20 μm below the mean surface plane and at least a 20 μm in diameter. These experimental parameters were chosen based on the mean distribution of collected surface points across all coupons analyzed.

**Analytical methods.** Crotonate loss was measured by HPLC (Dionex model IC-3000, Sunnyvale, CA) using an Alltech Prevail™ organic acid column (250mm × 4.6mm, particle size 5 μM; Grace, Deerfield, IL), and UV absorbance dector (Dionex model AD25, Sunnyvale, CA). The gradient pump was operated at a flow rate of 1.0 ml/min and mixed a mobile phase consisting of 60% (vol/vol) $KH_2PO_4$ (25 mM, pH 2.0) and 40% acetonitrile. The UV absorbance detector was set to 254 nm. Sulfate depletion was analyzed by ion chromatography (Dionex model IC-1000, Sunnyvale, CA) and methane production was monitored by gas chromatography (Packard model 427, Downers Grove, Ill.) and have been previously described (Lyles et al., 2013; Gieg et al., 2008).

## Results

### Anaerobic hydrocarbon biodegradation and the corrosion of carbon steel

There are many important ecological consequences associated with anaerobic hydrocarbon biodegradation in the environment. We used pure cultures and defined co-cultures to investigate the impact of this metabolism on one of the most important ecological consequences, the biocorrosion of carbon steel. *D. alkanexedens* strain ALDC and *M. hungatei* strain JF-1 were cultured axenically and as a syntophic partners

in the presence of carbon steel coupons. Coupon damage was assessed by periodically measuring the instantaneous corrosion rate during the course of the experiment and by surface profilometry at the end of the incubation period (Table 4).

After 44 d of incubation, *D. alkanexedens* strain ALDC cultured on *n*-decane reduced sulfate at a rate of 0.060 ± 0.014 mM $SO_4$•$day^{-1}$ (Figure S5) and produced an instantaneous corrosion rate of 7.8 x $10^{-3}$ ± 8.3 x $10^{-4}$ $ohms^{-1}$ $cm^{-2}$ (~0.381 mmpy; Figure 2). Approximately 18% of the *n*-decane was oxidized during the incubation period based on the amount of sulfate reduced within the incubation (data not shown). When *D. alkanexedens* strain ALDC and *M. hungatei* strain JF-1 were co-cultured on the same hydrocarbon, an average of 62.0 ± 22.5 µmol methane (Figure S6) was produced suggesting that ~ 0.2% of the parent hydrocarbon was utilized by the co-culture. The instantaneous corrosion rate for the co-culture was 7.0 x $10^{-4}$ ± 4.3 x $10^{-4}$ $ohms^{-1}$ $cm^{-2}$ (~0.0508 mmpy; Figure 2). Pure cultures of *M. hungatei* strain JF-1 cultured hydrogenotrophically ($H_2$/$CO_2$) produced ~1500 ± 700 µmol $CH_4$ over the initial 24 d incubation but the rate decreased with each headspace exchange over the entire incubation (Figure S7). The pure methanogen exhibited an instantaneous corrosion rate of 6.56 x $10^{-5}$ ± 4.4 x $10^{-5}$ $ohms^{-1}$ $cm^{-2}$ (<0.0254 mmpy); a value that was even lower than the comparable rate determination in the uninoculated control (1.01 x $10^{-4}$ ± 4.48 x $10^{-5}$ $ohms^{-1}$ $cm^{-2}$; <0.0254 mmpy).

When profilometry was used to assess localized corrosion in the coupons, differences between replicate incubations were evident (Table 4; Figure S8). One coupon replicate in the *D. alkanexedens* strain ALDC incubation exhibited substantial pitting (259 pits) while pits were not evident on the other replicate coupon despite

similar sulfate reduction (Figure S5) and instantaneous corrosion rates (Figure 2). Pitting was not as severe for coupon replicates incubated in the syntrophic co-culture. That is, 66 pits were counted on replicate one, 3 pits on replicate two, and 0 pits on replicate three. The pure culture incubation of *M. hungatei* strain JF-1 and the uninoculated control had 2 and 50 pits, respectively.

**Anaerobic fatty acid biodegradation and the corrosion of carbon steel**

The corrosion potential of the fatty acid-oxidizing syntroph, *S. aciditrophicus* strain SB, was evaluated in a similar manner by growing the bacterium, as a pure culture or in defined co-culture with *M. hungatei* strain JF-1 or *Desulfovibrio sp.* strain G11 (Table 4; Figure 3). The instantaneous corrosion rates were not substantially different between the pure culture of *S. aciditrophicus* strain SB and co-cultures *M. hungatei* strain JF-1 or *Desulfovibrio sp.* strain G11. However, localized corrosion increased when *S. aciditrophicus* strain SB was co-cultured with *Desulfovibrio sp.* strain G11 compared to when the syntroph was grown as a pure culture or when it was coupled with the methanogen (Table 4). Additionally, localized corrosion was also evident when coupons were exposed to pure cultures of *Desulfovibrio sp.* strain G11 grown in lactate-amended incubations with sulfate as the electron acceptor.

The instantaneous corrosion rates for pure cultures of *S. aciditrophicus* strain SB and related co-cultures are compared in Figure 3. Incubations containing axenic cultures of *S. aciditrophicus* strain SB were found to produce an instantanteous corrosion rate of $1.12 \times 10^{-3} \pm 9.65 \times 10^{-4}$ $ohms^{-1}$ $cm^{-2}$ (~0.0762 mmpy). In co-culture with *M. hungatei* strain JF-1, 15.65 ± 7.16 µmol methane was produced over the 16 d incubation period (Figure S9) and the instantaneous corrosion rate was $2.64 \times 10^{-3} \pm$

2.91 x $10^{-3}$ $ohms^{-1}$ $cm^{-2}$ (~0.178 mmpy). When co-cultured with *Desulfovibrio sp.* strain G11, the sulfate reduction rate was 0.34 ± 0.08 mM $SO_4$•$day^{-1}$ (Figure S10) and the instantaneous corrosion rate was 2.6 x $10^{-3}$ ± 1.19 x $10^{-3}$ $ohms^{-1}$ $cm^{-2}$ (~0.1524 mmpy). Uninoculated basal medium controls amended with 20 mM of crotonate had an instantaneous corrosion rate of 7.33 x $10^{-3}$ ± 2.01 x $10^{-3}$ $ohms^{-1}$ $cm^{-2}$ (~0.4318 mmpy). In all incubations containing *S. aciditrophicus* strain SB*,* crotonate was not detected by HPLC after 14 d of incubation (Figure S11). Additionally, the large standard deviations observed between $1/R_p$ values (Figure 3) associated with incubations of *S. aciditrophicus* strain SB and related co-cultures suggest that there is no difference in instantaneous corrosion rates, despite the formation of different metabolic endproducts (i.e. sulfide, methane, acetate) within each of the various incubation conditions.

Axenic incubations of *Desulfovibrio sp.* strain G11 cultured in the same media but amended with 20 mM of lactate produced an instantaneous corrosion rate of 1.5 x $10^{-3}$ ± 6.0 x $10^{-4}$ $ohms^{-1}$ $cm^{-2}$ (~0.089 mmpy; Figure 4). These incubations reduced sulfate at a rate of 2.00 ± 0.1 mM $SO_4$•$day^{-1}$ (Figure S10). The uninoculated media control containing 20 mM of lactate produced an instantaneous corrosion rate of 3.2 x $10^{-3}$ ± 6.0 x $10^{-4}$ $ohms^{-1}$ $cm^{-2}$ (~0.1778 mmpy; Figure 4). Thus, there is no significant difference for the instantaneous corrosion rates between *Desulfovibrio sp.* strain G11 and uninoculated control incubations. Additionally, when *Desulfovibrio sp.* strain G11 was cultured autotrophically with 138 kPa overpressure of $H_2/CO_2$ in the headspace as well as from hydrogen emanating from the metal surface, the sulfate reduction rate was 0.79 ± 0.04 mM $SO_4$•$day^{-1}$ and 0.35 ± 0.10 mM $SO_4$•$day^{-1}$, respectively (Figure S10). In all replicates of autotrophically-grown cultures of this microorganism, the

instantaneous corrosion rates (Figure 5) ranged between $5.17 \times 10^{-5} \pm 4.70 \times 10^{-5}$ and $5.51 \times 10^{-5} \pm 3.51 \times 10^{-5}$ ohms$^{-1}$ cm$^{-2}$ (<0.0208 mmpy), which is lower than the uninoculated controls containing either 138 kPa of $H_2/CO_2$ or $N_2/CO_2$ in the headspace ($1.02 \times 10^{-4} \pm 1.13 \times 10^{-4}$ ohms$^{-1}$ cm$^{-2}$).

Carbon steel coupons were assessed for localized corrosion using profilometry, and the numbers of pits counted from surface profiles (Figure S12) are compared in Table 4 (experiment 1). Even though pure cultures of *S. aciditrophicus* strain SB produced instantaneous corrosion rates of $10^{-3}$ and $10^{-4}$ only 2 pits were identified on the metal surface. When *S. aciditrophicus* strain SB was co-cultured with *Desulfovibrio sp.* strain G11 an average of 35 ± 2.6 pits were identified across the three replicates. Finally, when *S. aciditrophicus* strain SB was co-cultured with *M. hungatei* strain JF-1, one replicate produced 88 pits, while the other replicates had no detectable pits. When coupons were exposed to pure cultures of *Desulfovibrio sp.* strain G11 grown on lactate, replicate one had no pits, but replicates two and three had 23 and 12 pits, respectively. No pits were detected on coupons analyzed from incubations containing *Desulfovibrio sp.* strain G11 cultured under autotrophic conditions. Additionally, exposure to uninoculated medium amended with 20 mM crotonate caused one out of two metal samples to produce 45 pits.

Given the unexpectedly high level of variability encountered, the same experiments were repeated with the same degree of replication. With few exceptions, the instantaneous corrosion rates were largely in the $10^{-5}$ ohms$^{-1}$ cm$^{-2}$ range (Table 4 experiment 2; Figure S13) and pitting was mainly associated with the *S. aciditrophicus* strain SB and *Desulfovibrio sp.* strain G11 co-cultures (Table 4 experiment 2; Figure

S14). *S. aciditrophicus* strain SB alone or in co-culture with *Desulfovibrio sp.* strain G11 metabolized ~ 2 mM crotonate over the 30 d incubation (Figure S15) and the co-culture incubation reduced sulfate at 0.30 ± 0.08 mM $SO_4$•$day^{-1}$ (Figure S16). For comparison, *Desulfovibrio sp.* strain G11 cultured with lactate, $H_2/CO_2$ overpressure, or hydrogen emanating from the coupon reduced sulfate at 1.08 ± 0.006, 0.36 ± 0.06, and 0.16 ± 0.09 mM $SO_4$•$day^{-1}$, respectively (Figure S15). Thus, even though similar sulfate reduction rates were measured between cultures and co-cultures from experiment 1, the instantaneous corrosion rates as well as localized corrosion were substantially less within these repeat incubations (Table 4).

**Corrosivity of spent media**

The apparent corrosivity of uninoculated controls (Table 4) caused us to question the role of parent substrates and metabolic endproducts in exacerbating coupon damage. This prompted an experiment wherein acetate and sulfide were exogenously added to the sterile basal medium to simulate the concentration of these substances following the metabolism of crotonate by a co-culture of *S. aciditrophicus* strain SB and *Desulfovibrio sp.* strain G11. The same procedure was performed to simulate the products acetate and sulfide associated with lactate metabolism by *Desulfovibrio sp.* strain G11. These incubation conditions were chosen because localized corrosion was consistently assoicated with the production of acetate and sulfide. The results indicated that instantaneous corrosion rates typically ranged between $10^{-4}$ and $10^{-5}$ $ohms^{-1}$ $cm^{-2}$ and pitting was not detected on any of the metal surfaces (Table 4; Figures S17-S20).

## Discussion

Anaerobic hydrocarbon degradation is an important ecological process within petroleum-laden environments and one potential consequence of this metabolic activity is the sulfide-induced corrosion of carbon steel. However, the inherent complexity of the natural environment often makes it difficult to ascertain the biotic and abiotic factors that substantially influence biocorrosion. Our approach was to investigate this process in a more defined manner. That is, biocorrosion can be viewed as the interaction between electron donors of interest, a specific inoculum, the prevailing environmental conditions, and the composition of the metal (Suflita et al. 2013). Thus, we used defined microbial systems wherein the biological interactions with the electron donors were known and the metabolic endproducts could be reasonably anticipated. More specifically, we explored the impact of sulfate as an electron acceptor on metal biocorrosion in defined microbial assemblages and compared the damage to coupons when the same organisms were cultivated as syntrophic partnerships.

The corrosivity of the alkane-degrading, sulfate-reducing bacterium *D. alkanexedens* strain ALDC was previously assessed, and was found to produce higher instantaneous corrosion rates and more pits compared to an uninoculated medium control containing 20 mM sulfide (Suflita et al., 2013). Presumably, the production of sulfide by *D. alkanexedens* strain ALDC from *n*-decane oxidation was responsible for the increase in instantaneous corrosion rate and localized corrosion. In this study, when axenic incubations of *D. alkanexedens* strain ALDC were cultured on *n*-decane under sulfate reducing conditions, instantaneous corrosion rates were ~10 times higher than comparable pure cultures of *M. hungatei* strain JF-1 grown on $H_2/CO_2$ or in a co-culture

of the two microorganisms (Figure 2). Pitting also decreased when coupons were incubated with *M. hungatei* strain JF-1 alone or with the co-culture (Table 4; Figure S8). The biological replicates of *D. alkanexedens* strain ALDC pure culture incubations had similar sulfate reduction and instantaneous corrosion rates (Figure 2; Figure S5); however, despite theses similarities, the replicate incubations had a high variability in the number of pits observed on the individual coupons (Table 4). This result suggests that the coupons were differentially pitting even though the replicate incubations were biologically and chemically similar. Variability in localized corrosion was also observed in both the co-culture and the uninoculated control incubations, in which a single replicate produced pits under the respective incubation conditions (Table 4). This result suggested that pitting was not specifically a function of sulfide production, as this endproduct was not produced in either incubation. Nevertheless, coupon pitting under methanogenic conditions as well as with uninoculated controls was a relatively rare occurrence throughout our study. That is, one out of six coupons corroded under methanogenic conditions, while one out of twelve coupons corroded under uninoculated controls. For comparison, one out of every three coupons corroded under sulfate-reducing conditions.

Previous research has suggested that the acetate concentration can exacerbate carbon steel corrosion by multiple mechanisms (Hedges and Mcveigh, 1999; Garsany et al., 2003; Suflita et al., 2008; Crolet et al., 1999). At less than circumneutral pH values, at least some fraction of the acetate will exist acetic acid and cause direct damage to metal surfaces. Therefore, it may be that *S. aciditrophicus* strain SB can contribute to corrosion through the production of acetate from the metabolism of fatty acids as a pure

culture or when in syntrophic partnership. However, the instantaneous corrosion rates were not significantly different between axenic cultures of *S. aciditrophicus* strain SB and co-culture incubations with *M. hungatei* strain JF-1 or *Desulfovibrio sp.* strain G11 (Figure 3). However, when the coupons were subject to profilometric analysis, pitting was largely restricted to co-culture incubations of *S. aciditrophicus* strain SB and *Desulfovibrio sp.* strain G11 (Table 4 experiment 1; Figure S12). When *S. aciditrophicus* strain SB and *Desulfovibrio sp.* strain G11 co-culture incubations were repeated, instantaneous corrosion rates were substantially slower (Table 4 experiment 2; Figure S13), but pits were identified on all metal samples from the incubations (Table 4 experiment 2; Figure S14). Despite the 18 mM difference in crotonate metabolism between the experiments (Figure S11 and S15), the *S. aciditrophicus* strain SB and *Desulfovibrio sp.* strain G11 co-culture was the only incubation condition that produced localized corrosion in all six replicates. The results suggest that corrosion is likely increased due to the production of both acetate and sulfide during the metabolism of crotonate under sulfate reducing conditions.

The impact of lactate-grown *Desulfovibrio sp.* strain G11 on metal corrosion was similarly evaluated. This organism incompletely oxidizes lactate to acetate and uses sulfate as an external electron acceptor. Thus, if localized corrosion is at least a function of both acetate and sulfide production, pitting would be expected on the metal coupons. In fact, the results are largely consistent with this contention in that pitting occurred on metal surfaces in two of three replicate incubations (Table 4 experiment 1; Figure S12). Nevertheless, when these incubations were repeated, the instantaneous corrosion rates were substantially lower and no pits were evident by profilometry (Table

4 experiment 2; Figure S14) even though similar rates of sulfate reduction were measured between the two experiments (Figure S10 and S16). The variability in pitting behavior between replicate incubations and repeat experiments that exhibited similar rates of substrate utilization and metabolic endproduct formation is enigmatic. Since the biological activity and the resulting chemistry is both defined and controlled, we are forced to attribute the variability to incubation components we could not adjust. More specifically, we presume the variations can somehow be attributed to differences in the composition of the carbon steel coupons. However, according to the bulk analysis by the manufacturer, the coupons were compositionally similar (Table S1).

To exemplify, autotrophically cultured *Desulfovibrio sp.* strain G11 cultures are able to reduce sulfate at different rates depending on whether the coupon itself served as a hydrogen source or if the electron donor was supplied exogenously. In the latter case, the sulfate reduction rate was comparable to the co-culture of this organism with *S. aciditrophicus* strain SB (Figure S10 and S16). However, corrosion measures were substantially less with the pure culture relative to the co-culture, thus implicating acetate as a confounding factor in sulfide-induced corrosion. (Table 4 experiments 1 and 2). The only exception is one replicate from experiment two (Table 4), which produced an instantaneous corrosion rate of $10^{-3}$ $ohms^{-1}$ $cm^{-2}$ and had pitting on the side of the coupon (data not shown). Thus, only one metal coupon out of twelve substantially corroded upon exposure to autotrophically-grown *Desulfovibrio sp.* strain G11. Considering the relatively small amount of sulfide produced in these incubations (~2 mM), the lack of acetate production, and the relatively consistent levels of coupon

corrosion, differences in the corrosion behavior of a single replicate also point to potential differences in the coupons themselves.

Methanogens such as *Methanobacterium thermoautotrophicum* (Lorowitz et al., 1992) and *Methanococcus maripaludis* strain KA1 (Uchiyama et al., 2010) have been previously described to stimulate corrosion by either scavenging hydrogen or direct electron utilization from the surface of the metal coupons, respectively. *M. hungatei* strain JF-1 has not been reported to utilize either of these corrosion mechanisms, and when the metal was the only source of hydrogen in the incubation, methane production, instantaneous corrosion rates, and pitting were all negligible (data not shown) over the incubation period. Additionally, incubations of *M. hungatei* strain JF-1 amended with 138 kPa of $H_2/CO_2$ did not exacerbate corrosion on any metal sample (Table 4). However, *M. hungatei* strain JF-1 was associated with corrosion within two incubations. The first was in co-culture with *D. alkanexedens* strain ALDC (Table 4, replicate 1, 64 pits; Figure S8) and the second was in co-culture with *S. aciditrophicus* strain SB (Table 4 experiment 1, replicate 1, 88 pits; Figure S12). Considering methane production was similar between replicate incubations (Figures S6; Figure S9), the lack of sulfide production, and that pits were not detected on any other metal samples, the corrosion of these particular coupons are also attributed to the variability in the elemental composition of the metal sample.

Uninoculated media controls containing crotonate and lactate occasionally produced higher instantaneous corrosion rates (Figures 2 and 3) than the corresponding inoculated incubations and one replicate of a crotonate exposed coupon was found to have 45 pits at the end of the incubation (Table 4 experiment 1; Figure S12). Thus, we

concluded that the potential for metal corrosion due to exposure to various fatty acids could be important considering that formate, acetate, propionate, butyrate, and benzoate have all been detected in oil reservoirs with concentrations exceeding 20 mM (Magot et al., 2000). However, when comparable uninoculated controls were specifically evaluated, corrosion was found to be negligible (Table 4 experiment 2). Additionally, corrosion was not stimulated on metal samples that were exposed to uninoculated incubations amended with crotonate, lactate, acetate and sulfide to represent the spent medium of *S. aciditrophicus* strain SB and *Desulfovibrio sp.* strain G11 co-cultures as well as lactate-amended *Desulfovibrio sp.* strain G11 pure cultures (Table 4; Figures S17-S20). Thus, the differences between our initial observations and subsequent experimentation (Table 4) also seem to be a function of the variable nature of the coupons, despite identical manufacturer bulk analyses

Biocorrosion experiments exhibited high standard deviations for instantaneous corrosion rates and pitting for metal samples that was independent of inoculum type, biomass levels, initial substrate concentration, rates of microbial activity, or the degree of endproduct formation. Eliminating these factors as major contributors to the measured variability, forces us to attribute the large standard deviations to inconsistencies in the individual metal coupon samples. The bulk analysis of the metal from the manufacturer does not lend credence to this suggestion. However, low grade carbon steel is known to contain manganese sulfide inclusions (MnS) that are sites for pitting initiation and pit propagation (Vuillemin et al., 2003; Avci et al., 2013). The density of these submicron sized inclusions on carbon steel is typically thousands per square millimeter (Avci et al., 2013). It is unknown if the inclusions are evenly

(randomly) distributed in metal or if they are clustered (heterogeneous) to any degree. It also seems clear that some inclusions are more susceptible as sites of pit initiation than others (Wranglen, 1974; Davis, 2013). Thus, both the distribution and the reactivity of inclusion bodies within a metal sample could substantially influence corrosion processes and help explain why seemingly similar metal samples may behave differently in corrosion experiments.

There was generally no agreement between instantaneous corrosion rates and the number of pits; that is localized corrosion did not always occur on coupons with higher ($10^{-3}$ $ohms^{-1}$ $cm^{-2}$) $1/R_p$ values (Table 4; Figure 6). Electrochemical measurements, such as LPR are considered highly sensitive and accurate (<0.5% error; Jones, 1996) for monitoring generalized corrosion and profilometry can detect and quantify pits on a micron-scale. However, considering the electrochemistry and profilometry methods were not always in agreement, other methods of corrosion analysis would seem pertinent (e.g. weight loss, total iron determinations, manganese loss). Additionally, by differentially focusing our analysis on bulk fluids, the findings may not reflect reactions occurring in a biofilm on the metal surface. Localized metabolic activities in microbial biofilms, particularly the production of organic acids, can cause the pH to substantially decrease at the metal surface (Vroom et al., 1999). These points notwithstanding, our results generally show that localized corrosion was elevated when coupons were exposed to sulfide-producing cultures relative to methanogenic cultures or to uninoculated controls (Figure 6).

The major implications of this work are that the anaerobic biodegradation of hydrocarbons or associated fatty acid intermediates linked to sulfate reduction can have

important consequences with respect to the biocorrosion of carbon steel. That is, when sulfate is available as an electron acceptor, microbial assemblages will produce sulfide and low molecular weight organic acids that generally increase the corrosion of carbon steel. However, when the same organisms are in sulfate-limited environments and forced to live a syntrophic existence with a methanogen, biocorrosion is substantially reduced. These trends must be considered fairly general with more specific inferences being somewhat masked by the surprisingly high degree of variability associated with the corrosion assessments. Since the biological and chemical characteristics of the incubations were controlled, we were forced to attribute the high variability to differences with the metal samples themselves.

## References


Aktas, D. F., Lee, J. S., Little, B. J., Ray, R. I., Davidova, I. A., Lyles, C. N., and Suflita, J. M. (2010). Anaerobic metabolism of biodiesel and its impact on metal corrosion. *Energ. Fuel.* 24, 2924–2928.

Anderson, I., Ulrich, L. E., Lupa, B., Susanti, D., Porat, I., Hooper, S. D., Lykidis, A., Sieprawska-Lupa, M., Dharmarajan, L., Goltsman, E., et al. (2009). Genomic characterization of methanomicrobiales reveals three classes of methanogens. *PLoS One* 4, 1–9.

ASTM Standard G1-03 "Standard practice for preparing, cleaning, and evaluating corrosion test speciments" (2003). in *Corrosion of Metals; Wear and Erosion* (West Conshohocken, PA: ASTM International).

Avci, R., Davis, B. H., Wolfenden, M. L., Beech, I. B., Lucas, K., and Paul, D. (2013). Mechanism of MnS-mediated pit initiation and propagation in carbon steel in an anaerobic sulfidogenic media. *Corros. Sci.* 76, 267-274.

Bader, M. S. H. (2007). Sulfate removal technologies for oil fields seawater injection operations. *J. Pet. Sci. Eng.* 55, 93–110.

Blake, D. and Rowland, F. (1988). Continuing worldwide increase in tropospheric methane, 1978 to 1987. *Science* 239, 1129–1131.

Callaghan, A. V. (2013). Enzymes involved in the anaerobic oxidation of n-alkanes: from methane to long-chain paraffins. *Front. Microbiol.* 4, 1–9.

Cozzarelli, I. M., Baedecker, M. J., Eganhouse, R. P., and Goerlitz, D. F. (1994). The geochemical evolution of low-molecular-weight organic acids derived from the degradation of petroleum contaminants in groundwater. *Geochim. Cosmochim. Acta* 58, 863–877.

Crolet, J. L., Dugstad, A. L., and Thevenot, N. L. (1999). Role of free acetic acid on the $CO_2$ corrosion of steels. *Corrosion*, 1–16.

Davidova, I. A., Duncan, K. E., Choi, O. K., and Suflita, J. M. (2006). Desulfoglaeba alkanexedens gen. nov., sp. nov., an n-alkane-degrading, sulfate-reducing bacterium. *Int. J. Syst. Evol. Microbiol.* 56, 2737–2742.

Davis, B. H. (2013). MSc Thesis: Anaerobic pitting corrosion of carbon steel in marine sulfidogenic environment. Physics Department, Montana State University, pp 156.

Dinh, H. T., Kuever, J., Mußmann, M., Hassel, A. W., Stratmann, M., and Widdel, F. (2004). Iron corrosion by novel anaerobic microorganisms. *Nature* 427, 829–832.

Dolfing, J., Larter, S. R., and Head, I. M. (2008). Thermodynamic constraints on methanogenic crude oil biodegradation. *ISME J.* 2, 442–452.

Enning, D., Venzlaff, H., Garrelfs, J., Dinh, H. T., Meyer, V., Mayrhofer, K., Hassel, A. W., Stratmann, M., and Widdel, F. (2012). Marine sulfate-reducing bacteria cause serious corrosion of iron under electroconductive biogenic mineral crust. *Environ. Microbiol.* 14, 1772–1787.

Ferry, J. G., Smith, P. H., and Wolfe, R. S. (1974). Methanospirillum, a new genus of methanogenic bacteria, and characterization of Methanospirillum hangatii sp. nov. *Int. J. Syst. Bacteriol.* 24, 465–69.

Garsany, Y., Pletcher, D., and Hedges, B. (2003). The role of acetate in CO2 corrosion of carbon steel: studies related to oilfeild conditions. *Corrosion*, 1–15.

Gieg, L. M., Duncan, K. E., and Suflita, J. M. (2008). Bioenergy production via microbial conversion of residual oil to natural gas. *Appl. Environ. Microbiol.* 74, 3022–9.

Hamilton, W. A. (1985). Sulphate-Reducing Bacteria and Anaerobic corrosion. *Annu. Reveiw Microbiol.* 39, 195–217.

Head, I. M., Aitken, C. M., and Group, P. R. (2010). "Hydrocarbon Degradation in Petroleum Reservoirs," in *Handbook of Hydrocarbon and Lipid Microbiology*, ed. K. N. Timmis (Berlin, Heidelberg: Springer Berlin Heidelberg), 3098–3107.

Hedges, B., and Mcveigh, L. (1999). The role of acetate in $CO_2$ corrosion: the double whammy. *Corrosion,* 1-18.

Heider, J., and Schühle, K. (2013). "Anaerobic Biodegradation of Hydrocarbons Including Methane," in *The Prokaryotes*, eds. E. Rosenberg, E. F. DeLong, S. Lory, E. Stackebrandt, and F. Thompson (Berlin, Heidelberg: Springer Berlin Heidelberg), 605–634.

Hopkins, B. T., McInerney, M. J., and Warikoo, V. (1995). Evidence for anaerobic syntrophic benzoate degradation threshold and isolation of the syntrophic benzoate degrader. *Appl. Environ. Microbiol.* 61, 526–530.

Hubert, C., and Voordouw, G. (2007). Oil field souring control by nitrate-reducing Sulfurospirillum spp. that outcompete sulfate-reducing bacteria for organic electron donors. *Appl. Environ. Microbiol.* 73, 2644–52.

Jackson, B., Bhupathiraju, V., Tanner, R., Woese, C., and McInerney, M. (1999). Syntrophus aciditrophicus sp. nov., a new anaerobic bacterium that degrades fatty acids and benzoate in syntrophic association with hydrogen-using microorganisms. *Arch. Microbiol.* 171, 107–114.

Jenneman, G. E., McInerney, M. J., and Knapp, R. M. (1986). Effect of nitrate on biogenic sulfide production. *Appl. Environ. Microbiol.* 51, 1205–1211.

Jones, D. A. (1996). *Principles and Prevention of Corrosion*, eds. B. Stenquist, R. Kernan, and P. Daly. Upper Saddle River, NJ: Prentice Hall.

Jones, D. M., Head, I. M., Gray, N. D., Adams, J. J., Rowan, A. K., Aitken, C. M., Bennett, B., Huang, H., Brown, A., Bowler, B. F. J., et al. (2008). Crude-oil biodegradation via methanogenesis in subsurface petroleum reservoirs. *Nature* 451, 176–180.

Kermani, M. B., and Morshed, A. (2003). Carbon dioxide corrosion in oil and gas production—a compendium. *Corrosion* 59, 659–683.

King, R. A., and Miller, J. D. A. (1971). Corrosion by sulphate-reducing bacteria. *Nature* 233, 491–492.

King, R. A., Miller, J. D. A., and Smith, J. S. (1973a). Corrosion of mild steel by iron sulphides. *Br. Corros. J.* 8, 137–141.

King, R. A., Miller, J. D. A., and Wakerley, D. S. (1973b). Corrosion of mild steel in cultures of sulphate-reducing bacteria--effect of changing the soluble iron concentration during growth. *Br. Corros. J.* 8, 89–93.

King, R. A., and Wakerley, D. S. (1972). Corrosion of mild steel by ferrous sulphide. *Br. Corros. J.* 8, 41–45.

Lorowitz, W. H., Nagle, D. P., and Tanner, R. S. (1992). Anaerobic oxidation of elemental metals coupled to methanogenesis by Methanobacterium thermoautotrophicum. *Environ. Sci. Technol.* 26, 1606–1610.

Lyles, C. N., Aktas, D. F., Duncan, K. E., Callaghan, A. V, Stevenson, B. S., and Suflita, J. M. (2013). Impact of Organosulfur Content on Diesel Fuel Stability and Implications for Carbon Steel Corrosion. *Environ. Sci. Technol.* 47, 6052–6062.

Magot, M., Ollivier, B., and Patel, B. K. (2000). Microbiology of petroleum reservoirs. *A. Van Leeuw. J. Microb.* 77, 103–16.

Mayumi, D., Dolfing, J., Sakata, S., Maeda, H., Miyagawa, Y., Ikarashi, M., Tamaki, H., Takeuchi, M., Nakatsu, C. H., and Kamagata, Y. (2013). Carbon dioxide

concentration dictates alternative methanogenic pathways in oil reservoirs. *Nat. Commun.* 4, 1–6.

McInerney, M., Bryant, M., and Pfennig, N. (1979). Anaerobic bacterium that degrades fatty acids in syntrophic association with methanogens. *Arch. Microbiol.* 122, 129–135.

McInerney, M. J., Rohlin, L., Mouttaki, H., Kim, U., Krupp, R. S., Rios-Hernandez, L., Sieber, J., Struchtemeyer, C. G., Bhattacharyya, A., Campbell, J. W., et al. (2007). The genome of Syntrophus aciditrophicus: life at the thermodynamic limit of microbial growth. *P. Natl. Acad. Sci. USA.* 104, 7600–7605.

McInerney, M. J., Wofford, N. Q., and Sublette, K. L. (1996). Microbial control of hydrogen sulfide production in a porous medium. *Appl. Biochem. Biotechnol.* 57-58, 933–944.

Mouttaki, H., Nanny, M. A, and McInerney, M. J. (2007). Cyclohexane carboxylate and benzoate formation from crotonate in syntrophus aciditrophicus. *Appl. Environ. Microbiol.* 73, 930–938.

Nemati, M., Jenneman, G. E., and Voordouw, G. (2001). Impact of nitrate-mediated microbial control of souring in oil reservoirs on the extent of corrosion. *Biotechnol. Prog.* 17, 852–859.

Reiffenstein, R. J., Hulbert, W. C., and Roth, S. H. (1992). Toxicology of hydrogen sulfide. *Annu. Rev. Pharmacol. Toxicol.* 32, 109–134.

Van Stempvoort, D. R., Armstrong, J., and Mayer, B. (2007). Seasonal recharge and replenishment of sulfate associated with biodegradation of a hydrocarbon plume. *Ground Water Monit. R.* 27, 110–121.

Van Stempvoort, D. R., Millar, K., and Lawrence, J. R. (2009). Accumulation of short-chain fatty acids in an aquitard linked to anaerobic biodegradation of petroleum hydrocarbons. *Appl. Geochem.* 24, 77–85.

Struchtemeyer, C. G., Duncan, K. E., and McInerney, M. J. (2011). Evidence for syntrophic butyrate metabolism under sulfate-reducing conditions in a hydrocarbon-contaminated aquifer. *FEMS Microbiol. Ecol.* 76, 289–300.

Suflita, J. M., Lyles, C. N., Aktas, D. F., and Sunner, J. (2013). "Chapter 16: Biocorrosion issues associated with ultra low sulfur diesel and biofuel blends," in *Understanding Biocorrosion: Fundamentals & Applications* (Woodhead Publishing).

Suflita, J. M., Phelps, T. J., and Little, B. (2008). Carbon dioxide corrosion and acetate: a hypothesis on the influence of microorganisms. *Corrosion* 64, 854–859.

Tanner, R. S. (2002). “Cultivation of bacteria and fungi,” in *Manual of Environmental Microbiology*, eds. R. L. Crawford, G. R. Knudsen, M. J. McInerney, and L. D. Stetzenback (Washington, DC: ASM Press), 62–70.

Teske, A. (2010). “Sulfate-reducing and methanogenic hydrocarbon-oxidizing microbial communities in the marine environment,” in *Handbook of Hydrocarbon and Lipid Microbiology*, ed. K. N. Timmis (Berlin, Heidelberg: Springer Berlin Heidelberg), 2204–2216.

Uchiyama, T., Ito, K., Mori, K., Tsurumaru, H., and Harayama, S. (2010). Iron-corroding methanogen isolated from a crude-oil storage tank. *Appl. Environ. Microbiol.* 76, 1783–88.

Vroom, J. M., De Grauw, K. J., Gerritsen, H. C., Bradshaw, D. J., Marsh, P. D., Watson, G. K., Birmingham, J. J., and Allison, C. (1999). Depth penetration and detection of pH gradients in biofilms by two-photon excitation microscopy. *Appl. Environ. Microbiol.* 65, 3502–11.

Vuillemin, B., Philippe, X., Oltra, R., Vignal, V., Coudreuse, L., Dufour, L. C., and Finot, E. (2003). SVET, AFM and AES study of pitting corrosion initiated on MnS inclusions by microinjection. *Corros. Sci.* 45, 1143–1159.

Warikoo, V., McInerney, M. J., Robinson, J. A., and Suflita, J. M. (1996). Interspecies acetate transfer influences the extent of anaerobic benzoate degradation by syntrophic consortia. *Appl. Environ. Microbiol.* 62, 26–32.

Wranglen, G. (1974). Pitting and sulphide inclusions in steel. *Corros. Sci.* 14, 331–349.

**Acknowledgements**

This work was supported by a grant (Award No. N0001408WX20857) from the Office of Naval Research. We would also like to thank Karen Cloke of Phillips 66 for her assistance with the profilometry analysis.

**Table 1:** Substrate, sulfate, and headspace amendments for hydrocarbon-degrading incubations.

| Axenic or co-culture incubations | Substrate | Sulfate (mM) | Headspace atmosphere |
|---|---|---|---|
| *D. alkanexedens* ALDC | 1 ml *n*-decane | 20 | 138 kPa $N_2/CO_2$ (80:20) |
| *M. hungatei* JF-1 | $H_2/CO_2$ (138 kPa in ~40 mls of headspace) | - | 138 kPa $H_2/CO_2$ (5:95) |
| *D. alkanexedens* ALDC + *M. hungatei* JF-1 | 1 ml *n*-decane | - | 138 kPa $N_2/CO_2$ (80:20) |
| Uninoculated medium control | 1 ml *n*-decane | 20 | 138 kPa $H_2/CO_2$ (80:20) |

"-" = No amendment

**Table 2:** Substrate, sulfate, and headspace amendments for fatty acid-oxidizing incubations.

| Axenic or co-culture incubation | Substrate | Sulfate (mM) | Headspace atmosphere |
|---|---|---|---|
| *S. aciditrophicus* SB | 20 mM crotonate | - | 138 kPa $N_2/CO_2$ (80:20) |
| *S. aciditrophicus* SB + *Desulfovibrio sp.* G11 | 20 mM crotonate | 20 | 138 kPa $N_2/CO_2$ (80:20) |
| *S. aciditrophicus* SB + *M. hungatei* JF-1 | 20 mM crotonate | - | 138 kPa $N_2/CO_2$ (80:20) |
| *Desulfovibrio sp.* G11 (heterotrophic) | 20 mM lactate | 20 | 138 kPa $N_2/CO_2$ (80:20) |
| *Desulfovibrio sp.* G11 (autotrophic) | $H_2/CO_2$ (138 kPa in ~40 mls of headspace) | 20 | 138 kPa $H_2/CO_2$ (5:95) |
| *Desulfovibrio sp.* G11 (autotrophic) | $H_2$ from metal surface | 20 | 138 kPa $N_2/CO_2$ (80:20) |
| Uninoculated medium control | 20 mM crotonate | - | 138 kPa $N_2/CO_2$ (80:20) |
| Uninoculated medium control | 20 mM lactate | 20 | 138 kPa $N_2/CO_2$ (80:20) |
| Uninoculated medium control | - | 20 | 138 kPa $H_2/CO_2$ or 138 kPa $N_2/CO_2$ |

"-" = No amendment

**Table 3:** Uninoculated medium controls containing various concentrations of fatty acids and sulfide amended to represent crotonate metabolism by *S. aciditrophicus* strain SB or lactate metabolism by *Desulfovibrio sp.* strain G11.

| Crotonate metabolism | Lactate metabolism |
|---|---|
| 20 mM crotonate | 20 mM lactate |
| 10 mM crotonate + 20 mM acetate + 10 mM sulfide | 10 mM lactate + 10 mM acetate + 10 mM sulfide |
| 0 mM crotonate + 40 mM acetate + 20 mM sulfide | 0 mM lactate + 20 mM acetate + 20 mM sulfide |
| No amendment medium control | No amendment medium control |

**Table 4:** The number of pits and the instantaneous corrosion rates for replicates of the hydrocarbon-degrading and fatty acid-oxidizing cultures as well as the spent medium incubations. $1/R_p$ = ■ $10^{-5}$ ohms$^{-1}$ cm$^{-2}$, <0.0254 mmpy; ■ $10^{-4}$ ohms$^{-1}$ cm$^{-2}$, 0.0254-0.127 mmpy; ■ $10^{-3}$ ohms$^{-1}$ cm$^{-2}$, 0.0254-0.508 mmpy.

| Incubation condition (substrate amendment) | Number of pits + instantaneous corrosion rate ($1/R_p$) | | | | | | | | | | | |
|---|---|---|---|---|---|---|---|---|---|---|---|---|
| | Experiment 1 | | | | | | Experiment 2 | | | | | |
| | Replicate 1 | | Replicate 2 | | Replicate 3 | | Replicate 1 | | Replicate 2 | | Replicate 3 | |
| **Hydrocarbon-degrading cultures** | | | | | | | | | | | | |
| *D. alkanexedens* ALDC (*n*-decane) | ND | | 259 | | ND | | - | - | - | - | - | - |
| *D. alkanexedens* ALDC + *M. hungatei* JF-1 (*n*-decane) | 64 | | 3 | | ND | | - | - | - | - | - | - |
| *M. hungatei* JF-1 ($H_2/CO_2$) | 2 | | - | | - | | - | - | - | - | - | - |
| Uninoculated basal medium (*n*-decane) | 50 | | - | | - | | - | - | - | - | - | - |
| **Fatty acid-oxidizing cultures** | | | | | | | | | | | | |
| *S. aciditrophicus* SB (crotonate) | 1 | | ND | | 1 | | ND | | ND | | ND | |
| *S. aciditrophicus* SB + *M. hungatei* JF-1 (crotonate) | 88 | | ND | | ND | | - | - | - | - | - | - |
| *S. aciditrohpicus* SB + *Desulfovibrio sp.* G11 (crotonate) | 36 | | 37 | | 32 | | 158 | | 3 | | 32 | |
| *Desulfovibrio sp.* G11 (lactate) | ND | | 23 | | 12 | | ND | | ND | | ND | |
| *Desulfovibrio sp.* G11 ($H_2/CO_2$) | ND | | ND | | ND | | ND | | ND | | ND | |
| *Desulfovibrio sp.* G11 ($H_2$ from metal surface) | ND | | ND | | ND | | 1 | | ND | | ND* | |
| Uninoculated basal medium (crotonate) | ND | | 45 | | - | - | ND | | ND | | - | - |
| Uninoculated basal medium (lactate) | - | | - | | - | - | ND | | - | - | - | - |
| Uninoculated basal medium ($H_2/CO_2$) | ND | | ND | | - | - | ND | | ND | | - | - |
| **Spent medium incubations** | | | | | | | | | | | | |
| 20 mM crotonate | ND | | ND | | - | - | - | - | - | - | - | - |
| 10 mM crotonate + 20 mM acetate + 10 mM sulfide | ND | | ND | | - | - | - | - | - | - | - | - |
| 0 mM crotonate + 40 mM acetate + 20 mM sulfide | ND | | ND | | - | - | - | - | - | - | - | - |
| 20 mM lactate | ND | | ND | | - | - | - | - | - | - | - | - |
| 10 mM lactate + 10 mM acetate + 10 mM sulfide | ND | | ND | | - | - | - | - | - | - | - | - |
| 0 mM lactate + 20 mM acetate + 20 mM sulfide | ND | | ND | | - | - | - | - | - | - | - | - |
| Unamended basal medium control | ND | | ND | | - | - | - | - | - | - | - | - |

ND = Not detectable "-" = Replicate not done or data not available
*The metal had pitting on the side but could not be quantified by the profilometer

**Table S1:** Elemental composition of C1020 steel coupons used within this study. Two lots of the same type of metal samples were ordered and both had the exactly the same chemical and physical test report containing this elemental composition table. Lot one coupons were used in the *D. alkanexedens* strain ALDC incubations as well as the first experiment of *S. aciditrophicus* strain SB incubations. Lot two coupons were used in the repeat *S. aciditrophicus* strain SB experiment and also for the spent medium incubations.

| C | Mn | P | S | Si | Cu | Ni | Cr | Mo | V | Nb | N | Sn | Al | Ti | Ca | Zn | Co |
|---|---|---|---|---|---|---|---|---|---|---|---|---|---|---|---|---|---|
| .20 | .58 | .008 | .016 | .20 | .25 | .12 | .12 | .017 | .025 | .002 | .0091 | .008 | .003 | .00100 | .00140 | .00100 | .008 |

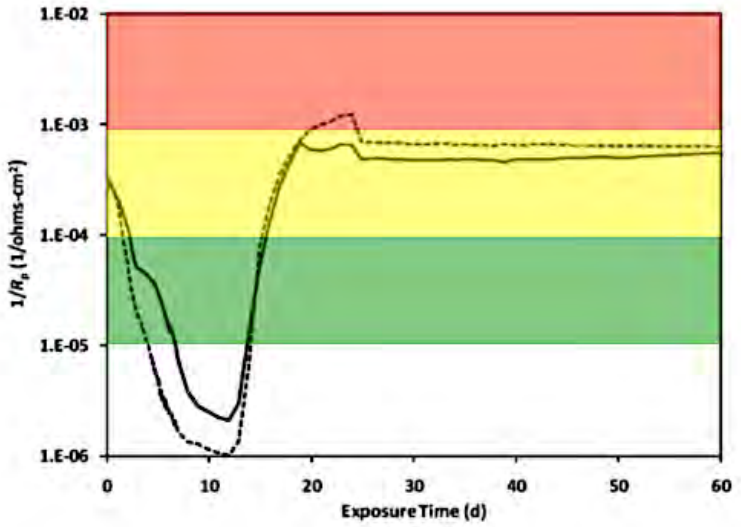


**Figure 1:** An instantaneous corrosion rate ($1/R_p$) curve adapted from Aktas et al. (2010) The basic shape of the curve represents the corrosion of C1020 metal over time. $1/R_p$ = ■ $10^{-5}$ $ohms^{-1}$ $cm^{-2}$, <0.0254 mmpy; ■ $10^{-4}$ $ohms^{-1}$ $cm^{-2}$, 0.0254-0.127 mmpy; ■ $10^{-3}$ $ohms^{-1}$ $cm^{-2}$, 0.0254-0.508 mmpy.

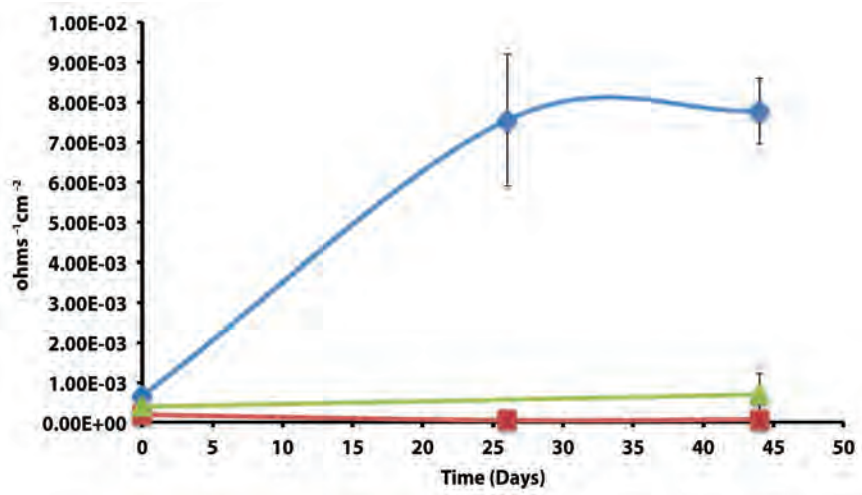


**Figure 2:** Instantaneous corrosion rates (1/Rp) for pure cultures of *D. alkanexedens* strain ALDC (◆) and *M. hungatei* strain JF-1 (■) as well as the syntrophic co-culture (▲) of the two microorganisms (standard deviation incubations *n*=3, axenic *D. alkanexedens* strain ALDC incubations *n*=2).

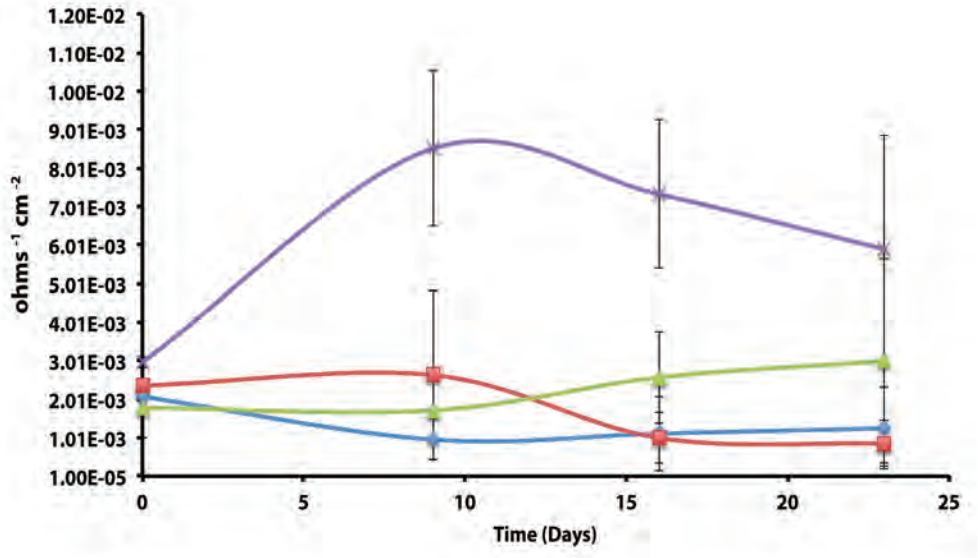


**Figure 3:** Instantaneous corrosion rates (1/Rp) for pure cultures of *S. aciditrophicus* strain SB (◆) and syntrophic co-cultures with *M. hungatei* strain JF-1 (■) and *Desulfovibrio sp.* strain G11 (▲) as well as an uninoculated basal medium controls amended with 20 mM of crotonate (×) (standard deviation incubations *n*=3, medium controls *n*=2).

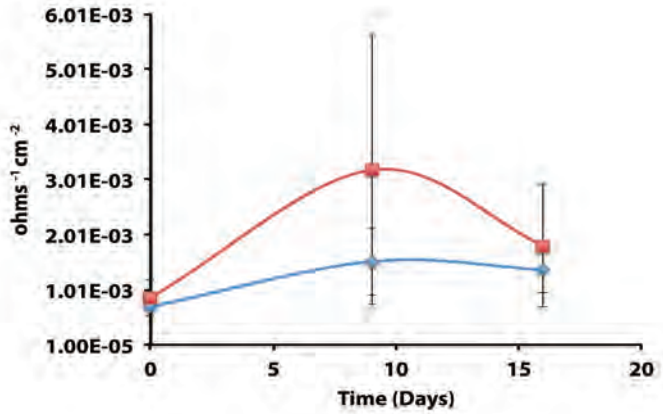


**Figure 4:** Instantaneous corrosion rates (1/Rp) for lactate-amended pure cultures of *Desulfovibrio sp.* strain G11 (◆) and uninoculated basal medium controls amended with 20 mM lactate (■) (standard deviation incubations *n*= 3, medium controls *n*= 2).

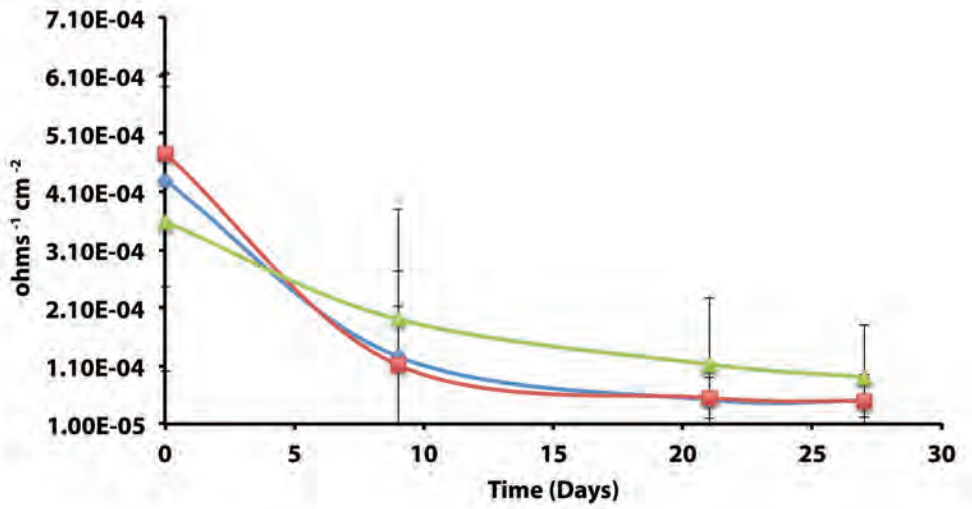


**Figure 5:** Instantaneous corrosion rates (1/Rp) for axenic incubations of *Desulfovibrio sp.* strain G11 cultured autotrophically on 138 kPa of $H_2/CO_2$ (◆) and hydrogen from the metal surface (■), as well as an uninoculated basal medium controls (▲) amended with 138 kPa of $H_2/CO_2$ or $N_2/CO_2$ (standard deviation incubations *n*= 3, medium controls *n*= 2).

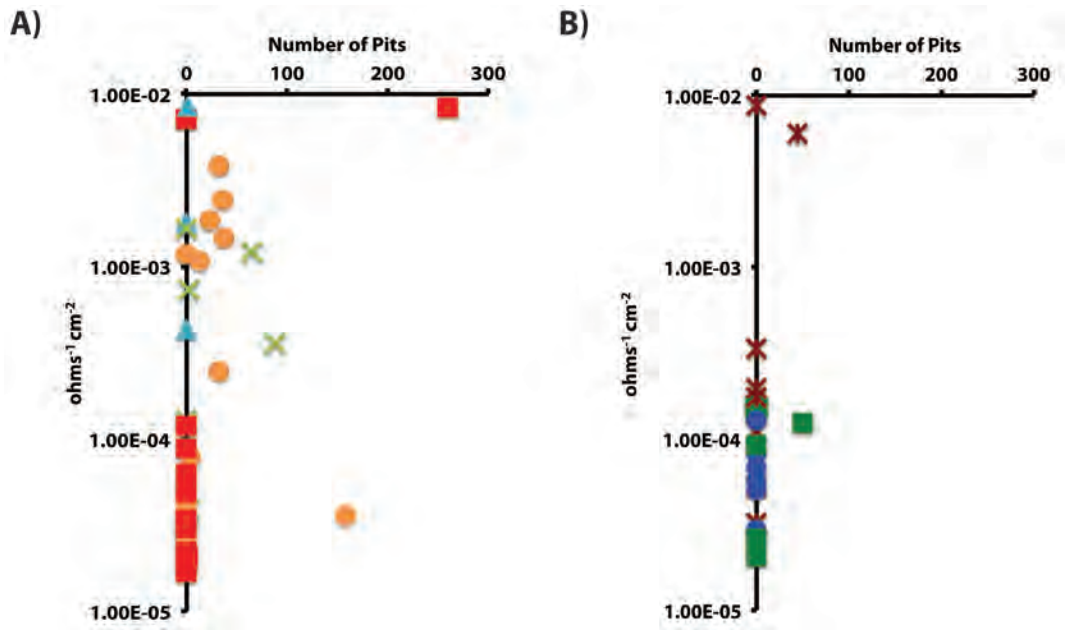


**Figure 6**: The impact of A) microbial cultures producing sulfide and acetate (●), sulfide only (■), acetate only (▲), and methane (×) on localized corrosion. Compared to B) uninoculated medium controls amended with crotonate (✱), lactate (●), or no VFA (■).


**Figure S1:** A 100 ml culture bottle used as an electrochemical cell during corrosion experiments with *D. alkanexedens* strain ALDC and *S. aciditrophicus* strain SB pure cultures and related co-cultures.

**Figure S2:** A number six-rubber stopper modified to hold a graphite counter electrode and a luggin probe (bridge tube) for the saturated calomel reference electrode.

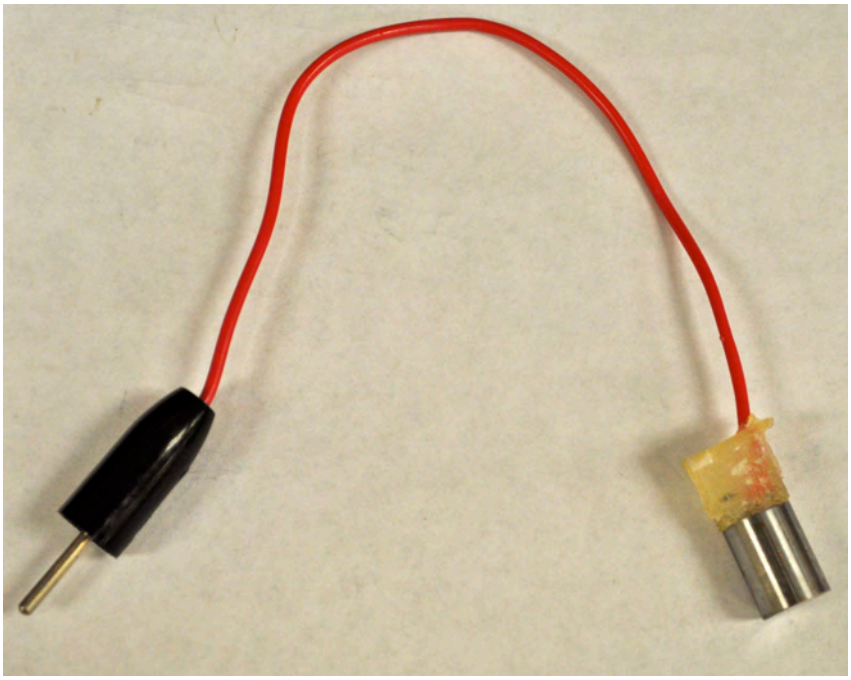

**Figure S3:** A C1020 working electrode. The wire was attached to the coupon using rosin core solder and epoxy sealed to prevent galvanic corrosion. The electrode pin (black) connects to the corresponding alligator clip from the potentiostat. This was incubated within the culture bottles during the experimental time.

**Figure S4:** Complete electrochemical cell assembly inside the anaerobic chamber. Culture bottles were periodically brought into the anaerobic chamber and opened so that the sterile stopper assembly (Figure S2) could be placed inside the incubation. Corrosion was monitored using LPR curves taken every 5 minutes for a 30 minute period. Once complete the culture bottles were resealed with sterile stoppers and the headspace exchanged to the appropriate atmosphere.

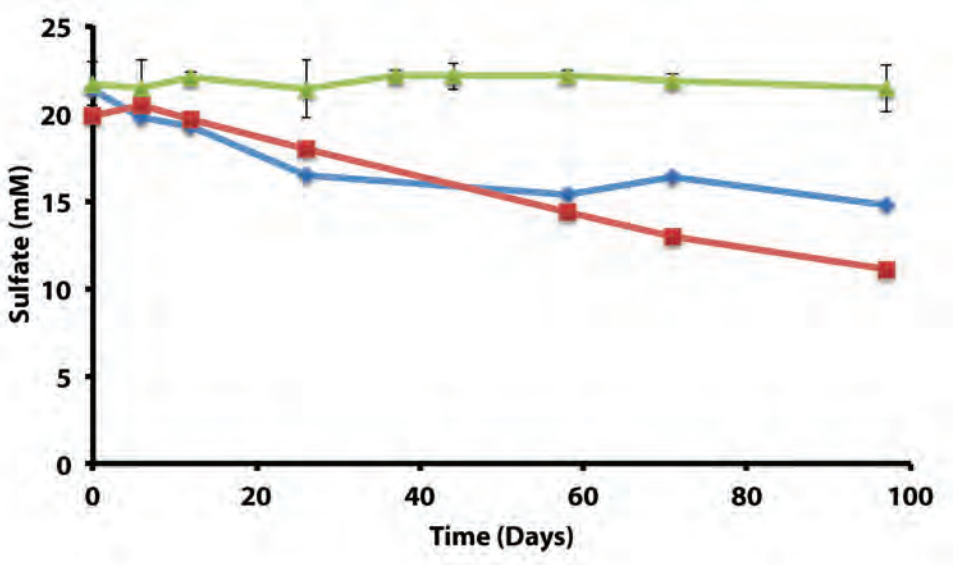


**Figure S5:** Sulfate reduction observed in axenic incubations of *D. alkanexedens* strain ALDC cultures replicates one (◆) and two (■). No sulfate loss was observed in uninoculated medium controls (▲; standard deviation *n*=3).

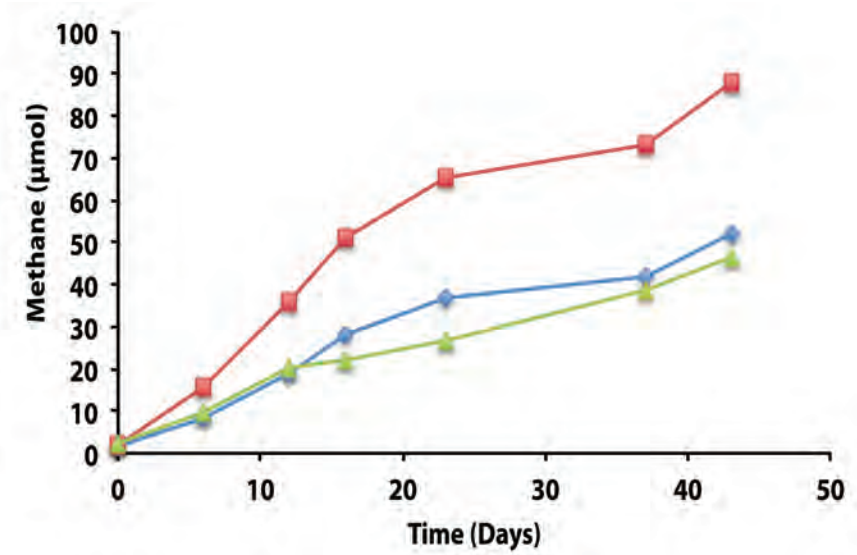


**Figure S6:** Methane production observed in co-culture incubations of *D. alkanexedens* strain ALDC and *M. hungatei* strain JF-1. Replicate 1 (◆) Replicate 2 (■) Replicate 3 ( ▲)

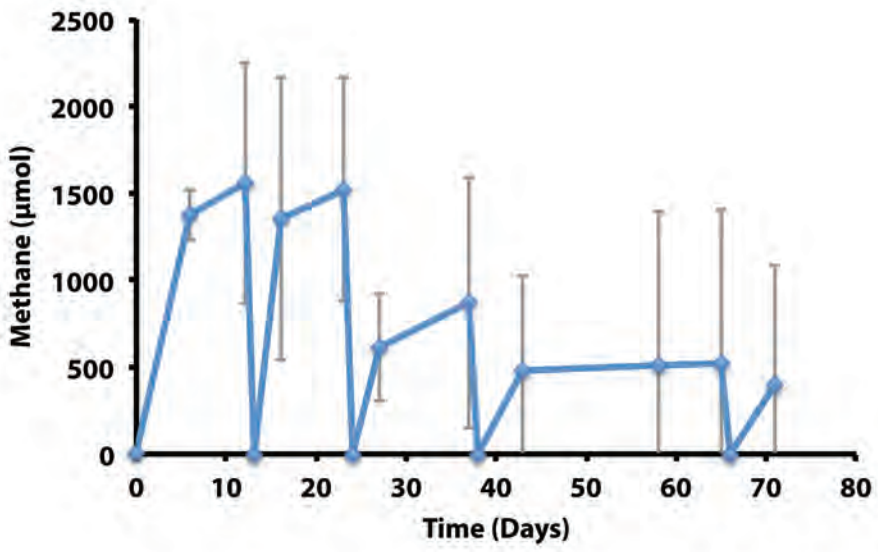


**Figure S7:** Methane production from pure cultures of *M. hungatei* strain JF-1 (◆) amended with 138 kPa of $H_2/CO_2$. The methane decreased to zero during the incubation because the headspace was periodically exchanged and repressurized with $H_2/CO_2$. Methane was not detected in uninoculated controls (standard deviation $n$=3).

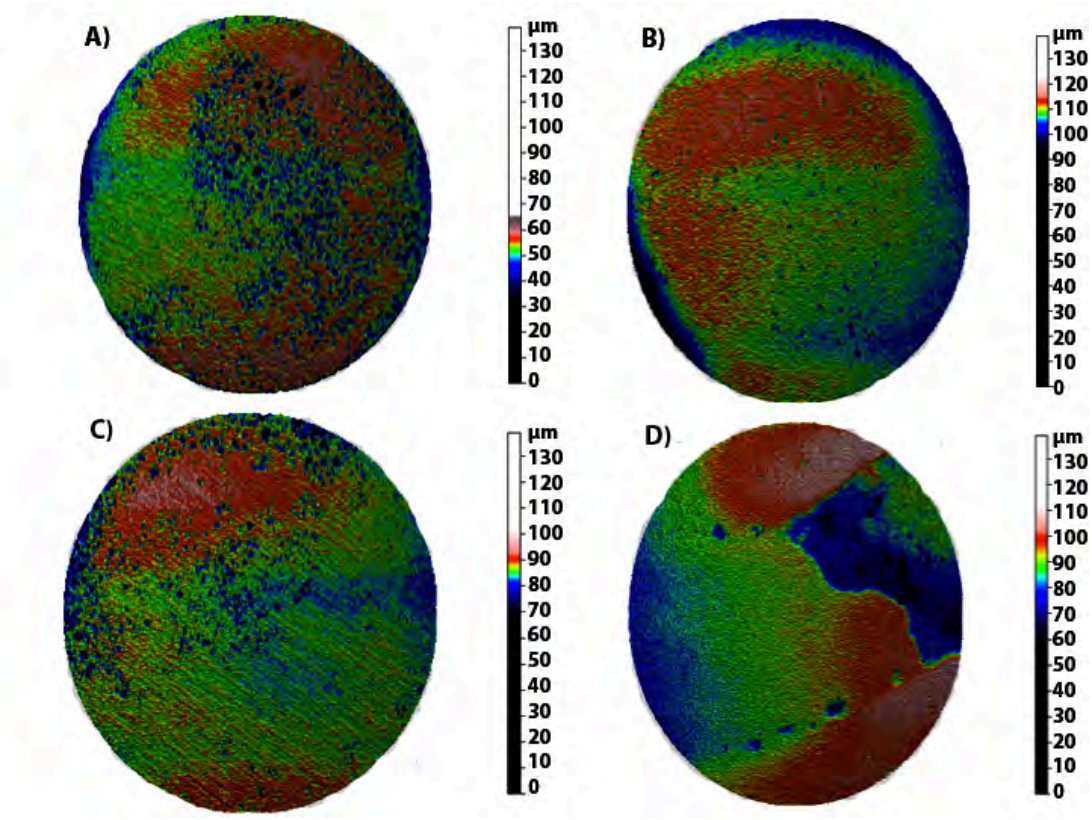


**Figure S8:** Surface profiles of C1020 metal coupons exposed to pure cultures of A) *D. alkanexedens* strain ALDC B) *M. hungatei* strain JF-1 as well as a C) syntrophic co-culture of the two microorganisms and a D) media culture. The profilometry scanning was done at Phillips 66 (Bartlesville, OK, USA) surface analysis was done at the University of Oklahoma.

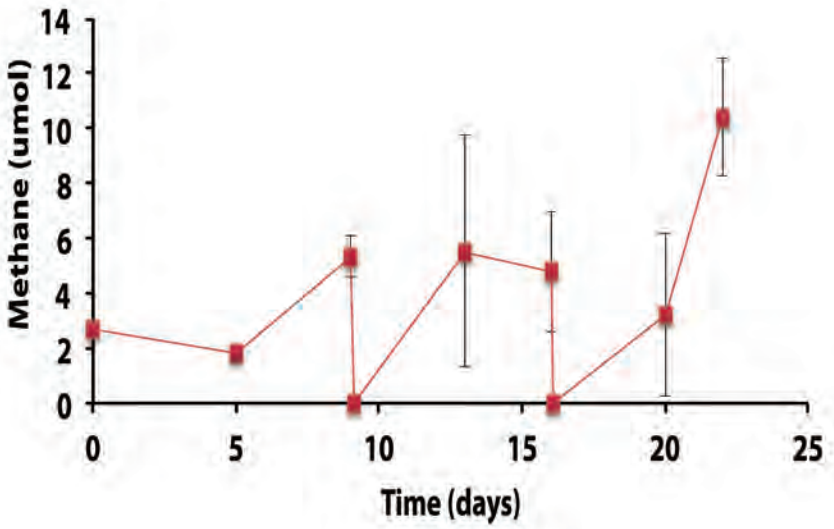


**Figure S9**: Methane production from co-cultures of *S. aciditrophicus* strain SB and *M. hungatei* strain JF-1 (■). When methane decreased to zero, the cultures were opened to take LPR measurements within the anaerobic chamber. Methane was not detected in uninoculated controls (standard deviation *n*=3).

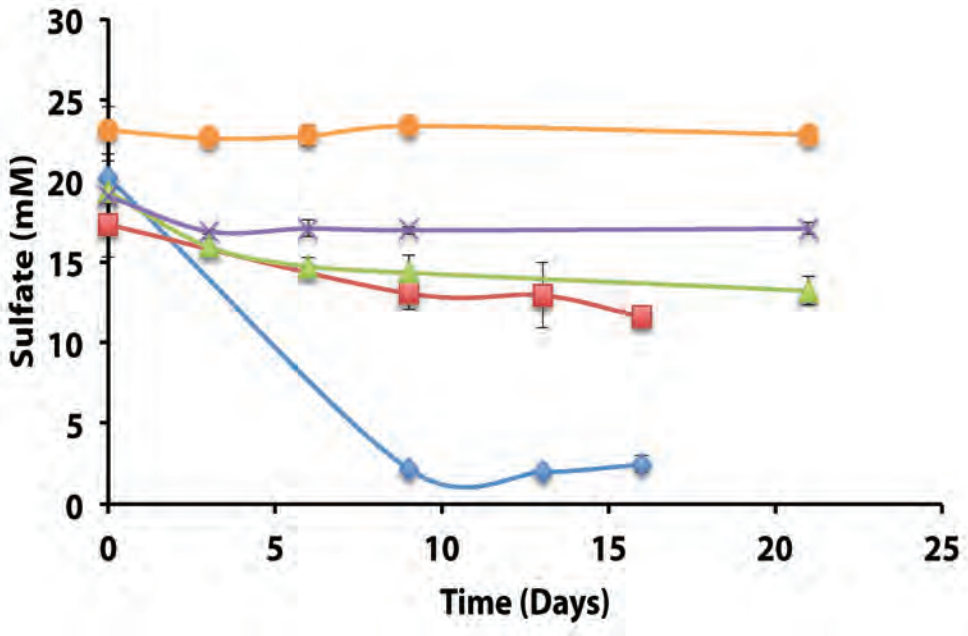


**Figure S10:** Sulfate reduction observed during experiment one in axenic *Desulfovibrio sp.* strain G11 cultures amended with lactate (◆), 138 kPa of $H_2/CO_2$ (▲), hydrogen from the metal surface (×), and co-cultured with *S. aciditrophicus* strain SB (■). Uninoculated basal medium controls (●) were also monitored but no sulfate depletion was observed (standard deviation $n$=3).

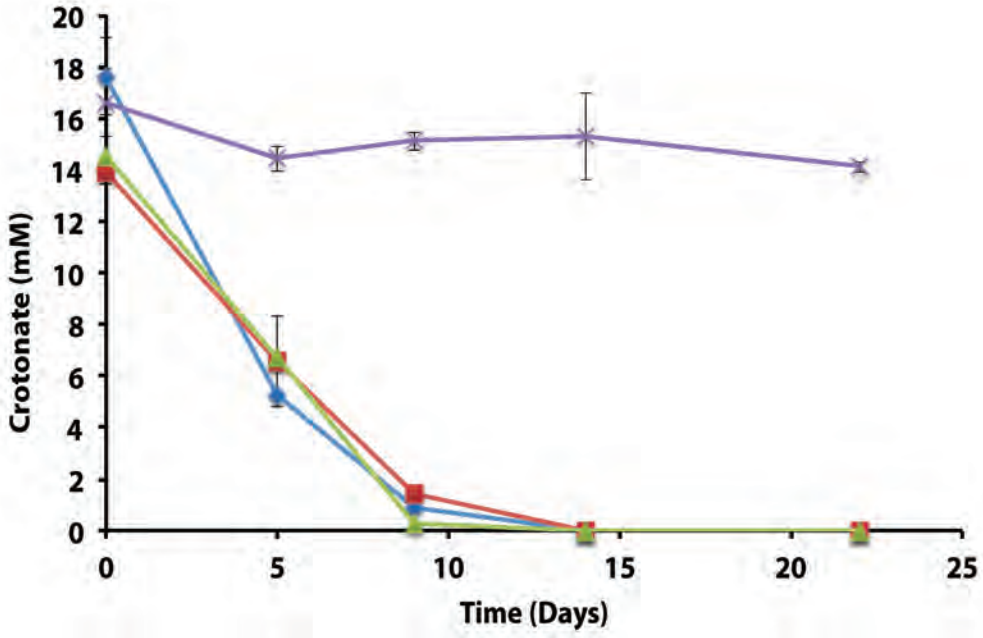


**Figure S11:** Crotonate depletion observed during experiment one in *S. aciditrophicus* strain SB incubations cultured axenically on crotonate (◆), in co-culture with *M. hungatei* strain JF-1 (■), and in co-culture with *Desulfovibrio sp.* strain G11 (▲). No crotonate loss was observed in uninoculated basal medium controls (×) (standard deviation *n*=3).

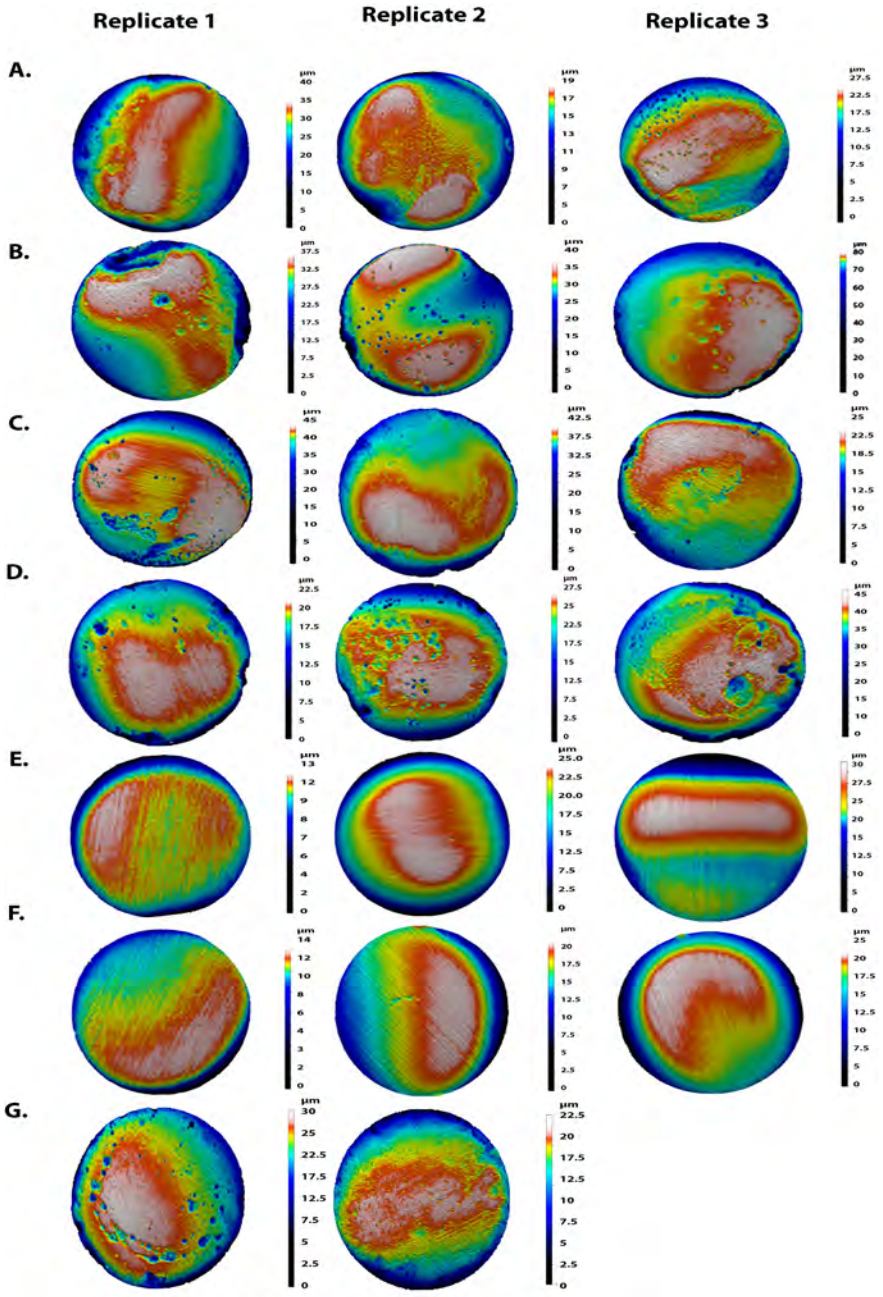


**Figure S12:** Surface profiles of C1020 metal coupons from experiment one exposed to pure cultures of A) *S. aciditrophicus* strain SB and co-cultures with B) *Desulfovibrio sp.* strain G11 and C) *M. hungatei* strain JF-1. Additionally, *Desulfovibrio sp*. strain G11 was cultured axenically on D) lactate, E) 138 kPa of $H_2/CO_2$, and F) on hydrogen from the metal surface. Also shown is an uninoculated medium control G) amended with 20 mM of crotonate.

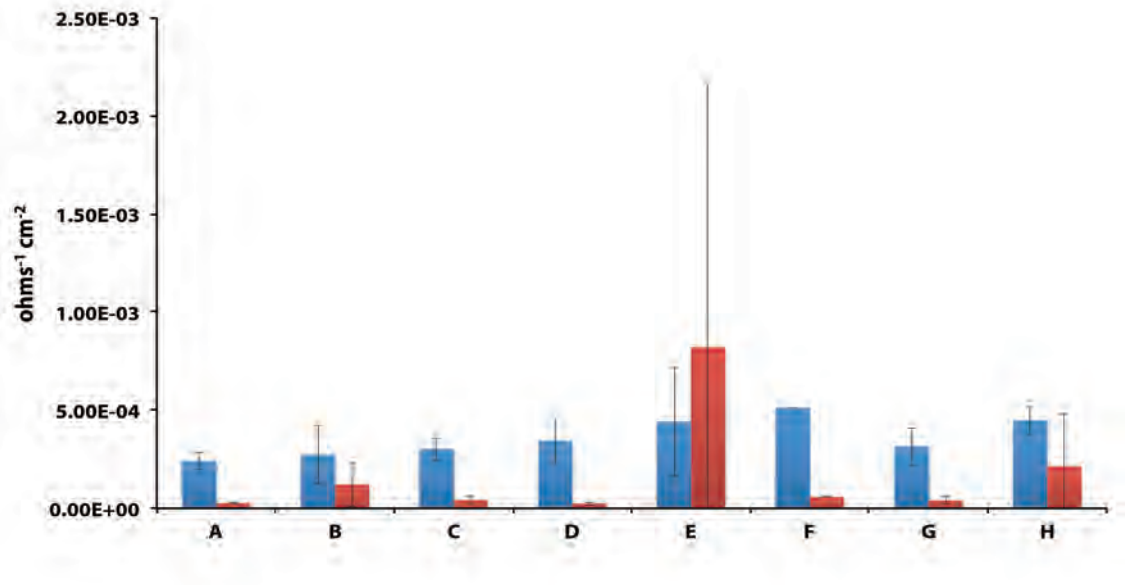


**Figure S13:** Instantaneous corrosion rates ($1/R_p$) for experiment two at time 0 (■) and after 28 days (■) for incubations of *S. aciditrophicus* strain SB axenically cultured on A) crotonate and B) co-cultured with *Desulfovibrio sp.* strain G11, as well as *Desulfovibrio sp.* strain G11 cultured axenically on C) lactate, D) 138 kPa of $H_2/CO_2$, and E) hydrogen from the metal surface. Additionally, uninoculated basal media amended with F) 20 mM of lactate G) 20 mM of crotonate, and H) 138 kPa of $H_2/CO_2$ or $N_2/CO_2$ were also monitored for corrosion.

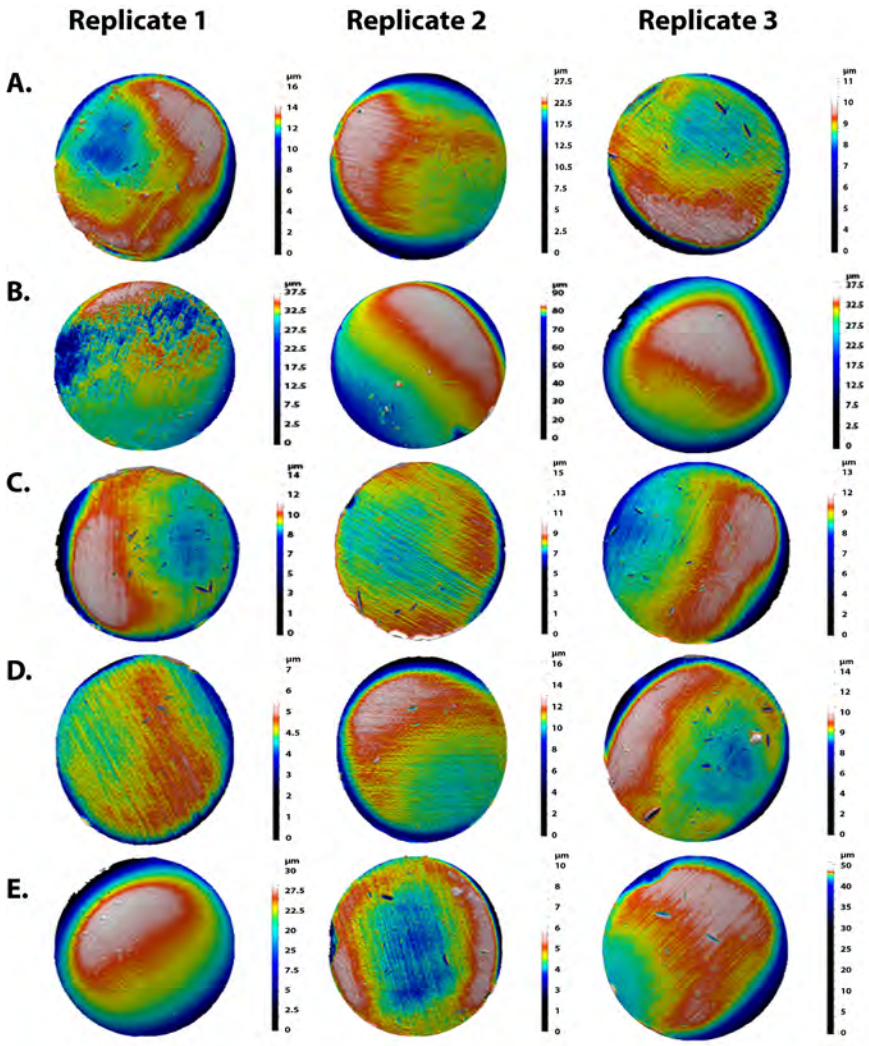


**Figure S14:** Surface profiles of C1020 metal coupons from experiment two exposed to pure cultures of A) *S. aciditrophicus* strain SB and co-culture incubations with B) *Desulfovibrio sp.* strain G11. Additionally, *Desulfovibrio sp*. strain G11 was axenically cultured on C) lactate, D) 138 kPa of $H_2/CO_2$, and E) on hydrogen from the metal surface. Replicate 3 from *Desulfovibrio sp.* strain G11 autotrophically cultured on hydrogen from the metal surface had pitting on the sides of the metal sample but the profilometer could not quantify the damage due to the curvature nature of the coupon.

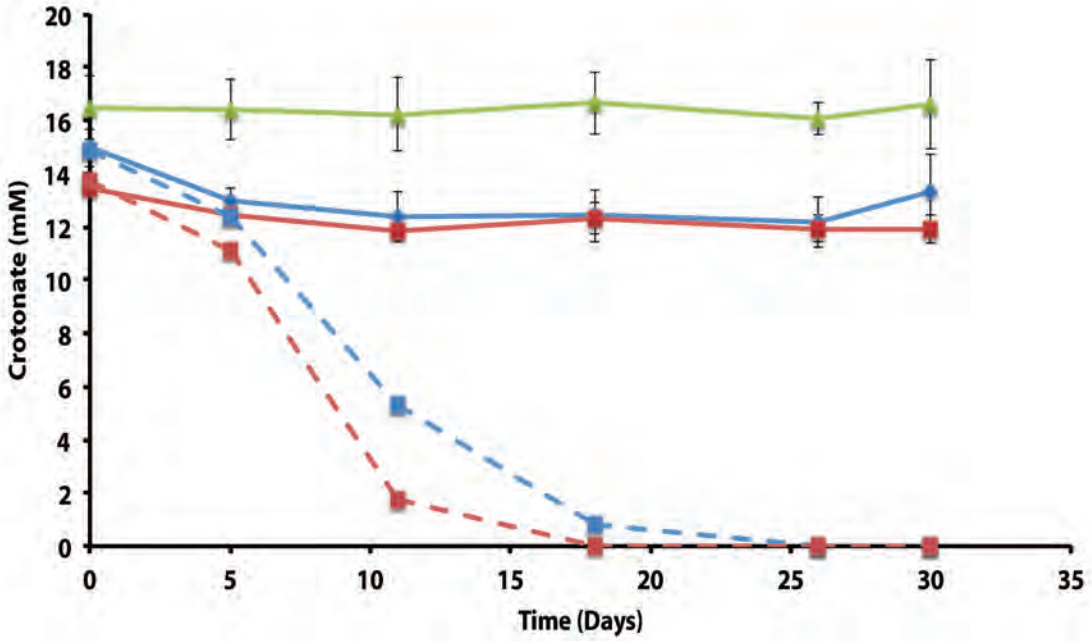


**Figure S15:** Crotonate depletion observed in experiment two for *S. aciditrophicus* strain SB incubations cultured axenically on crotonate (◆) and in co-culture with *Desulfovibrio sp.* strain G11 (■). No crotonate loss was observed in uninoculated basal medium controls (▲) (standard deviation *n*=3). For incubations that did not contain metal samples (positive controls) crotonate was not detectable after ~18 days in axenic cultures of *S. aciditrophicus* strain SB (blue dashed line ■) and the co-culture with *Desulfovibrio sp.* strain G11 (red dashed line ■).

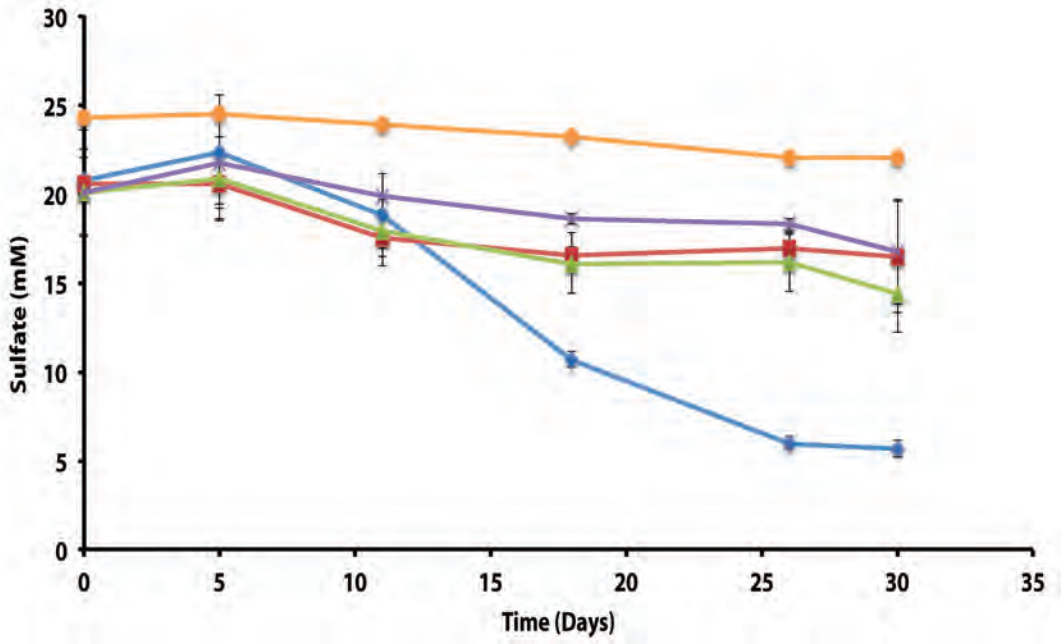


**Figure S16:** Sulfate reduction observed during experiment two with axenic *Desulfovibrio sp.* strain G11 cultures amended with lactate (◆), 138 kPa of $H_2/CO_2$ (▲), hydrogen from the metal surface (×), and in co-culture with *S. aciditrophicus* strain SB (■). No sulfate depletion was observed in uninoculated basal medium controls (●) (standard deviation *n*=3).

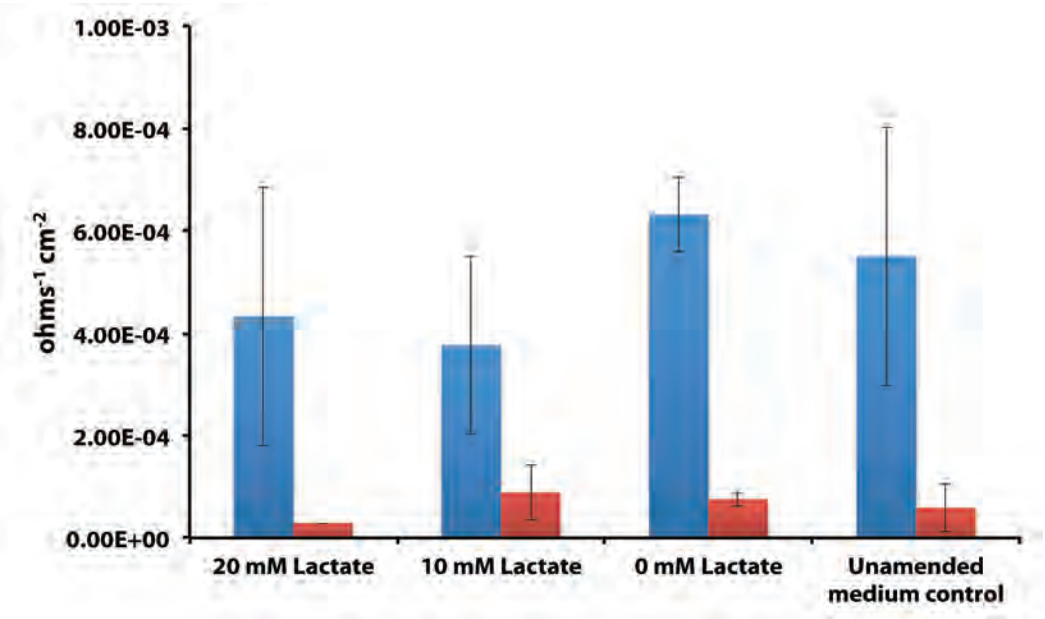


**Figure S17:** Instantaneous corrosion rates ($1/R_p$) at time 0 (■) and after 17 days (■) for uninoculated incubations containing exogenous amendments of lactate, acetate, and sulfide (standard deviation $n$=2).

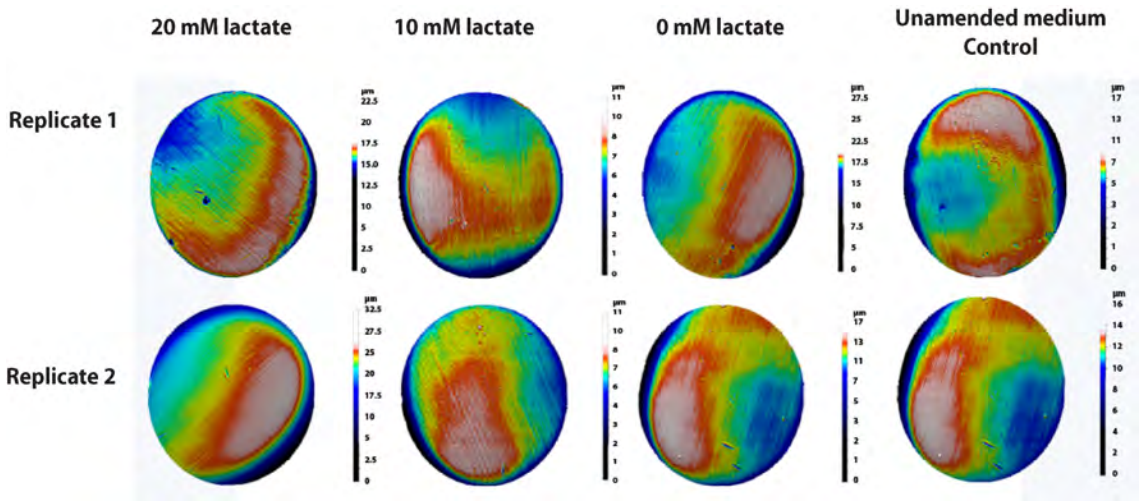


**Figure S18:** Surface profiles for metal samples associated with uninoculated incubations containing exogenous amendments of lactate, acetate, and sulfide.

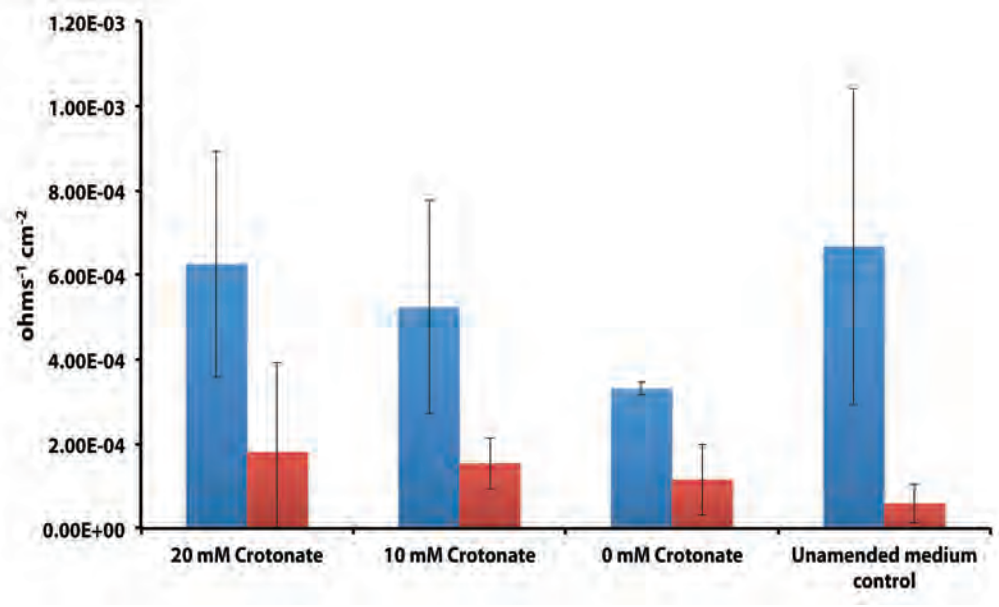


**Figure S19:** Instantaneous corrosion rates ($1/R_p$) rates at time 0 (■) and after 17 days (■) for uninoculated incubations containing exogenous amendments of crotonate, acetate, and sulfide (standard deviation $n$=2).

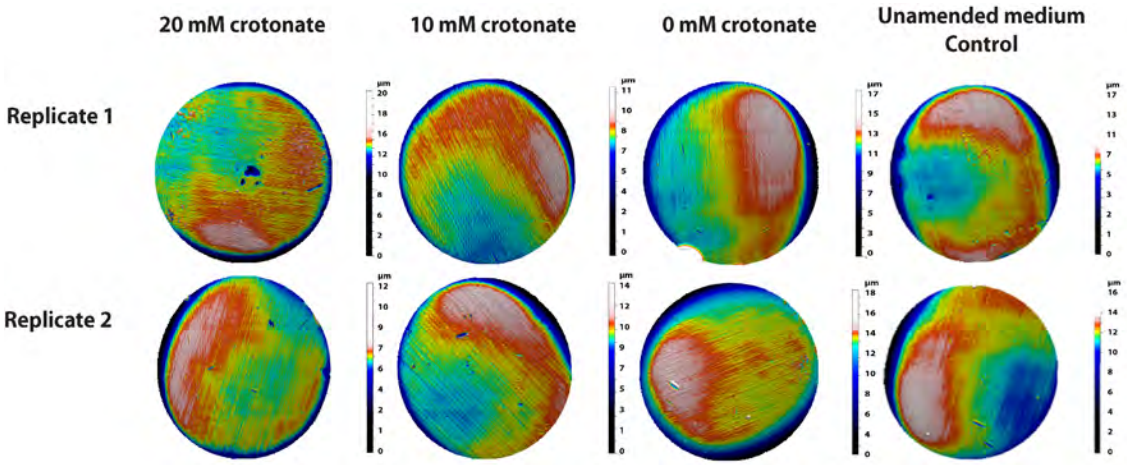


**Figure S20:** Surface profiles for metal samples associated with uninoculated incubations containing exogenous amendments of crotonate, acetate, and sulfide.

# Appendix A: Anaerobic metabolism of biodiesel and its impact on metal corrosion


## Abstract

Biodiesels have gained widespread acceptance because they are domestically produced carbon-neutral fuels that ultimately decrease greenhouse gas emissions and reduce dependence on fossil imports. While they are chemically and physically stable fuels, their susceptibility to biological degradation in the absence of oxygen is underexplored. We incubated five anaerobic inocula with biodiesel. The microorganisms originated from fresh and marine environments with differing histories of exposure to hydrocarbons, biodiesel, and oxygen. All inocula were able to biodegrade biodiesel within 1 month. Biodiesel metabolism accelerated the rate of both sulfate reduction and methanogenesis above biodiesel-unamended controls. Metabolite profiling indicated that the methyl esters of biodiesel were readily hydrolyzed to the corresponding suite of fatty acids, and the latter were also metabolized. Electrochemical/corrosion experiments showed that the anaerobic microbial metabolism of biodiesel in coastal seawater samples accelerated the rate of pitting corrosion in carbon steel. The susceptibility of biodiesel to anaerobic biodegradation and its propensity to stimulate biocorrosion suggest caution when integrating this alternate fuel with the existing infrastructure.

## Reference

Aktas, D.F. Lee, J.S., Little, B.J., Ray, R.I., Davidova, I.A., Lyles, C.N., Suflita, J.S. 2010. Anaerobic Metabolism of Biodiesel and Its Impact on Metal Corrosion. *Energy & Fuels*, 24(5), 2924–2928.

# Appendix B: Biocorrosion issues associated with ultra low sulfur diesel and biofuel blends


## Abstract

Microorganisms catalyze multiple mechanisms of biocorrosion throughout the carbon steel energy infrastructure. We contend that the primary energy source(s) supporting the proliferation of biocorrosive biofilms are the energy constituents themselves. As societies alter their formulations to make fuels more environmentally acceptable, they can impact biocorrosion in unanticipated ways. For instance, the removal of organosulfur compounds from fuel had relatively little effect on stability, while additives like biodiesel biodegrade rapidly and exacerbate corrosion problems. Biocorrosion can thus be viewed as the interplay between a metal surface, the predominant carbon and energy source in the environment and the availability of an inoculum capable of growth under the prevailing ecological conditions.

## Reference

Suflita, J.M., Lyles, C.N., Aktas, D.F., Sunner, J. 2013. Chapter 16: Biocorrosion issues associated with ultra low sulfur diesel and biofuel blends. In *Understanding Biocorrosion: Fundamentals & Applications*. Woodhead Publishing.

# Appendix C: Methane formation from residual oil, shale and coal: potential importance and biocorrosion aspects


## Abstract

There is an ever-increasing demand for energy to supply a burgeoning world population. Meeting such energy challenges in an environmentally acceptable manner is likely to require a reexamination of how conventional resources are utilized as well as the exploitation of unconventional assets. Examples are provided of the use of biotechnology to convert residual oil from a marginal reservoir, organic matter from several shale deposits and coal to methane. Inoculation with an oil-degrading methanogenic consortium was utilized in all cases, but required with the marginal oil and shale experiments. For coal, the best results were obtained when the fossil substrate was initially oxidized with ozone followed by incubation with the consortium. The relationship of such transformations to metal biocorrosion was probed with a hydrocarbonoclastic sulfate reducing bacterium. When grown as a pure culture with sulfate as an electron acceptor, hydrocarbon was oxidized, sulfate was reduced, sulfide was produced and the corrosion of carbon-steel was elevated. However, when grown syntrophically using a methanogen as an electron acceptor, biocorrosion was minimal. Collectively, the results help illustrate how the interconversion of plentiful domestic energy reserves to methane could potentially play an important role in addressing global energy needs and yet minimize apprehension associated with biocorrosion.

## Reference

Suflita, J.M., Gieg L., Mendivelso M., Lyles, C.N. 2012. Methane Formation from Residual Oil, Shale and Coal: Potential Importance and Biocorrosion Aspects. In *Proceedings of the VI International Scientific Conference: Microbial Biodegradation and Biodeterioration of Technical Materials*. Łódź, Poland: published in the journal Ochrona Przed Korozją (Protection From Corrosion), pp. 305–400.